©2012

James G. Bollinger

Development and Application of Novel Methodologies for the Characterization of Phospholipase A_2 Activity: Targeted Lipidomic Profiling and Interfacial Binding Analysis

James G. Bollinger

A dissertation
submitted in partial fulfillment of the
requirements for the degree of

Doctor of Philosophy

University of Washington

2012

Reading Committee:

Michael H. Gelb, Chair

Sarah L. Keller

Dustin J. Maly

Program Authorized to Offer Degree:

Chemistry

In presenting this dissertation in partial fulfillment of the requirements for the Doctoral degree at the University of Washington, I agree that the Library shall make its copies freely available for inspection. I further agree that extensive copying of the dissertation is allowable only for scholarly purposes, consistent with “fair use” as prescribed in the U.S. Copyright Law. Requests for copying or reproduction of this dissertation may be referred to Proquest Information and Learning, 300 North Zeeb Road, Ann Arbor, MI 48106-1346, to whom the author has granted “the right to reproduce and sell (a) copies of the manuscript in microform and/or (b) printed copies of the manuscript made from microform.”

Signature _____

Date _____

University of Washington

Abstract

Development and Application of Novel Methodologies for the Characterization of Phospholipase A_2 Activity: Targeted Lipidomic Profiling and Interfacial Binding Analysis

James G. Bollinger

Chairperson of the Supervisory Committee:
Professor Michael H. Gelb
Department of Chemistry

Phospholipases A_2 are a family of enzymes that hydrolyze membrane glycerophospholipids to yield free fatty acids and lysophospholipids. Both products serve as precursors for an array of lipid mediators that play known roles in a variety of signal transduction processes. Discussed herein is the development and application of novel analytical methods to characterize both the kinetic and interfacial binding parameters of members of the secreted and cytosolic phospholipase A_2 families. Specifically, the discussion involves the development of assays that utilize the triple quadrupole LC-ESI-MS/MS analytical platform to profile the products and relevant downstream metabolites for the PLA_2 enzymatic reaction; lysophospholipids, free fatty acids, and eicosanoids, a family of bioactive lipid mediators derived from arachidonic acid. Additionally, the discussion includes methods to characterize the interfacial binding behavior for several prominent members of the secreted and cytosolic phospholipase A_2 families.

Table of Contents

List of Abreviations ..... **iv**

List of Figures ..... **viii**

List of Tables ..... **x**

Chapter 1 Phospholipase A_2 and the Production of Lipid Mediators **1**
Section 1 : Introduction 1
Section 2 : Fatty Acid Structure and Molecular Diversity 3
Section 3 : Glycerophospholipid Structure and Molecular Diversity 5
Section 4 : Biological Roles of Lipids 11
Section 5 : Phospholipase A_2 and the Production of Lipid Mediators 13
The $sPLA_2$ Family of Enzymes 16
The $cPLA_2$ Family of Enzymes 20

Chapter 2 Improved Method for the Quantification of Lysophospholipids Including Enol Ether Species by Liquid Chromatography-Tandem Mass Spectrometry **25**
Section 1 : Introduction 25
Section 2 : Methods 27
Materials 27
Sample Preparation 29
Sample Analysis 31
Analysis of Isobars 34
Section 3 : Results and Discussion 35
General features of the LC/ESI-MS/MS analysis. 38
LC/ESI-MSMS analysis of LPL mixtures. 45
Section 4 : Summary 49
Section 5 : Addendum to Chapter 2 63

Chapter 3 Improved Sensitivity Mass Spectrometric Detection of Eicosanoids by Charge Reversal Derivatization **65**
Section 1 : Introduction 65
Section 2 : Methods 67
Synthesis of AMPP 67
Preparation of eicosanoid stock solutions 68
Preparation of samples prior to derivatization with AMPP 69
3.2.a Standard curves. 69
3.2.b Mouse serum 69
3.2.c Lung epithelial cells 70

3.2.d Rat 3Y1 cells 71
Derivatization with AMPP 72
LC/ESI-MS/MS analysis 73
Eicosanoid recovery studies 76
Section 3 : Results and Discussion 77
Design and preparation of AMPP amides 77
LC/ESI-MSMS analysis of eicosanoid AMPP amides 80
Section 4 : Summary 86
Section 5 : Addendum to Chapter 3 90
3.5.a Method parameters for Waters Xevo TQ/Acquity UPLC 90
3.5.b Substitution of HOBt with HOAt 94
3.5.c Eicosanoids from $sPLA_2$ incubations of platelet derived microparticles 95

Chapter 4 Improved Sensitivity Mass Spectrometric Detection of Fatty Acids by Charge Reversal Derivatization 100
Section 1 : Introduction 100
Section 2 : Materials and Methods 104
Preparation of reagents and materials for fatty acid analysis 104
4.2.a Synthesis of AMPP 104
4.2.b Pre-derivitization work-up of glassware, solvents, and reagents 105
Preparation of fatty acid stock solutions 105
Preparation of samples prior to derivatization with AMPP 106
4.2.a Standard curves. 106
4.2.b Preparation of recombinant $sPLA_2$'s 106
4.2.c Preparation of platelet derived microparticles 106
4.2.d Isolation of mitochondria 106
4.2.e Incubation of mitochondria and platelet derived microparticles in presence of $sPLA_2$. 107
4.2.f Extraction of fatty acids from platelet derived microparticles treated with $sPLA_2$'s. 107
4.2.g Extraction of fatty acids from platelet derived mitochondrion treated with $sPLA_2$'s. 108
4.2.h Extraction of fatty acids from mouse serum 108
Derivatization with AMPP 110
LC/ESI-MS/MS analysis 111
Section 3 : Results 113

Chapter 5 Comparison of the PLA_1 and PLA_2 Enzymatic Activities of a Panel of Mammalian $cPLA_2$ Isoforms 119
Section 1 : Introduction 119
Section 2 : Methods 119

Materials 119
Kinetic Studies 120
Section 3 : Results and Discussion 121

Chapter 6 Interfacial Binding of Bee Venom sPLA$_2$ Occurs Predominantly By a Non-Electrostatic Mechanism 125
Section 1 : Introduction 125
Section 2 : Methods 128
Preparation of Recombinant Bee Venom PLA2's 128
Interfacial Binding Studies 128
Section 3 : Results 130
Approach to study Interfacial binding of bvPLA$_2$ 130
Binding of wild-type and mutant bvPLA$_2$'s to vesicles 131
Section 4 : Discussion 136

Chapter 7 Interfacial Binding Studies and Sensitivity to DTT of the Secreted Phospholipases A$_2$ 141
Section 1 : Introduction 141
Section 2 : Methods 142
Materials 142
sPLA$_2$ sensitivity to DTT 143
Interfacial binding to vesicles 143
Section 3 : Results 144
Sensitivity of mouse and human sPLA$_2$'s to DTT 144
Interfacial Binding of sPLA$_2$ to GPL vesicles 145
Section 4 : Discussion 149

List of References 155

Appendix A: Chronological Personal Publication List 166
A1 : Publications up to December 2012 166

Appendix B: List of Funded Proposals, Awards, and Presentations 169
B1 : Funded Proposals 169
B2 : Awards 169
B3 : Selected Presentations 169

List of Abbreviations

A23187 – Calcium Ionophore
AA – Arachidonic Acid
ACN – Acetonitrile
AMPP – *N*-(4-Aminomethylphenyl)-Pyridinium
APCI – Atmospheric Pressure Chemical Ionization
Bis-Tris – 2-[Bis(2-Hydroxyethyl)-Amino]-2-Hydroxymethyl)-Propane-1,3-Diol
BSA – Bovine Serum Albumin
bv-sPLA$_2$ – Bee Venom Secreted Phospholipase A2 Type III
bvPLA$_2$-E5 – (K14E/R23E/K85E/K94E/K133E) mutant of bv-sPLA$_2$
bvPLA$_2$-Q5 – (K14Q/R23Q/K85Q/K94Q/K133Q) charge reversal mutant of bv-sPLA$_2$
C2 – Protein Structural Domain Involved in Lipid Binding
CH – Cholesterol
CID – Collision Induced Dissociation
CL – Cardiolipin
cPLA$_2$ – Cytosolic Phospholipase A2
cPLA$_2$-α – Cytosolic Phospholipase A2 Type IVA
cPLA2-β – Cytosolic Phospholipase A2 Type IVB
cPLA$_2$-γ – Cytosolic Phospholipase A2 Type IVC
cPLA$_2$-δ – Cytosolic Phospholipase A2 Type IVD
cPLA$_2$-ε – Cytosolic Phospholipase A2 Type IVE
cPLA$_2$-ζ – Cytosolic Phospholipase A2 Type IVF
CV – Coefficient of Variation
DMAP – 4-Dimethylaminopyridine
DCM – Dichloromethane
DMEM – Dulbecco's Modified Eagle Medium
DMF – *N,N*-Dimethylformamide
DMSO – Dimethyl Sulfoxide
DO$_{et}$PC – 1,2-di-O-(9*Z*-octadecenyl)-*sn*-Glycero-3-Phosphatidylcholine
DO$_{et}$PS – 1,2-di-O-(9*Z*-octadecenyl)-*sn*-Glycero-3-Phosphatidylserine
DOPC – 1,2-dioleoyl-*sn*-Glycero-Phosphatidylcholine
DOPS – 1,2-dioleoyl-*sn*-Glycero-Phosphatidylserine
DTT – Dithiothreitol
EDCI – 1-Ethyl-3-(3-Dimethylaminopropyl) Carbodiimide Hydrochloride
EGTA – Ethylene Glycol Tetraacetic Acid
ESI – Electrospray Ionization
ESI-MS/MS – Electrospray Tandem Mass Spectrometry
FA – Fatty Acid

G3P – *sn*-Glycerol-3-Phosphate
GPA – *sn*-Glycero-3-Phosphatidic Acid
GPC – *sn*-Glycero-3-Phosphatidylcholine
GPCR – G-Protein Coupled Receptor
GPE – *sn*-Glycero-3-Phosphatidylethanolamine
GPG – *sn*-Glycero-3-Phosphatidylglycerol
GPI – *sn*-Glycero-3-Phosphatidyl-*myo*-inositol
GPL – Glycerophospholipid
GPS – *sn*-Glycero-3-Phosphatidylserine
HEK293 – Human Embryonic Kidney Immortalized Cell Line
HEPES – (4-(2-hydroxyethyl)-1-piperazineethanesulfonic acid)
HOAt – 1-Hydroxy-7-azabenzotriazole
HOBt – 1-Hydroxybenzotriazole
HPLC – High-Pressure Liquid Chromatography
K_d – Dissociation Constant
LPA – Lysophosphatidic Acid
LPC – Lysophosphatidylcholine
LPE – Lysophosphatidylethanolamine
LPG – Lysophosphatidylglycerol
LPI – Lysophosphatidyl-*myo*-inositol
LPL – Lysophospholipid
LPS – Lysophosphatidylserine
LC – Liquid Chromatography
LT – Leukotriene
MeOH – Methanol
MOPS – 3-(*N*-Morpholino)Propanesulfonic Acid
MS – Mass Spectrometry
MS/MS – Tandem Mass Spectrometry
MUFA – Monounsaturated Fatty Acid
NMR – Nuclear Magnetic Resonance
PAPC – 1-Palmitoyl-2-Arachidonyl-*sn*-Glycero-Phosphatidylcholine
PBS – Phosphate Buffered Saline
PG – Prostaglandin
PLA_2 – Phospholipase A2
POPA – 1-palmitoyl-2-Oleoyl-*sn*-Glycero-3-phosphate
POPC – 1-Palmitoyl-2-Oleoyl-*sn*-Glycero-Phosphatidylcholine
POPE – 1-Palmitoyl-2-Oleoyl-*sn*-Glycero-Phosphatidylethanolamine
POPG – 1-Palmitoyl-2-Oleoyl-*sn*-Glycero-Phosphatidylglycerol
POPI – 1-Palmitoyl-2-Oleoyl-*sn*-Glycero-Phosphatidyl-*myo*-Inositol

POPS – 1-Palmitoyl-2-Oleoyl-*sn*-Glycero-Phosphatidylserine
PUFA – Polyunsaturated Fatty Acid
RPMI – Roswell Park Memorial Institute Medium
SFA – Saturated Fatty Acid
SM – Sphingomyelin
sn – Stereospecific Numbering
$sPLA_2$ – Secreted Phospholipase A2
$sPLA_2$-GIB – Secreted Phospholipase A2 Type IB
$sPLA_2$-GIIA – Secreted Phospholipase A2 Type IIA
$sPLA_2$-GIIC – Secreted Phospholipase A2 Type IIC
$sPLA_2$-GIID – Secreted Phospholipase A2 Type IID
$sPLA_2$-GIIE – Secreted Phospholipase A2 Type IIE
$sPLA_2$-GIIF – Secreted Phospholipase A2 Type IIF
$sPLA_2$-GIII – Secreted Phospholipase A2 Type III
$sPLA_2$-GV – Secreted Phospholipase A2 Type V
$sPLA_2$-GX – Secreted Phospholipase A2 Type X
$sPLA_2$-GXIIA – Secreted Phospholipase A2 Type XIIA
$sPLA_2$-GXIIB – Secreted Phospholipase A2 Type XIIB
SRM – Single Reaction Monitoring
TQ – Triple Quadrupole
Tris – Tris(hydroxymethyl)aminomethane
UPLC – Ultra High-Pressure Liquid Chromatography

Units
amu – Atomic Mass Unit (Dalton)
°C – Degrees Celsius
f – Femto
g – Grams
g – Gravitational Acceleration
hrs – hours
kDa – Kilodalton
L – Liter
min – Minutes
mm – Millimeter
M – Molar
mol – Moles
n – Nano
p - Pico
RPM – Revolutions Per Minute

RT – Room Temperature
sec – Seconds
μ - Micro
Å – Angstrom

NMR
d – Doublet
MHz – Megahertz
s – Singlet
t – Triplet

List of Figures

Chapter 1:

FIGURE 1.1: Major variations of the glycerophospholipid molecular structure……..**7**

Chapter 2:

FIGURE 2.1: LC/ESI-MSMS detection of a standard mixture of LPL's……**46**
FIGURE 2.2: Distribution of coefficient of variances (CV's) for the analysis of LPL's in mouse serum……**47**
FIGURE 2.3: LPL molecular species changes in HEK293 cells in response to group X sPLA2 action……**48**
FIGURE 2.4: Summary of the concentration of LPL's in mouse serum……..**56**
FIGURE 2.5: Standard curves for commercially available LPL's……..**60-62**

Chapter 3:

FIGURE 3.1: Structure of AMPP and an AMPP amide along with the reagents used for derivatization……..**76**
FIGURE 3.2: B3LYP/6-31G* calculated potential energy profile for the N—CH_2 benzylic bond dissociation in the charge tag……..**78**
FIGURE 3.3: Fragment ion spectra of eicosanoid AMPP amides……**79**
FIGURE 3.4: LC/ESI-MSMS traces of eicosanoids after workup from a solution in phosphate buffered saline……**81**
FIGURE 3.5: AMPP method cross-validation with commercial EIA kit……**83**
FIGURE 3.6: Selected ion traces for LC/ESI-MSMS analysis of eicosanoids in mouse serum……**84**
FIGURE 3.7: Eicosanoid profile of $sPLA_2$ incubations of platelet derived microparticles. **……98**

Chapter 4:

FIGURE 4.1: Unsaturated Fatty acid profile of $sPLA_2$-GIIA, $sPLA_2$-GV, and $sPLA_2$-GX incubations with platelet derived microparticles…**……113**
FIGURE 4.2: Unsaturated Fatty acid profile of $sPLA_2$-GIIA, $sPLA_2$-GV, and $sPLA_2$-GX incubations with mitochondria isolated from mouse liver…**……114**
FIGURE 4.3: Fragment ion spectra of fatty acid AMPP amides…**……115-117**

Chapter 6:

FIGURE 6.1: Binding of bvPLA$_2$ and bvPLA$_2$-E5 to DOetPS/DOet-PC vesicles……**132**
FIGURE 6.2: Binding of bvPLA$_2$'s to 25% DOetPS/75% DOetPCvesicles as a function of pH. ……**134**
FIGURE 6.3: Binding of bvPLA$_2$'s to DOPS/DOPC/CH/SM vesicles as a function of the amount of DOPS……**136**

Chapter 7:

FIGURE 7.1: Interfacial binding of sPLA$_2$'s to phospholipid vesicles……**145**

List of Tables

Chapter 2:

TABLE 2.1: Extraction yields, liquid chromatography retention times, and tandem mass spectrometry parameters for lysophospholipid molecular species……**32-34**
TABLE 2.2: Autosampler (2795 Alliance HT LC) and ESI-MS/MS (Waters Quattro Micro) data collection parameters……..**51**
TABLE 2.3: Isobar analysis of LPA, LPE, LPG, LPI and LPS species……**52-55**
TABLE 2.4: Analysis of LPL's in mouse serum……..**57**
TABLE 2.5: LPL molecular species changes in HEK293 cells in response to human $sPLA_2$-GX action……..**58-59**

Chapter 3:

TABLE 3.1: Extraction yields, liquid chromatography retention times, and tandem mass spectrometry parameters for eicosanoid AMPP amide molecular species……..**76**
TABLE 3.2: Coefficient of variation (%) for LC/ESI-MSMS analysis of eicosanoid AMPP amides……**85**
TABLE 3.3: Eicosanoid levels (pg/μl) in mouse serum……..**85**
TABLE 3.4: Eicosanoid levels (pg/ml) from primary human bronchial cells……**86**
TABLE 3.5: Autosampler (2795 Alliance HT LC) and ESI-MS/MS (Waters Quattro Micro) data collection parameters……**88**
TABLE 3.6: Autosampler (Waters ACQUITY UPLC) and ESI-MS/MS (Waters Quattro Premier) data collection parameters……**89**
TABLE 3.7: Autosampler (Waters ACQUITY UPLC) and ESI-MS/MS (Waters Xevo TQ) data collection parameters for underivatized and AMPP amide eicosanoids……..**92**
TABLE 3.8: Liquid chromatography retention times (Acquity **UPLC**) and ESI-MS/MS parameters for eicosanoid AMPP amides and underivatized eicosanoids……**93-94**
TABLE 3.9: Eicosanoid levels (pg/μl) of $sPLA_2$ enzymatic incubations of platelet derived microparticles……**96**

Chapter 4:

TABLE 4.1: Liquid chromatography retention times (Acquity UPLC) and ESI-MS/MS parameters for eicosanoid AMPP amides and underivatized eicosanoids……**109-110**
TABLE 4.2: Autosampler (Waters ACQUITY UPLC) and ESI-MS/MS (Waters Quattro Premier) data collection parameters……**112**
TABLE 4.3: Calculated concentrations along with Inter-assay and Intra-assay Coefficients of Variation for fatty acid AMPP amides in mouse serum……**118**

Chapter 5:

TABLE 5.1: PLA_1 versus PLA_2 activities of $cPLA_2$s (POPC vesicles)……..**122**
TABLE 5.2: PLA_1 versus PLA_2 activities of $cPLA_2$'s (mixed GPL vesicles)……**124**

Chapter 6:

TABLE 6.1: Binding of $bvPLA_2$ to vesicles as a function of pH dependence……..……**138**
TABLE 6.2: Binding of $bvPLA_2$ to Vesicles at pH 7.4-GPS as a function of Calcium Dependence……..**139**

Chapter 7:

TABLE 7.1: Remaining enzymatic activity of human and mouse $sPLA_2$'s after treatment with 10 mM DTT……..**145**
TABLE 7.2: Interfacial kinetic and binding properties of human and mouse $sPLA_2$'s……**148**

Acknowledgements

I would like to formally acknowledge my advisor Michael H. Gelb for all his support and guidance throughout my research career. In the eleven years I was privileged to work in his interdisciplinary laboratory, I was given every opportunity to learn a multitude of biochemical techniques, interact with accomplished scientists, and contribute to research efforts that have had a tangible impact on human health. I would also like to thank a multitude of Gelb lab members (you know who you are!) for your moral and intellectual support over the years. I must also acknowledge the University of Washington, the Huckabay Foundation, and the National Institutes of Health for financial support during my time in graduate school. Finally, I would like to sincerely thank my family and friends, who's love and support have given me the audacity to live my dreams.

Dedication

This body of work is dedicated to my loving wife, Anne Powell. You continue to inspire the best in me and make me want to be a better human being. I would also like to dedicate these efforts to my mother, Nancy Bollinger. Your belief in me has always given me the courage to take that next step.

Chapter 1

Phospholipase A_2 and the Production of Lipid Mediators

Section 1: Introduction

Biological lipids are a structurally diverse class of biomolecules with an array of chemically distinct species that numbers in the tens of thousands[1]. The structural diversity of this family owes its origins partly to the fact that lipids were initially categorized more on the basis of their similar physical properties (*i.e.* solubility in nonpolar organic solvents and amphipathic behavior in aqueous solutions) than on the basis of any specific similarity in structure. As a result, the term "biological lipid" has been generally applied to describe a wide variety of compounds assembled from an assorted array of structural subunits. The kind of molecular diversity imparted by the heterogeneous building blocks of lipids is unique when compared to the diversity inherent to any of the other three primary classes of biomolecules; proteins, carbohydrates, and nucleic acids. For these classes, variation in molecular structure is usually a function of the polymerization of a finite and limited set of structural monomers (ie. peptides/proteins from amino acids, oligosaccharides from mono-saccharides, or DNA/RNA from nucleic acids). Conversely, lipids are not merely "poly-lipids" but rather, complex mosaics of multiple different structural motifs. Perhaps the best indicator of the extent of this structural diversity of biological lipids is the fact that

there even still remains an ongoing debate as to their precise and comprehensive definition. One camp suggests taking into account a compound's amphipathic properties as well as the biosynthetic origins of its structural motifs from either "carbanion-based condensations of fatty acyl thio-esters or carbocation-based condensations of isoprene units"[2]. Yet another camp favors a more reductionist approach and simply defines lipids as "fatty acids, their derivatives, and substances related biosynthetically or functionally to these compounds" [3]. Although the specifics of a precise definition pose fodder for scholarly debate, it is largely agreed upon that the empirical study of lipids requires a general consensus on definition as well as a standardized classification system. To meet these ends, a recent report has suggested classifying lipids into eight distinct classes according to similarities in some of their key structural subunits: fatty acids, glycerolipids, glycerophospholipids, sphingolipids, sterol lipids, prenol lipids, saccharolipids, and polyketides[2]. Within this structurally diverse family of compounds, those species most relevant to the current dissertation are the fatty acids (FA's) as well as the glycerophospholipids (GPL's). Particular emphasis is given to downstream bioactive metabolites of these compounds that are produced as a result of the interfacial hydrolytic activity of the cytosolic and secreted phospholipase A_2 (cPLA_2 and sPLA_2, respectively) families of enzymes. Collectively, these biological compounds are discussed in this dissertation with regard to their role in promoting interfacial interactions with PLA_2's and in the context of the development of sensitive and specific

assays for their quantification utilizing liquid chromatography in conjunction with triple-quadrupole mass spectrometry as an analytical platform.

Section 2: Fatty Acid Structure and Molecular Diversity

Considering that FA's are essential building blocks of nearly all complex lipids and that they independently exemplify the key physiochemical properties on which the biological lipid class was initially defined, no discussion on the topic of lipids is complete without an introduction to FA's and the structural features from which their hallmark properties derive. In their simplest form, FA's are comprised of a nonpolar poly-methylene chain that is functionalized on one end with a comparably polar carboxylic acid group. At physiological pH, the acid moiety is typically ionized to its respective carboxylate, which imparts even more contrasting hydrophilic character to its respective end of the hydrophobic hydrocarbon chain. Where as the solubility of a fatty acid in nonpolar organic solvents is dictated by the length and degree of unsaturation of its respective hydrocarbon chain, its amphipathic behavior (*i.e.* self-assembly into higher order structures when dissolved in aqueous solution above a certain critical concentration) is a function of the contrast in polarity between that chain and its respective carboxylate terminus. Self-aggregation of FA's into micelles takes its origins from the principles underlying the hydrophobic effect[4]. The hydrophobic "tails" of the fatty acids associate to minimize the surface area exposed to water where as the hydrophilic carboxylate "heads" align at the solvent/solute interface. This self-assembly

limits the entropic penalty that would be incurred by solvent molecules that order at the interface of the hydrophobic "cavity" created by the aliphatic portion of a non-aggregated amphipath.

Molecular diversity of FA's results from different possible lengths and degrees of unsaturation of their hydrocarbon chains. Where as aliphatic chains with branch points and an odd number of carbon atoms are commonly observed in prokaryotic biology, most fatty acids relevant to eukaryotic biology contain unbranched chains comprised of an even number of carbons ranging from four to thirty-six. Even numbers of carbons in FA's result from FA catabolism and metabolism that is based on two-carbon (acetate) chemistry. For reasons believed to be related to optimal membrane properties such as bilayer thickness, fluidity, and curvature, plants and animals typically utilize fatty acids with chains between twelve and twenty-four carbons long, with a preponderance of chains that contain either sixteen or eighteen carbons[3]. Regarding the degree of unsaturation, fatty acids vary with respect to the number and relative position of double bonds along the carbon backbone. The saturated series of fatty acids (SFA) contain no double bonds and are comparably more hydrophobic than those with identical chain lengths in the monounsaturated (MUFA) and polyunsaturated (PUFA) series. The double bonds of most unsaturated fatty acids are, with a few notable exceptions, in the *cis* orientation. The double bonds of PUFA's are almost never conjugated and are typically separated by single methylene group.

Systematic nomenclature for fatty acids starts with the name for the parent hydrocarbon. Fatty acid carbons are numbered starting at the carboxylate carbon. The penultimate carbon in the chain is often referred to as the ω carbon and carbons two and three are often referred to as the α and β carbons, respectively. The position of a double bond may be identified by either indicating its respective carbon number or by indicating its distance from the ω carbon. Complete nomenclature also includes the stereochemistry designations for the configuration of each double bond. In some instances, the use of trivial names has replaced the use of the systematic name. Additionally, another simplified nomenclature for fatty acids is also commonly used and cleanly specifies the number of carbons in the alkyl chain followed by the number of double bonds after a colon. Using this shorthand notation, the position of the double bonds are indicated by carbon number as a superscript symbol after the greek symbol Δ. For example, a fatty acid with eighteen carbons and one double bond in the *cis* orientation at carbon nine can be referred to as (*9Z*)-octadecenoic acid (systematic name), oleic acid (common name), or 18:1 Δ^{9cis} (shorthand notation).

Section 3: Glycerophospholipid Structure and Molecular Diversity

Glycerophospholipids are an important set of fatty acid derivatives that comprise the bulk of the lipid fraction in most biological membranes. Similar to FA's, GPL's are amphipathic molecules that self-assemble into higher order structures when in aqueous

media. For reasons related to the relative cross-sectional surface area between their hydrophilic "heads" and hydrophobic "tails", GPL's tend to aggregate into vesicles and membrane bilayers rather than micelles[4].

At the core of the GPL structure is *sn*-glycerol-3-phosphate (G3P), a phosphorylated three-carbon carbohydrate. The asymmetric substitution of the prochiral compound glycerol converts its secondary carbon into a chiral center. For the current discussion, the stereospecific numbering (*sn*-) system will be employed to unambiguously assign the stereoisomer of G3P found in most biological lipids. Using this system, the *sn-1* position is, by definition, the position of the prochiral glycerol molecule that occupies the pro-*S* position[5]. G3P serves as the scaffold on which the hydrophilic and hydrophobic moieties of the amphipathic GPL structure are assembled. The hydrophobic moiety of a GPL is comprised of a FA chain esterified to the *sn-2* position of the glycerol backbone and either a FA or fatty alcohol linked to the *sn-1* position via an ester or ether bond, respectively. The hydrophilic portion of a GPL is comprised of either the *sn-3* phosphate itself (for the phosphatidic acid (GPA) series of GPL's) or a polar alcohol attached to the *sn-3* carbon of glycerol via a phosphodiester linkage. Collectively, the hydrophilic segment of a GPL is often referred to as its polar head group. In eukaryotes, the alcohols most commonly found in head groups are choline, ethanolamine, glycerol, *myo*-inositol, and the amino acid serine. Cardiolipin (CL) represents a non-traditional GPL enriched in prokaryotic and mitochondrial

membranes that is comprised of two di-acyl PA subunits linked to a common glycerol backbone at the *sn-1* and *sn-3* positions. Figure 1.1 summarizes the major variations of the core GPL structure, the stereochemistry of a GPL's asymmetric carbon, as well as the structures of the polar alcohols commonly utilized as GPL head groups.

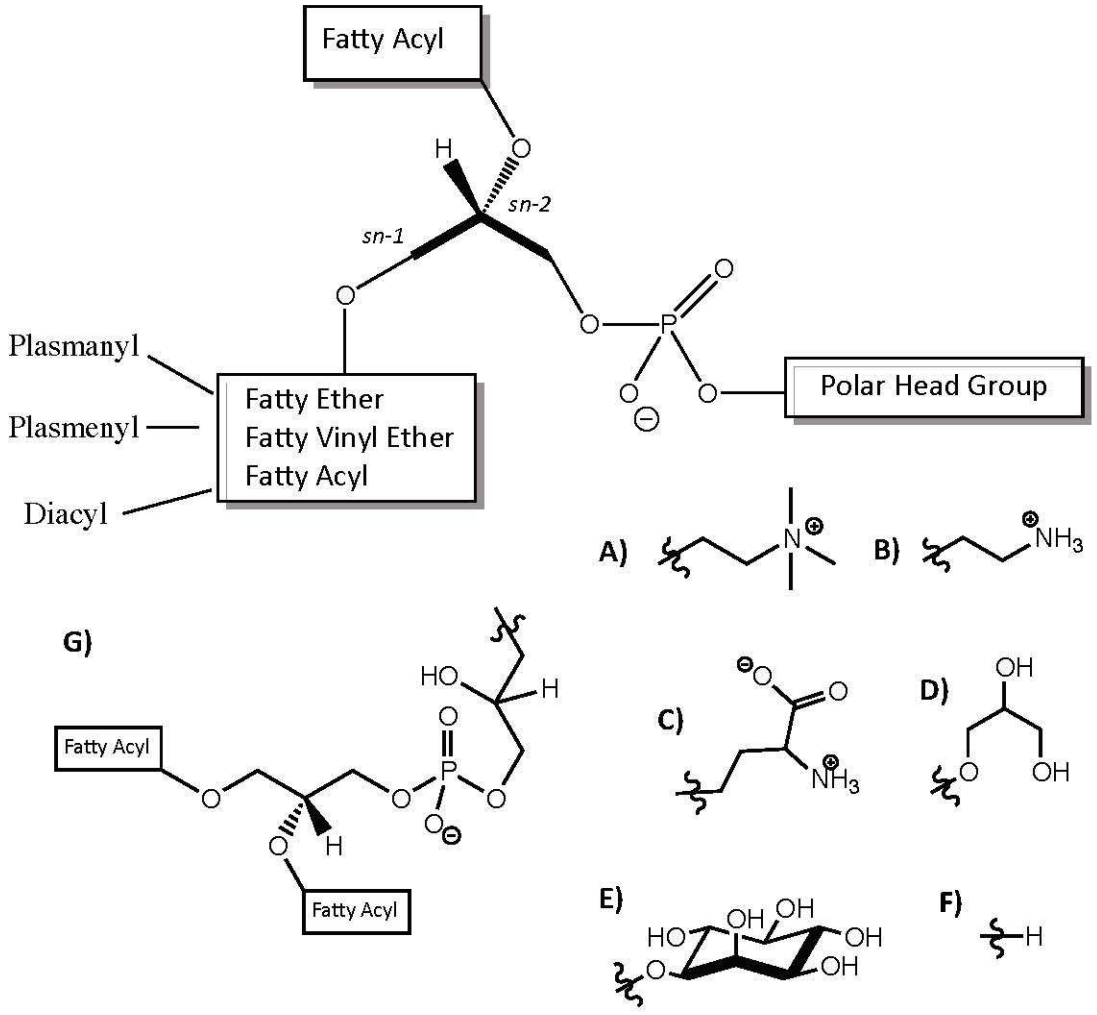


Figure 1.1 : Major variations of the glyycerophospholipid structure utilized by eukaryotic biology. Polar head group structures are detailed for (A) phosphatidyl choline, (B) phosphatidyl ethanolamine, (C) phosphatidyl serine, (D) phosphatidyl glycerol, (E) phosphatidyl myo-inositol, (F) phosphatidic acid, and (G) cardiolipin molecular species.

Lysophospholipids (LPL's) are a family of GPL derivatives that have only a single FA or fatty alcohol moiety linked to the glycerol backbone. These species are produced either as GPL biosynthetic intermediates or as secondary messengers in signaling cascades involving the enzymatic activity of phospholipases. LPL's, with their monomeric hydrophobic moiety, are considerably more polar than their GPL analogs. This feature increases their relative solubility in aqueous media and permits monomers to partition out of bilayers and participate in inter- and intracellular signaling events[6].

The systematic nomenclature for GPL's utilized for the current text includes the stereospecific numbering system mentioned above and names GPL species according to their polar alcohol moieties as derivatives of a phosphatidic acid parent compound. When referring to a class of GPL's by their common head group, the abbreviations GPC, GPE, GPS, GPI, GPG, GPA, and CL are frequently used to describe phosphatidylcholine, phosphatidylethanolamine, phosphatidylserine, phosphatidyl-*myo*-inositol, phosphatidylglycerol, phosphatidic acid, and cardiolipin species, respectively. Occasionally, and only where specifically noted, the first letter of the trivial name for the fatty acyl substituents are included in the abbreviation. For example, a GPL with choline as the head group, palmitate in the *sn-1* position, and arachidonate in the *sn-2* position is described as PAPC (1-palmitoyl-2-arachidonyl-*sn*-glycero-phosphatidylcholine). Species with either an ether or vinyl ether (fatty alcohol with an unsaturation between C1 and C2) linkage in the *sn-1* position are referred to as plasmanyl-GPL's or plasmenyl-

GPL's, respectively. LPL, plasmanyl-LPL, and plasmenyl-LPL species are treated in a similar fashion to their GPL counterparts with respect to head group class abbreviations (*i.e.* LPC, LPE, LPS, LPI, LPG, and LPA). Similarly, their nomenclature includes a complete description of their single FA or fatty alcohol substituent as well as, in examples where it is not immediately evident, the *sn*- designation for that hydrophobic substituent.

Molecular diversity of GPL's and LPL's is a function of both their head group identity as well as the composition of their FA's and fatty alcohols. Although the systematic variation of these elements predicts thousands of distinct chemical species[1], the library of GPL/LPL species utilized in eukaryotic biology is considerably smaller. The manner in which individual molecular species are distributed within the various types of cellular membranes follows a handful of relatively conserved principles. First of all, the polar head group distribution within a specific membrane is neither homogenous nor random. Living cells commit energy resources to generating and maintaining the GPL distributions of their various membranes. In general, GPC and GPE species are the most abundant GPL's in most eukaryotic membranes, where as the other five polar head groups comprise relatively minor GPL mole fractions[3]. Furthermore, the GPL composition of membranes is asymmetric with respect to their individual leaflets[3]. For example, the extracellular face of a eukaryotic cell's plasma membrane tends to be enriched in GPC, sphingomyelin, and cholesterol relative to the cytosolic face. Conversely, GPE, GPS, GPI, and GPG tend to be enriched in the cytosolic face of the

plasma membrane as well as in the membranes of various organelles[7]. This inter-bilayer asymmetry has important consequences for the recognition of specific membranes by PLA_2's and other interfacial enzymes.

A second principle of the GPL composition of eukaryotic membranes is that each polar head group has its own distinct panel of hydrophobic moieties[3]. As discussed in the section on FA molecular diversity, acyl and alky chains of sixteen and eighteen carbons with zero, one, or two double bonds are the most frequently encountered species in biological membranes. The other chain lengths, particularly the twenty and twenty-two carbon PUFA's constitute smaller fractions but often maintain crucial roles in signaling pathways. Generalizing across the different head groups, GPE, GPS, GPI, GPE, and CL species tend to have a higher percentage of unsaturated chains in their hydrophobic moieties than their GPG and GPC counterparts[3, 8]. A further illustration of this principle is that plasmanyl and plasmenyl species occur predominantly in the GPC and GPE fractions of membrane GPL's[9].

A third conserved principle involves the trends of the *sn-1*/*sn-2* distribution of FA's and fatty alcohols within individual GPL species. This principle applies across all head groups and is best summarized by pointing out that the *sn-1* position of most GPL's is occupied by SFA's and MUFA's for canonical GPL's or saturated and monounsaturated fatty alcohols for plasmanyl-GPL and plasmenyl-GPL species, respectively. Conversely, PUFA species, when present, tend to occupy the *sn-2* position exclusively[3, 8]. This last

principle is essential in the understanding of the connection between PLA_2 enzymatic activity and various downstream signaling events.

Section 4: Biological Roles of Lipids

The immense structural diversity of the biological lipid family is accompanied by a multiplicity of biological roles. These roles are generally grouped into four distinct categories[10]: structure, energy storage, post-translational protein modification, and signal transduction. First of all, as major constituents of cellular membranes, lipids serve an important structural function by segregating cells and organelles from their external environments. The amphipathic structure of lipids drives the formation of phospholipid bilayers, which compartmentalize the biochemical reactions of the cell and can raise the effective molarity of protein substrates and cofactors. Additionally, the structural subunits of membrane lipids can also serve as recognition motifs for protein recruitment to various locations within the cell[5]. A second functional category of lipids function is related to their role as a cellular energy reservoir. Due to the relatively low oxidation state of their aliphatic subunits, lipids represent an efficient source of substrates for the oxidative pathways from which cells typically derive a bulk of their required energy. Thirdly, lipids are utilized by cellular systems for post-translational modifications of proteins. These modifications help facilitate protein-protein and inducible protein-lipid interactions. Lastly, and of greatest relevance to the current discussion, biological lipids

can also function as precursors to potent inter- and intra-cellular signaling molecules. Multistep enzymatic pathways release water-soluble intermediates from membrane lipid reservoirs. These intermediates then go on to participate in cell signaling events via specific interactions with cognate receptors[10].

Our understanding of the biological roles of lipids has gone through two distinct iterations. Up until the early twentieth century, it was widely believed that these roles were confined to structure and energy storage. Then, in a series of seemingly unrelated studies in the early 1930's, it became evident that membrane-derived lipids could also function as potent signaling molecules. One study described the production of a "slow-reacting substance of anaphylaxis," now known to be a member of the leukotriene (LT) family, by organs and lymph treated with snake venom[11]. Another set of studies proposed a family of molecules named 'prostaglandins' (PGs) to account for the smooth muscle stimulating effects of an acidic lipid fraction isolated from seminal fluid[12]. Three decades later, in a series of studies that would eventually result in a Nobel Prize, the structures of these PGs and LTs were solved[13]. Their biosynthesis was linked to a common arachidonic acid (AA) precursor[14], and the anti-inflammatory effects of aspirin were correlated to their biosynthesis[15]. The pioneering work on these AA metabolites, now collectively referred to as the eicosanoids, provided some of the first insight into the importance and interconnectedness of lipid signaling pathways and ultimately validated the therapeutic strategy of manipulating these networks.

In the decades since this pioneering work on the eicosanoids, a host of other bioactive lipid mediators have been identified and some common themes of lipid signaling have emerged[10, 16]. In general, lipid mediators are synthesized on demand in a calcium-dependent manner from membrane derived lipid precursors. The resulting bioactive metabolites act on type I G-protein coupled (GPCR) and/or nuclear receptors. These metabolites usually have relatively short half-lives in serum due to both enzymatic and non-enzymatic degradation. This rapid degradation usually limits their efficacy to autocrine and paracrine signaling networks. In addition to their initial correlation with inflammation, lipid mediators and their respective signaling pathways have been implicated in nearly every cellular process. Furthermore, imbalances within these pathways contribute to disease progression in a host of different ailments including cancer, autoimmunity, atherosclerosis, hypertension, and metabolic syndrome[10, 16].

Section 5: Phospholipase A_2 and the Production of Lipid Mediators

Early work on the eicosanoids established that the intracellular level of free AA is kept low and tightly regulated. Furthermore it was shown that virtually all cellular AA is esterified in the *sn-2* position of GPL's[17]. Concurrent efforts in the field of interfacial enzymology began to characterize a family of phospholipase A_2 (PLA_2) enzymes capable of selectively catalyzing the hydrolysis the *sn-2* esters of GPL's to yield free FA's as well

as LPL's. Despite these observations, the connection between PLA_2 activity and lipid mediator production was correlative at best until the early 1990's with the discovery of a cytosolic PLA_2 ($cPLA_2$-α) selective for GPL substrates with PUFA's esterified in the *sn-2* position[18]. Follow-up studies with transgenic mice and a panel of first generation of inhibitors confirmed a significant role for $cPLA_2$-α in the liberation of AA destined for eicosanoid generation (*Reviewed in* [10]). However, the fact that residual levels of lipid mediators are still observed in studies utilizing the $cPLA_2$-α knockout mouse suggests that there are alternative pathways for their production. In the years since these seminal studies, multiple other members of the mammalian PLA_2 family have been identified (*Reviewed in* [19]). Much effort is currently dedicated to elucidating if and how these newly discovered PLA_2's are involved in the production of lipid mediators and to identifying their other potential roles in cellular biology. Of those PLA_2's, the most relevant to the current discussion are the eleven known $sPLA_2$ isoforms ($sPLA_2$-GIB, $sPLA_2$-GIIA, $sPLA_2$-GIIC, $sPLA_2$-GIID, $sPLA_2$-GIIE, $sPLA_2$-GIIF, $sPLA_2$-GIII, $sPLA_2$-GV, $sPLA_2$-GX, $sPLA_2$-GXIIA, and $sPLA_2$-GXIIB) as well as the five other known isoforms of $cPLA_2$ ($cPLA_2$-β, $cPLA_2$-δ, $cPLA_2$-γ, $cPLA_2$-ε, and $cPLA_2$-ζ).

Due to a potential role in the liberation of LPL's and PUFA's from membrane reservoirs and possible subsequent initiation of downstream signaling cascades, a considerable amount of effort is currently invested in elucidating the physiological and pathological roles of various PLA_2's in a host of cellular pathways. Characterization of

these enzymes via classic *in vitro* medicinal enzymology techniques such as the interfacial binding analysis detailed in Chapter Six and Seven has provided insight. However, interpretation of these studies is challenging due to multiple isoforms with overlapping substrate/inhibitor specificities and the likely temporal-spatial regulation via cell-cell, protein-protein and protein-membrane interactions inherent to interfacial enzymes *in vivo*. Genetic manipulation techniques have also proved useful yet limited in this analytical endeavor. Multiple PLA_2's implicated in eicosanoid and LPL biology has been disrupted by gene targeting mechanisms or effectively silenced by RNA interference mechanisms[10]. The observations obtained from these studies have resulted in a few clinical trials for novel therapeutics[20]. Despite this progress, the precise role(s) for each of the recently discovered isoforms and their respective splice variants has remained elusive due to several analytical caveats including the aforesaid compensatory effects resulting from overlapping substrate specificities and interspecies differences between humans and the animals used in disease models[21]. Taken together, the limitations of traditional biochemical techniques highlight the need for a metabolite-driven approach for top-down analysis of these pathways[22]. This 'targeted lipidomic' approach seeks to elucidate the regulatory mechanisms of these pathways via profiling all relevant downstream lipid metabolites. Top-down analysis requires rapid, sensitive analytical techniques and high-resolution chromatographic techniques amenable to high-throughput screens. Electrospray tandem mass spectrometry (ESI-MS/MS) coupled

with high-pressure liquid chromatography (HPLC) or alternatively, ultra high-pressure liquid chromatography (UPLC) has emerged as the premier technique for the targeted analysis of lipid mediators[23].

The $sPLA_2$ Family of Enzymes

The $sPLA_2$'s are family of relatively small (14-19 kDa) globular enzymes that are characterized by short N-terminal extensions (that target them for secretion into the extracellular matrix), multiple disulfide bridges, and active sites with conserved calcium binding loops and aspartic acid/histidine catalytic dyads[24]. These enzymes typically require μM levels of calcium for their ester hydrolase activity and display enhanced activity on lipid aggregates (*i.e.* bilayers and vesicles) over lipid monomers. The enhanced stability of these enzymes is attributed to their small size and disulfide rich tertiary structure. Unlike $cPLA_2$-α, $sPLA_2$'s typically display little selectivity for substrates containing PUFA's esterified in the *sn-2* position of GPL's. However, they do show trends in their preference for binding to specific GPL head groups. In general, the $sPLA_2$'s with interfacial binding surfaces enriched in tryptophan residues (*i.e.* $sPLA_2$-GV and $sPLA_2$-GX) display the highest affinity for membranes enriched in zwitterionic GPL's (i.e. GPC). Conversely, the other $sPLA_2$'s tend to have higher specific activities on membranes enriched in negatively charged GPL's (i.e. GPS, GPI, GPG, GPA, and CL)[25]. A summary of the $sPLA_2$ isoforms' head group preferences can be found in table 3.2 of

chapter seven. Of the eleven $sPLA_2$ isoforms common to mammalian genomes, eight $sPLA_2$'s share a common three-dimensional structure and are categorized as conventional (groups I, II, V, and X). The remaining three atypical $sPLA_2$'s (groups III and XII) only share a minimal set of features with the conventional $sPLA_2$'s[24].

The common tertiary structure of conventional $sPLA_2$'s is their six conserved disulfide bridges as well as up to two additional unique ones. The $sPLA_2$-GIB enzyme has a unique five amino acid segment in its catalytic domain referred to as the "pancreatic loop" and is secreted in pancreatic juice as an inactive zymogen with an additional seven amino acid N-terminal sequence. This sequence is removed by trypsin as the enzyme reaches its functional destination and performs its role in the digestion of dietary GPL's [26]. The $sPLA_2$-IIA, $sPLA_2$-GIIC, $sPLA_2$-GIID, $sPLA_2$-GIIE, and $sPLA_2$-GIIF genes are clustered on the same chromosome in higher mammals and each have a characteristic C-terminal extension with a seventh disulfide bridge[27]. The $sPLA_2$-GIIF isoform has a longer, proline-rich C-terminal extension that contains an additional unpaired cysteine residue of unknown function. Although expressed as an active enzyme in *mus musculus*, the $sPLA_2$-GIIC is merely a pseudogene in humans[24]. The $sPLA_2$-gV gene is also clustered with the group II genes. It is considered a minimal $sPLA_2$ because it lacks any apparent characteristic amino acid extension or unique fold and has only the minimum of six disulfide bridges. Similar to the $sPLA_2$-GIB isoform, the $sPLA_2$-GX enzyme also has a N-terminal extension and is synthesized as an inactive zymogen. However, the principles

underlying the *in vivo* activation of the $sPLA_2$-gX pro-enzyme seem to be context dependent and are still not completely understood[28] .

The atypical $sPLA_2$ isoforms share homology with the conventional ones only in their calcium binding loops and catalytic domains. The gIII cDNA predicts for a slightly larger (55 kDa) enzyme with lengthy C-terminal and N-terminal extensions that are not required for enzymatic activity[24]. The catalytic domain of $sPLA_2$-GIII has a unique fold and is expected to be similar in structure to one of the first characterized PLA_2's from bee venom[29]. Similarly, save for its catalytic domain, the primary sequences of $sPLA_2$-gXIIA and $sPLA_2$-gXIIB are markedly different from any of the other $sPLA_2$'s. In support of the notion that $sPLA_2$'s may function as ligands for cellular receptors, the $sPLA_2$-gXIIB isoform completely lacks phospholipase activity due to a natural mutation of the normally conserved histidine residue in the active site[30].

With regard to their cellular roles, $sPLA_2$'s may function in secretory vesicles, in the extracellular matrix, or during the re-internalization into neighboring cells. Regulation of $sPLA_2$ activity takes place via transcriptional control, proteolytic processing of pro-enzymes, binding events to their target membranes, and by inhibition and degradation facilitated by specific binding to cell surface proteins[24]. Although cPLA2-α's role in the production of eicosanoids has been firmly established[21a], the role of $sPLA_2$ in this process is less clear. Early evidence for a $sPLA_2$ involvement in the inflammatory processes came from observations of $sPLA_2$-GIIA's accumulation in the synovial fluid of

rheumatoid arthritis patients as well as its increased concentration in the sera of those in sepsis[31]. Although further evidence for $sPLA_2$-GIIA's role in augmenting eicosanoid generation has begun to appear in the literature, most of these studies rely on *in vitro* experiments with either exogenous addition or forceful overexpression of enzyme and thus, caution should be used when interpreting the results. It is interesting to note that of all the $sPLA_2$ isoforms, $sPLA_2$-GV and $sPLA_2$-GX are the most efficient at hydrolyzing membranes enriched in GPC's such as the external leaflets of non-apoptotic cultured cells[32]. This observation is in good agreement with our systematic study described in chapter 7 in which we found that these two enzymes display a relatively high affinity for both anionic and zwitterionic vesicles, whereas the other isoforms display an affinity only for vesicles enriched in anionic GPL's[25]. These observations, coupled with the fact that $sPLA_2$-GV and $sPLA_2$-GX are both highly expressed in immune cells, highlight the potential role of these enzymes in the production of inflammatory mediators. Indeed, a few studies with $sPLA_2$-GV knockout mice and their derived cell lines have noted the $sPLA_2$-GV's role in augmenting cPLA2-α's production of eicosanoids[33]. Perhaps the strongest evidence for an *in vivo* role of a $sPLA_2$ in the production of lipid mediators comes from our recent studies utilizing $sPLA_2$-GX knockout mice in an asthma model[34]. Compared to wild-type mice, the $sPLA_2$-GX knockout mice displayed a dramatic reduction of eicosanoid production and subsequent type 2 T-helper cell mediated responses. The $cPLA_2$-α knockout mice also displayed a dramatic reduction in airway

inflammation, which again highlights the cooperative role that $sPLA_2$ and $cPLA_2$ likely play in eicosanoid production.

Other than their potential involvement in augmenting the release of lipid mediators, a few $sPLA_2$'s have other documented roles in eukaryotic biology. One example of an alternative physiological role is $sPLA_2$-GIB's high expression in pancreatic juice and proposed function in the digestion of dietary GPL's [26]. Furthermore, it has been observed that $sPLA_2$-GIIA as well as a subset of other $sPLA_2$'s can act as potent antimicrobial agents via hydrolysis of the anionic lipids of prokaryotic membranes[35, 36]. Finally, there is also some evidence that $sPLA_2$'s can participate in cell signaling events independent of their enzymatic activity via high-affinity interactions with a set of cellular receptors[24, 37, 38]. Much like their role in eicosanoid production, the specific mechanisms that underlie $sPLA_2$ involvement in these processes are still either actively debated or largely unknown[24].

The $cPLA_2$ Family of Enzymes

The group IV phospholipase A_2 ($cPLA_2$) family is comprised of six intracellular enzymes ranging in size from about 60 to 110 kDa (*Reviewed in* [39]). These enzymes are characterized by a C2 lipid-binding domain linked to an α/β hydrolase domain that utilizes an aspartic acid/serine catalytic dyad as well as another conserved arginine residue in the active site. Although these enzymes are usually described as calcium

dependent, the divalent cation is not required for enzymatic activity as it is for the $sPLA_2$ family. Rather, elevated intracellular calcium concentrations induce conformational changes in the C2 lipid-binding domain, which results in the translocation of the enzyme from the cytosol to various membranes/substrate pools within the cell. Consistent with other lipid acylhydrolases that utilize a serine residue in the active site, $cPLA_2$'s display a variety of distinct enzymatic activities. These include PLA_1, lysophospholipase, and transacylase activities.

Due to its relatively early discovery and established role in the regulation of eicosanoid biosynthesis, $cPLA_2$-α is the most extensively characterized isoform. Thus, features of the other isoforms are commonly discussed in reference to what is known about $cPLA_2$-α. The active site of $cPLA_2$-α has a unique fold that is distinct from most other α/β lipid hydrolases. Specifically, the active site residues sit in a deep cleft at the bottom of a hydrophobic funnel. The entrance to this funnel has a flexible lid attached via a short linker. Although this flexible lid is unique to $cPLA_2$-α, the hydrophobic funnel is relatively conserved across the other $cPLA_2$ isoforms. The lid is thought to play a role in interfacial activation, whereas the subtle differences in the architecture of the hydrophobic cleft are speculated to be the source of cPLA2-α's observed selectivity for AA containing GPL species[40].

The C2 domain of each isoform of $cPLA_2$'s is on the N-terminus and is a β-

sandwich structure (*Reviewed in* [21a]). The exception to this generalization is cPLA$_2$-γ, which lacks a C2 domain entirely, is calcium independent, and instead utilizes an isoprenylation site on its C-terminus as well as a putative myristoylation site on its N-terminus for its membrane associations[41]. Furthermore, the functional splice variant of cPLA$_2$-β expressed in most human tissues contains an additional N-terminal sequence upstream of the C2 domain that contains a truncated Jmjc domain of unknown function[21a]. Alignment of the cPLA$_2$ C2 domains reveals that each domain shares a common fold comprised of an eight-stranded anti-parallel β-sheet. The conserved elements of this β-sheet are three distinct calcium binding loops that play a significant role in governing a particular isoform's interfacial interactions. When in the presence of excess calcium ligand, these loops undergo a conformational change in the distal edge of the domain to expose hydrophobic and aromatic amino acid residues that promote the association of a cPLA$_2$ with specific intracellular membranes. In the case of cPLA$_2$-α, a few amino acid residues in calcium binding loops one and three dictate the enzyme's preference for membranes enriched in GPC substrates[42]. The C2 domains of the cPLA$_2$-β sub-family (cPLA$_2$-β, cPLA$_2$-δ, cPLA$_2$-ε, and cPLA$_2$-ζ) are more homologous to each other (~35-40%) than they are to cPLA$_2$-α (~25%)[21a]. A key difference between the cPLA$_2$-β sub-family and cPLA$_2$-α is the length of the linker that connects the C2 domain to the catalytic domain. The cPLA$_2$-α isoform has a relatively short linker region that is five

amino acid residues in length, whereas each of the other isoforms has a longer linker about 120 residues in length. These longer linker regions represent areas of low homology within the $cPLA_2$-β sub-family[21a]. This variation in linker length may play a role in modulating each enzyme's interfacial interactions. The low homology observed in the various C2 domains and their linker regions implies that each $cPLA_2$ enzyme has distinct membrane targets and thus, distinct functional roles.

In reference to its intracellular regulation, cPLA2-α is constitutively and ubiquitously expressed in most mammalian cells and tissues. However, the isoform may be up-regulated in response to a host of inflammatory stimuli or down-regulated in response to glucocorticoids[43]. Under resting conditions, $cPLA_2$-α resides in the cytosol. Upon cellular activation and the subsequent release of intracellular calcium stores, $cPLA_2$-α translocates to the golgi apparatus, endoplasmic reticulum, and/or perinuclear membrane. Once localized to its target membrane, $cPLA_2$-α undergoes interfacial activation via displacement of the mobile lid near the entrance to the active site's hydrophobic funnel[21a]. It is also at these target membranes that $cPLA_2$-α is functionally coupled with the cyclooxygenase and lipooxygenase enzymes that initiate the eicosanoid signaling pathways[44]. In addition to interfacial activation and functional coupling to oxidative enzymes, there is some evidence that $cPLA_2$-α activity can be stimulated by interacting with lipid second messengers such as phosphatidylinositol-

(4,5)-bisphosphate[45]. The cPLA2-α isoform also contains a few functionally important serine phosphorylation sites that augment its activity during activation of either the mitogen-activated protein kinase or calmodulin kinase signaling cascades[46].

In humans, the genes for the cPLA$_2$-β subfamily, (cPLA$_2$-β, cPLA$_2$-δ, cPLA$_2$-ε, and cPLA$_2$-ζ) are clustered on the same chromosome, whereas the genes for cPLA$_2$-α and cPLA$_2$-γ maintain their own distinct loci. On average, the cPLA$_2$ isoforms retain about 50% sequence identity in their active sites and about 35% identity overall. Although cPLA$_2$-α is the only isoform to possess a known selectivity for GPL's with PUFA's in the *sn-2* position and to maintain a tie to the production of the eicosanoids, the other isoforms might augment lipid mediator production in ways that have yet to be determined.

Chapter 2

Improved Method for the Quantification of Lysophospholipids Including Enol Ether Species by Liquid Chromatography-Tandem Mass Spectrometry

Section 1: Introduction

Detection and quantification of LPL species are important in lipid biology because such species mark the action of lipolytic enzymes such as the PLA_2 family[47] and are themselves ligands for numerous signaling receptors[48]. Combined high pressure LC/ESI-MS/MS is a powerful method to detect and quantify a large number of GPL molecular species in a single analysis[49]. In this study we focus on the use of LC/ESI-MS/MS to detect and quantify an array of LPL molecular species.

Prior to LC/ESI-MS/MS it is often necessary to partially purify the LPL's by some form of liquid-liquid or liquid-solid extraction. Although extraction of biological aqueous samples with chloroform and methanol is useful for many LPL species, including LPG, LPE, LPS, and LPC, the extraction of LPA and LPI are low yielding unless the aqueous phase is acidified[50]. It is also possible to extract LPL's using 1-butanol[50b, 51], but high yield extraction also requires acidification, and 1-butanol is more cumbersome to remove than chloroform and methanol. The problem with acidification during extraction is that plasmenyl-LPL's are rapidly degraded at low pH due to spontaneous cleavage of

their *sn*-1 enol ether chains to give the corresponding *sn*-1 hydroxyl group[52]. This leads to formation of *sn*-2 acyl-LPC and *sn*-2 acyl-LPE and possible other species. These *sn*-2 LPLs behave similarly to the corresponding *sn*-1-acyl LPL's when examined by ESI-MS/MS since they are isobaric and give rise to the same major fragment ions. This acid-catalyzed breakdown leads to an underestimation of the amount of enol ether GPL species and an overestimation of the amount of LPL species. Currently, we describe a simple multi-step extraction procedure that allows for the rapid analysis of LPL and enol ether LPL molecular species using LC/ESI-MS/MS and that avoids the decomposition problems described above. We also carried out an analysis of isobaric LPL species and show that the use of LPL's with perdeuterated fatty acyl chains as internal standards is preferred over the use of those with fatty acyl chains with odd carbon numbers and that LC prior to ESI-MS/MS is required to avoid problems with isobars. We show that LPS species breakdown in the mass spectrometer source to generate LPA species, which underscores the need for LC separation of these species prior to mass spectrometry. Finally, we apply the new method to quantify LPL in serum and in cells expressing or treated with human sPLA$_2$-GX.

Section 2: Methods

Materials

$CHCl_3$ and CH_3OH are from Fisher Scientific (HPLC grade), and n-hexane and isopropanol are from Fisher (Optima grade). Water is purified with a Milli-Q system (Millipore). Phosphate buffer saline without Ca^{2+} and Mg^{2+} is from Gibco (Cat. 14190-144). The following lipids were purchased from Avanti Polar Lipids: 14:0-LPA, 17:0-LPA, 18:1-LPA, 12:0-LPC, 17:0-LPC, egg-LPC, 24:0-LPC, 19:2-enyl-LPC, 14:0-LPE, 16:0-LPE, 17:1-LPE, 18:0-LPE, 19:2-enyl-LPE, 14:0-LPG, 16:0-LPG, 17:1-LPG, 18:0-LPG, liver LPI, 17:1-LPI, 17:1-LPS, brain-LPS, 1-O-1'-(*Z*)-octadecenyl-2-arachidonyl-sn-glycero-3-phosphocholine, and 1-O-1'-(*Z*)-octadecenyl-2-arachidonyl-sn-glycero-3-phosphoethanolamine. 16:0-alkyl-LPC is from BioMol, and d_4-16:0-alkyl-LPC is from Cayman Chemicals.

Deuterated LPL internal standards were prepared as follows. Into a 1.5 mL polypropylene microfuge tube was added 10 μg of each of the following deuterated phospholipids (all from Avanti Polar Lipids) in $CHCl_3/CH_3OH$ (2/1, v/v): 1-d_{31}-palmitoyl-2-palmitoyl-glycero-*sn-3*-phosphoinositol, 1-d_{31}-palmitoyl-2-palmitoyl-glycero-*sn-3*-phospho-(rac)-glycerol; 1-d_{31}-palmitoyl-2-palmitoyl-glycero-*sn-3*-phosphoethanolamine, 1-d_{31}-palmitoyl-2-palmitoyl-glycero-*sn-3*-phosphoserine, and 1-d_{31}-palmitoyl-2-palmitoyl-glycero-*sn-3*-phosphate. $CHCl_3/CH_3OH$ was removed with a stream of N_2. To

the residue was added 50 µL of 10 mM MOPS, pH 7.2, 0.5 mM EGTA, 100 mM KCl, 4 mM $CaCl_2$, and the capped tube was placed in a high-powered bath sonicator for ~30 sec (a microtip probe sonicator can also be used). A stock solution of bee venom phospholipase A_2 (Sigma Cat. P9279, 1020 Units per mg of solid) was prepared at 17.9 Units/µL in the above buffer, and a 2 µL aliquot was added to the phospholipid mixture. The sample was left at room temperature for 3 hours and then placed in a centrifugal evaporator (Speed-Vac) to remove all liquid. The residue was taken up in ethanol and stored at -80 °C in a capped vial. d_{31}-16:0-LPC (Avanti Polar Lipids) and d_4-alkyl-16:0-LPC were added to the internal standard stock solution to give a mixture of all 6 internal standards. It was determined by mass spectrometry that bee venom phospholipase A_2 hydrolyzed GPA acid poorly. Thus, we generated d_{31}-16:0-LPA by treating commercial d_{31}-16:0-LPC with cabbage phospholipase D as described [53] and added it to the internal standard stock solution. To determine the concentration of each deuterated LPL in the stock solution, an aliquot was spiked with known amounts of 16:0-LPA, 16:0-LPE, 16:0-LPG, 16:0-LPI, 16:0-LPS, 16:0-LPC, and alkyl-16:0-LPC (stock solutions calibrated by inorganic phosphorous assay as described above), and the mixture was analyzed by LC-MS/MS as described below. By comparing the peak area for each internal standard to that from the corresponding non-deutrated LPL peak, the amount of each internal standard was obtained. We assumed that the deuterated and the non-deuterated LPL species give the same mass spectrometry peak area per mole, which is not true because

of likely slight differences in the intrinsic ionization efficiencies of these species and because the deuterated species contains a significant amount of d_{30} and d_{29} species (discussed further below), and we select only the d_{31} species in the first quadrupole mass analyzer. However, the factor by which the deuterated and non-deuterated samples differ is not needed since it cancels out of all calculations to derive the absolute moles of LPL analytes in test samples.

Sample Preparation

Stock solutions of phospholipids were made in $CHCl_3/CH_3OH$ (2/1, v/v) and stored at minus 80°C under Argon in Teflon septum-capped glass vials. Concentrations were determined by total phosphorous assay [54]. For convenience, multiple aliquots of LPL's containing 25 pmole of each molecular species were dried down and stored at -80 °C under Argon.

Aqueous samples for LPL analysis were extracted in 16 x 125 mm disposable glass culture tubes, and extraction solvent was transferred with glass Pasteur pipets. Aqueous samples with volumes larger than 1 mL were lyophilized overnight and reconstituted in 1 mL PBS prior to extraction. Cell pellets were thawed on ice in 1 mL PBS. Prior to extraction, each sample was spiked with 10 µL of the internal standard mix. Each 1 mL of PBS was first extracted under neutral conditions with 4 mL of $CHCl_3/CH_3OH$ (2/1, v/v) followed by 2 mL of PBS-saturated $CHCl_3/CH_3OH$ (2/1, v/v). Each extraction step was followed by a 60 sec vortex and a 1 min centrifugation step in a

bench-top clinical centrifuge in a cold room at 4 °C at ~3,000 RPM to resolve the organic and aqueous phases. The lower organic phases from both neutral extraction steps were pooled and dried under a gentle stream of N_2. The remaining aqueous phase was chilled on ice for 10 min and then acidified with ice-cold 0.3 M citric acid solution to pH ~ 3-4 (small aliquot spotted on pH paper, checked on the first 2 samples to determine the volume of citric acid needed per sample thereafter). The sample was then extracted twice with ice-cold PBS-saturated $CHCl_3/CH_3OH$ (2/1, v/v). The sample was vortexed as above, and the organic phases were again resolved by centrifugation. The lower organic phases were pooled and neutralized to pH ~ 6-7 (checked with pH paper as above) with 1% triethylamine in $CHCl_3/CH_3OH$ (2/1, v/v) on ice. The neutralized organic phase from the acidic extraction was combined with the initial neutral fraction and dried under a stream N_2. The resulting residue was reconstituted in 0.5 mL of $CHCl_3/CH_3OH$ (2/1, v/v), and after briefly vortexing, the solution was transferred to the auto-sampler vial (Waters Total Recovery 186000385C). The tube was subsequently rinsed with 250 µL of the same solvent, and this was combined with the initial reconstitution. Solvent was removed with a stream of N_2 and the residue was taken up in 100 µL of initial LC solvent (see below). The vial was caped with a Teflon-Silicone cap (Agilent 5185-5838). The samples were analyzed by LC/ESI-MS/MS or stored at -20 °C under argon.

Analysis of LPL's in serum was carried out with mouse serum from Atlantic Biologicals. 100 µL of serum was extracted as above and analyzed by LC/ESI-MS/MS.

The analysis was repeated with 3 additional 100 µL portions of serum. The growth of HEK293 cells, establishment of cells stably transfected with human $sPLA_2$-GX and treatment of non-transfected cells with exogenous $sPLA_2$-GX were carried out as described [32]. Four million cells were seeded in a 10 cm dish, which was placed in the CO_2 incubator for 48 h at 37°C. Cells were washed with PBS and then washed twice with RPMI-1640 medium without serum. Washed cells were covered with serum-free RPMI-1640 medium with or without recombinant human $sPLA_2$-GX (200 ng/ml) and placed for 4 h at 37°C in the CO_2 incubator. Cells were washed once with PBS and scraped into 1 ml of PBS on ice. The cell suspension was stored at -80°C prior to lipid extraction. Cells stably transfected with human $sPLA_2$-GX were processed in the same way except that exogenous PLA_2 was not added.

Sample Analysis

LC/ESI-MS/MS was carried out on a Waters Quattro triple quadrupole mass spectrometer, a 2795 Alliance HT LC/autosampler system and the QuanLynx software package. Chromatography was carried out with a normal phase column (Phenomenex Luna, 5□□□ silica, 100 Å, 250 x 2.0 mm, Cat 00G-4274-BO) equipped with a guard column (Phenomenex Security Guard Column Cat KJ0-4282) with a column temperature of 30°C. Solvent A is 30/40 (v/v) *n*-hexane/isopropanol, and solvent B is 30/60/15 (v/v/v) *n*-hexane/isopropanol/5 mM ammonium acetate in water. The solvent program is: 0-18 min, 50-86% linear B gradient (0.2 mL/min); 18-22 min, 86% B (0.2 mL/min); 22-25 min,

86-100% linear B gradient (0.2 mL/min); 25-42 min, 100% B (0.2 mL/min). At 42 min, solvent B was stepped to 50%, and the flow rate was stepped to 0.3 mL/min. At 52 min, the flow rate was stepped to 0.2 mL/min. The vials were held at 15 °C in the auto-sampler chamber, and 20 μL injection volumes were utilized. Other injector parameters are given in Table 2.2.

The ESI-MS/MS parameters are given in Table 2.2. Parent and fragment ion *m*/*z* values, cone voltages and collision energies for each analyte are given in Table 2.1.

TABLE 2.1: Extraction yields, liquid chromatography retention times, and tandem mass spectrometry parameters for LPL molecular species.

LPL Species[1]	Extraction Yield (%)[2]	LC Retention Time (min)	Limit of quant. (fmole)[3]	Parent Ion[4]	Fragment Ion[4]	Cone Voltage[5]	Collision Energy[5]
(12:0)-LPG		9.8		-427.22	(-) 199.22	(-) 38	26
(14:0)-LPG	65	9.5	80	-455.25	(-) 227.25	(-) 38	26
(16:1)-LPG		9.3		-481.26	(-) 253.26	(-) 38	26
(16:0)-LPG	93	9.2	120	-483.28	(-) 255.28	(-) 38	26
d_{31}-(16:0)-LPG		9.2		-514.44	(-) 286.44	(-) 38	26
(18:3)-LPG		9.2		-505.25	(-) 277.25	(-) 38	26
(18:2)-LPG		9.1		-507.27	(-) 279.27	(-) 38	26
(18:1)-LPG		9.0		-509.29	(-) 281.29	(-) 38	26
(18:0)-LPG	106	8.9	200	-511.31	(-) 283.31	(-) 38	26
(20:4)-LPG		9.1		-531.25	(-) 303.25	(-) 38	26
(20:3)-LPG		9.0		533.27	(-) 305.27	(-) 38	26
(20:2)-LPG		8.8		-535.29	(-) 307.29	(-) 38	26
(20:1)-LPG		8.7		-537.31	(-) 309.31	(-) 38	26
(20:0)-LPG		8.7		-539.33	(-) 311.33	(-) 38	26
(22:6)-LPG		9.0		-555.24	(-) 327.24	(-) 38	26
(22:5)-LPG		8.9		-557.26	(-) 329.26	(-) 38	26
(22:4)-LPG		8.8		-559.28	(-) 331.28	(-) 38	26
(12:0)-LPI		13.9		-515.12	(-) 199.22	(-) 45	35
(14:0)-LPI		13.5		-543.23	(-) 227.25	(-) 45	35
(16:1)-LPI		13.1		-596.26	(-) 253.26	(-) 45	35
(16:0)-LPI	55	12.9	65	-571.28	(-) 255.28	(-) 45	35
d_{31}-(16:0)-LPI		12.9		-602.44	(-) 286.44	(-) 45	35
(18:3)-LPI		13.0		-593.25	(-) 277.25	(-) 45	35
(18:2)-LPI		12.8		-595.27	(-) 279.27	(-) 45	35
(18:1)-LPI	72	12.6	120	-597.29	(-) 281.29	(-) 45	35
(18:0)-LPI	71	12.4	25	-599.31	(-) 283.31	(-) 45	35
(20:4)-LPI		12.3		-619.26	(-) 303.25	(-) 45	35
(20:3)-LPI		12.2		-621.28	(-) 305.27	(-) 45	35
(20:2)-LPI		11.9		-623.30	(-) 307.29	(-) 45	35
(20:1)-LPI		11.9		-625.32	(-) 309.31	(-) 45	35
(20:0)-LPI		11.7		-627.34	(-) 311.33	(-) 45	35
(22:6)-LPI		12.3		-643.25	(-) 327.24	(-) 45	35
(22:5)-LPI		12.2		-645.27	(-) 329.26	(-) 45	35
(22:4)-LPI		12.0		-647.29	(-) 331.28	(-) 45	35
(12:0)-LPE		15.6		(-) 396.23	(-) 199.22	(-) 32	23
(14:0)-LPE	94	15.2	40	(-) 424.26	(-) 227.25	(-) 32	23
(16:1)-LPE		14.9		(-) 450.27	(-) 253.26	(-) 32	23

LPL Species[1]	Extraction Yield (%)[2]	LC Retention Time (min)	Limit of quant. (fmole)[3]	Parent Ion[4]	Fragment Ion[4]	Cone Voltage[5]	Collision Energy[5]
(16:0)-LPE	95	14.7	60	(-) 452.29	(-) 255.28	(-) 32	23
d_{31}-(16:0)-LPE		14.7		(-) 483.44	(-) 286.44	(-) 32	23
(18:3)-LPE		14.6		(-) 474.26	(-) 277.25	(-) 32	23
(18:2)-LPE		14.4		(-) 476.28	(-) 279.27	(-) 32	23
(18:1)-LPE	80	14.3	60	(-) 478.3	(-) 281.29	(-) 32	23
(18:0)-LPE	85	14.0	50	(-) 480.32	(-) 283.31	(-) 32	23
(20:4)-LPE		13.6		(-) 500.27	(-) 303.25	(-) 32	23
(20:3)-LPE		13.6		(-) 502.29	(-) 305.27	(-) 32	23
(20:2)-LPE		13.9		(-) 504.31	(-) 307.29	(-) 32	23
(20:1)-LPE		13.7		(-) 506.33	(-) 309.31	(-) 32	23
(20:0)-LPE		13.5		(-) 508.35	(-) 311.33	(-) 32	23
(22:6)-LPE		13.6		(-) 524.26	(-) 327.24	(-) 32	23
(22:5)-LPE		13.4		(-) 526.28	(-) 329.26	(-) 32	23
(22:4)-LPE		13.2		(-) 528.3	(-) 331.28	(-) 32	23
(12:0)-LPS		17.4		(-) 440.2	(-) 153.05	(-) 28	30
(14:0)-LPS		17.2		(-) 468.23	(-) 153.05	(-) 28	30
(16:1)-LPS		16.6		(-) 494.26	(-) 153.05	(-) 28	30
(16:0)-LPS	67	16.3		(-) 496.28	(-) 153.05	(-) 28	30
d_{31}-(16:0)-LPS		16.3		(-) 527.44	(-) 153.05	(-) 28	30
(18:3)-LPS		16.3		(-) 518.25	(-) 153.05	(-) 28	30
(18:2)-LPS		16.1		(-) 520.27	(-) 153.05	(-) 28	30
(18:1)-LPS	77	15.9		(-) 522.29	(-) 153.05	(-) 28	30
(18:0)-LPS		15.6	180	(-) 524.31	(-) 153.05	(-) 28	30
(20:4)-LPS	82	15.9		(-) 544.26	(-) 153.05	(-) 28	30
(20:3)-LPS	83	15.7		(-) 546.28	(-) 153.05	(-) 28	30
(20:2)-LPS	98	15.7		(-) 548.3	(-) 153.05	(-) 28	30
(20:1)-LPS		16.2		(-) 550.32	(-) 153.05	(-) 28	30
(20:0)-LPS		15.6		(-) 552.34	(-) 153.05	(-) 28	30
(22:6)-LPS		15.8		(-) 568.25	(-) 153.05	(-) 28	30
(22:5)-LPS		15.6		(-) 570.27	(-) 153.05	(-) 28	30
(22:4)-LPS		15.4		(-) 572.29	(-) 153.05	(-) 28	30
(12:0)-LPA		22.8		(-) 353.22	(-) 153.05	(-) 28	20
(14:0)-LPA	96	22.2	300	(-) 381.25	(-) 153.05	(-) 28	20
(16:1)-LPA		22.0		(-) 407.26	(-) 153.05	(-) 28	20
(16:0)-LPA		21.6		(-) 409.28	(-) 153.05	(-) 28	20
d_{31}-(16:0)-LPA		21.6		(-) 440.44	(-) 153.05	(-) 28	20
(18:3)-LPA		21.9		(-) 431.25	(-) 153.05	(-) 28	20
(18:2)-LPA		21.6		(-) 433.27	(-) 153.05	(-) 28	20
(18:1)-LPA		21.2	250	(-) 435.29	(-) 153.05	(-) 28	20
(18:0)-LPA		20.9		(-) 437.31	(-) 153.05	(-) 28	20
(20:4)-LPA		21.2		(-) 457.26	(-) 153.05	(-) 28	20
(20:3)-LPA		21.2		(-) 459.28	(-) 153.05	(-) 28	20
(20:2)-LPA		21.0		(-) 461.3	(-) 153.05	(-) 28	20
(20:1)-LPA		20.5		(-) 463.32	(-) 153.05	(-) 28	20
(20:0)-LPA		20.2		(-) 465.34	(-) 153.05	(-) 28	20
(22:6)-LPA		21.2		(-) 481.25	(-) 153.05	(-) 28	20
(22:5)-LPA		21.2		(-) 483.27	(-) 153.05	(-) 28	20
(22:4)-LPA		20.9		(-) 485.29	(-) 153.05	(-) 28	20
(12:0)-LPC	137	37.5	20	(+) 440.27	(+) 184.15	(+) 35	30
(14:0)-LPC	109	35.8		(+) 468.30	(+) 184.15	(+) 35	30
(16:1)-LPC	105	35.1		(+) 494.31	(+) 184.15	(+) 35	30
(16:0)-LPC	98	34.4	20	(+) 496.33	(+) 184.15	(+) 35	30
d_{31}-(16:0)-LPC		34.4		(+) 527.49	(+) 184.15	(+) 35	30
(18:3)-LPC		34.8		(+) 518.30	(+) 184.15	(+) 35	30
(18:2)-LPC		34.4		(+) 520.32	(+) 184.15	(+) 35	30
(18:1)-LPC	106	33.8		(+) 522.34	(+) 184.15	(+) 35	30
(18:0)-LPC	102	33.0	14	(+) 524.36	(+) 184.15	(+) 35	30
(20:4)-LPC		33.0		(+) 544.32	(+) 184.15	(+) 35	30
(20:3)-LPC		33.4		(+) 546.33	(+) 184.15	(+) 35	30
(20:2)-LPC	87	32.9		(+) 548.35	(+) 184.15	(+) 35	30
(20:1)-LPC	91	32.4		(+) 550.37	(+) 184.15	(+) 35	30
(20:0)-LPC	107	31.6		(+) 552.39	(+) 184.15	(+) 35	30
(22:6)-LPC		33.7		(+) 568.34	(+) 184.15	(+) 35	30
(22:5)-LPC		32.7		(+) 570.36	(+) 184.15	(+) 35	30
(22:4)-LPC		31.7		(+) 572.38	(+) 184.15	(+) 35	30
(24:0)-LPC	89	29.3		(+) 608.45	(+) 184.15	(+) 35	30

LPL Species[1]	Extraction Yield (%)[2]	LC Retention Time (min)	Limit of quant. (fmole)[3]	Parent Ion[4]	Fragment Ion[4]	Cone Voltage[5]	Collision Energy[5]
(16:1)-PlasLPE		13.2	1200	(-) 436.21	(-) 196.12	(-) 52	29
(18:2)-PlasLPE	89	12.9		(-) 462.22	(-) 196.12	(-) 52	29
(18:1)-PlasLPE	84	12.6	1400	(-) 464.24	(-) 196.12	(-) 52	29
(16:1)-PlasLPC		32.2		(+) 480.30	(+) 181.12	(+) 45	31
(18:2)-PlasLPC	105	32.0		(+) 506.31	(+) 181.12	(+) 45	31
(18:1)-PlasLPC		30.8		(+) 508.33	(+) 181.12	(+) 45	31
(16:0)-LysoPAF	68	34.0		(+) 482.28	(+) 184.15	(+) 37	30
d4-(16:0)-LysoPAF		34.0		(+) 486.41	(+) 184.15	(+) 37	30
(18:1)-LysoPAF		33.4		(+) 508.4	(+) 184.15	(+) 37	30
(18:0)-LysoPAF		33.7		(+) 510.41	(+) 184.15	(+) 37	30

[1]The internal standard used for enol ether LPE and LPC species are d_{31}-16:0-LPE and d_{31}-16:0-LPC, respectively (see Main Text). Other internal standards are as indicated.
[2]Extraction yields were determined only for a subset of LPL's as indicated.
[3]Limit of quantification is defined as a signal-to-noise ratio of ~10/1, as measured with the Waters QuanLynx software. Values are given only for those LPL species which were prepared as standardized stock solutions.
[4]*m*/*z* Values listed were derived from instrument tuning using a set of commercially available LPL standards (see Main Text for the list). Values for other species were obtained by subtracting or adding the appropriate exact atomic masses. Exact *m*/*z* values will vary in an instrument-dependent manner.
[5]Cone voltages and collision energies were optimized for each commercially available LPL (see Main Text for the list). We used the same values across the set of molecular species in each LPL head group class. Values were derived from instrument tuning and are instrument dependent.

Analysis of Isobars

To look for isobaric species, we considered the masses of a general set of LPL's that contain either a fatty acyl *sn*-1 chain or an ether linked *sn*-1 chain (both enol ether and alkyl ether). Polar head groups included were GPA, GPC, GPE, GPG, GPI, and GPS. We considered acyl and alkyl *sn*-1 chains 12:0, 14:0, 16:0, d_{31}-16:0, 16:1,18:0, 18:1, 18:2, 18:3, 20:0, 20:1, 20:2, 20:3, 20:4, 22:4, 22:5, and 22:6. As a first step, we ignored isobars due to different positions of the double bonds in the fatty chain. We considered all LPL's that are analyzed in negative mode (LPA, LPE, LPG, LPI, and LPS) as one group, and positive mode analytes (LPC) as a second group. Isobars between these two groups are not considered to cause an issue because of the different charge polarity used to

analyze ions in negative mode and in positive mode and because it is highly likely that the LC step will lead to separation of all LPC species from all other LPL species (the group of LPC species are well separated from the group of LPA species). For each of the above LPL's we also analyzed the ion mass + 1 since natural heavy isotopic substitution results in a satellite peak whose intensity is about 30% of the mono-isotopic peak (lacking heavy isotopes). We also considered the ion mass –1, -2, and +2 to account for the isotope distribution for the d_{31}-16:0 internal standard for each head group. Thus, the number of negative mode masses considered is 360 (17 fatty chains x 5 polar head groups = 85 *sn*-1-acyl LPL's plus 16 fatty chains (all but d_{31}-16:0) x 5 polar head groups = 80 *sn*-1-ether LPL's gives 165 species, which gives 330 species after consideration of the ion mass + 1 ions). We also considered 6 LPL's with the *sn*-1 fatty acyl chains 17:0 and 17:1 since these are commonly used commercially available internal standards (17:1-LPG, 17:1-LPI, 19:2-enyl-LPE, 17:1-LPE, 17:1-LPS, 17:0-LPA). As a second independent analysis, we considered 74 positive mode masses (all of negative mode masses plus 24:0). Thus, we considered a total of 440 LPL masses. Table 2.3 lists all isobars derived from the set of 360 masses for negative mode LPL's (LPA, LPE, LPG, LPI, and LPS).

Section 3: Results and Discussion

Extraction of LPL's.

The method that we developed involves extraction of the pH neutral aqueous

biological sample with $CHCl_3/CH_3OH$ (2/1), which is expected to extract all LPL's except LPA and LPI. The use of neutral pH conditions avoids spontaneous loss of species that contain the highly acid sensitive *sn-1* enol ether. To extract LPA and LPI species, the remaining aqueous phase was acidified on ice, and the mixture was extracted again with $CHCl_3/CH_3OH$ (2/1). Ice was used to minimize acid decomposition of any enol ether species that were not extracted in first round. The organic layer was neutralized with triethylamine before it was combined with the first organic phase, again to avoid loss of enol ether species. The use of triethylamine avoids any possible transacylation reactions that might occur had a primary amine been used. The pH varies from 7.4 (phosphate buffered saline) to 3-4 (after citrate addition) to 6-7 (after triethylamine addition). A previous study of spontaneous migration of fatty acyl chains between the *sn*-1- and *sn*-2 position of LPC showed that the rate is pH dependent with a half-life at pH 7.4 of ~6 hrs and at pH 3 of ~90 hrs at room temperature[55]. Thus, during the above extraction procedure, acyl chain migration should be minimal.

By applying the above extraction procedure to a standard mix of LPL's and comparing the ESI-MS/MS peak areas of the species detected in the extracted sample versus those from a standard stock solution of LPL's that were directly injected on to the LC column without extraction, we determined the percent recovery values for several LPL species (Table 2.2). The yields were acceptable, the lowest being 55% for 16:0-LPI. In previous work, 1-butanol has been used together with acidification of the aqueous

sample medium to ensure high yield recovery of LPA species[50b, 51]. If we extracted the sample with 1-butanol without acidification of the aqueous phase, yields of LPA species were very low (~10%) as were yields of LPI (~20%). If $CHCl_3/CH_3OH$ (2/1, v/v) was used in the absence of acidification, yields of LPA species were ~5%. In another study, $CHCl_3/CH_3OH$ was used as the extraction solvent in the absence of acidification[56], but we could not reproduce the yields of LPA that were reported in that study. We prefer the use of $CHCl_3/CH_3OH$ versus 1-butanol since the former is easier to remove by evaporation. We also the stress the need to acidify the aqueous phase to ensure high yield extraction of LPA and LPI species.

To examine whether the new extraction procedure leaves plasmenyl phospholipids intact, we subjected a mixture of plasmenyl-GPC and plasmenyl-GPE to the extraction procedure and analyzed the sample by LC/ESI-MSMS. When 100 pmole of 1-*O*-1'-(*Z*)-octadecenyl-2-arachidonyl-*sn*-glycero-3-PC and 100 pmole of 1-*O*-1'-(*Z*)-octadecenyl-2-arachidonyl-*sn*-glycero-3-PE were added to phosphate buffered saline and submitted to the extraction procedure given in Methods, the amount of 20:4-LPC and 20:4-LPE detected by LC/ESI-MS/MS corresponded to 1.6 % and 0.6 %, respectively of the plasmenyl phospholipids present. When 100 pmoles of plasmenyl GPL's were analyzed by LC/ESI-MS/MS without sample processing, the amount of 20:4-LPC and 20:4-LPE were 0.02 % and 0.1 %, respectively, of the plasmenyl species. Thus, the extraction procedure leads to a small amount of plasmenyl phospholipid breakdown.

However, the amount of breakdown is very small compared to that which occurs if the aqueous sample of plasmenyl phospholipids is acidified with citric acid and then extracted with $CHCl_3/CH_3OH$. This latter procedure results in breakdown of 38% of the plasmenyl GPC and 10% of the plasmenyl GPE. We also tested the extraction procedure given by the Lipid Maps consortium[56], which involves quenching the lipid residue with ice-cold 1:1 CH_3OH/0.1 N aqueous HCl (0.8 mL) plus $CHCl_3$ (0.4 mL). This resulted in 4 % and 2% breakdown of the plasmenyl GPC and plasmenyl GPE, respectively. Thus, acidification leaves the plasmenyl species mainly intact when the extraction is done with cold solvents, but use of the procedure described in Methods is superior if LPL's are to be analyzed. The use of acidification with 1-butanol extraction[50b, 51] is problematic for analysis of LPL species as well. If LPA and LPI species are the only ones analyzed, acid catalyzed breakdown would be a problem if the sample contains enol ether GPA and GPI species. If LPC and LPE species are analyzed, acid catalyzed breakdown is a major problem since most cell membranes containing a relatively large amount of plasmenyl-GPC and plasmenyl-GPE species.

General features of the LC/ESI-MS/MS analysis.

All LPL's except LPC, plasmenyl-LPC and plasmanyl-LPC species were analyzed in negative ion mode. In the case of LPE, LPG and LPI species, the major anionic fragment detected after collision induced dissociation is the fatty acid carboxylate chain[49], and this was used for detection. For LPA species, the major fragment is due to loss of the *sn*-

1 fatty acyl chain followed by attack of the *sn*-1 hydroxyl to form the the cyclic-phosphate mono anion (*m*/*z* = -153)[49], and this was used for analyte detection. For LPS species, serine is lost from the phosphate to give the LPA intermediate, which then converts to the same cyclic phosphate with a *m*/*z* = -153. For plasmenyl-LPE species, we detected the fragment at *m*/*z* = -196, presumably due to cleavage of the enol ether and formation of the phosphate diester mono anion (*analogous to Figure 7 of* [57]). For plasmenyl-LPC species, we detected the *m*/*z* =+181 fragment ion due to formation of a phosphate di-ester mono cation (*see Figure 7 of* [57]). Lastly, for LPC and plasmanyl-LPC species, we detected *m*/*z*=+184 fragment ion due to formation of the phosphocholine cation[49].

We developed a simple procedure to prepare all of the deuterated internal standard LPLs using commercially available reagents. We used a separate internal standard for each LPL head group class. For example, we used d_{31}-16:0-LPC as the internal standard to quantify all fatty acyl LPC species, and we assumed that all fatty acyl LPC species ionize with the same efficiency in the mass spectrometer source (however, see below). It is simply not practical to have an internal standard for each of the 116 LPL species analyzed by LC/ESI-MS/MS in this study. We obtained standard curves for all of the commercially available LPLs used in this study (see Figure 2.5). A linear response was obtained for all species in the 50-1000 fmole range. This suggests that aggregation of LPLs during LC does not occur. In the case of commercial LPC species we obtained data

for 12:0-LPC, 16:0-LPC, 18:1-LPC and 24:0-LPC. The relative peak areas of the ion trace peaks are as follows: 12:0-LPC (1.0), 16:0-LPC (1.0), 18:1-LPC (1.0), 24:0-LPC (3.0). For LPG, LPI, LPE and LPS, the relative areas vary by less than 1.3-fold in going from 14:0-18:1. For LPA species, the relative areas are: 14:0-LPA (1.0), 16:0-LPA (0.37), 18:1-LPA (0.27). Since we did not correct the ESI-MS/MS responses for the variation of ionization efficiency with fatty acyl chain length, the absolute values of the amounts of LPL's reported in this study may be off by as much as ~3-fold. However, in our study of group X $sPLA_2$-induced LPL generation described below, it is the relative change in analyte levels that we are most interested in (i.e. the fold-increase in LPL levels when the PLA_2 is added to cells or comparing non-transfected to PLA_2-transfected cells). Relative quantification of LPL's is not influenced by fatty acyl chain dependence on ESI-MS/MS ionization efficiencies.

We assumed that each fatty acyl LPC species fragmented to the same extent, which should be valid since the fragment ion chosen is the major ion after collision induced dissociation. For quantification of enol ether LPC species, we injected a standard amount of 19:2-plasmenyl-LPC and 16:0-LPC to obtain the relative integrals of the fragment ion traces after LC/ESI-MS/MS analysis. This factor was then used to quantify all enol ether LPC species based on the signal for d_{31}-16:0-LPC. We used d_4-16:0-plasmanyl-LPC as the internal standard to quantify alkyl ether LPC species. Likewise, for LPE, we used d_{31}-16:0-LPE to quantify all fatty acyl LPE species, and we

analyzed a standard amount of 19:2-plasmenyl-LPE and 16:0-LPE to obtain the relative detection signals. We made no attempt to quantify alkyl ether LPE species or enol ether and alkyl ether species of LPA, LPG, LPI and LPS. Accurate quantification of these species would require ESI-MS/MS analysis of stock solutions of appropriate LPL standards of known concentration. Table 2.2 also gives the optimized ESI-MS/MS conditions (cone voltage and collision energy) for several LPL species. Cone voltages and collision energies were optimized for 1-2 LPL species representative of each head group class, and we used the same conditions for each member of each class. According to the User Manual for the Waters Quattro mass spectrometer, the optimal cone voltage is generally higher as the molecular weight of the analyte increases. In the case of LPC species, the optimal cone voltage for 12:0-LPC was found to be +30 V, and it was +35 V for 24:0-LPC. The analyte signal versus cone voltage peaks are fairly broad; the use of +30 V for all LPC species reduces detection sensitivity only by ~5% in the worst case. The same trends are seen for other LPL head group species. This justifies our use of a single cone voltage for each LPL head group class.

We found that LPS species undergo in-source conversion to the corresponding LPA species (data not shown). The amount of this decomposition depends on the ESI source conditions. As noted above the pathway for collision induced fragmentation of LPS involves first conversion to LPA as an intermediate. This in-source LPS to LPA conversion underscores the need to resolve LPA and LPS species by LC prior to ESI-

MS/MS.

To look for isobaric species, we carefully considered the masses of a general set of LPL's that contain either a fatty acyl *sn*-1 chain or an ether linked *sn*-1 chain (both enol ether and alkyl ether). LPL species included were LPA, LPC, LPE, LPG, LPI, and LPS. We considered acyl and ether *sn*-1 chains 12:0, 14:0, 16:0, 16:1, 18:0, 18:1, 18:2, 18:3, 20:0, 20:1, 20:2, 20:3, 20:4, 22:4, 22:5, and 22:6 (and 24:0 for LPC only). We also considered fatty chains with an odd number of carbons (17:0, 17:1 and 19:2) since commercially available LPL's with these chains are often used as internal standards in earlier studies. Table 2.3 lists all isobars along with a statement about whether an unambiguous identification of the LPL species can be made. Several general points emerge. Within each polar head group LPL class, there are no isobars other than double bond positional isomers as long as the deuterated internal standards described in this study are used. On the other hand, use of the commercially available internal standards with an *sn-1* chain containing an odd number of carbons[50b] is not advised. For example, 17:0-LPC is isobaric with 18:0-alkyl-LPC, and 17:1-LPC is isobaric with 18:1-alkyl-LPC. It is not known *a priori* whether all of these isobaric species resolve by LC. Likewise 19:2-enyl-LPC and 19:2-enyl-LPE were not used as internal standards. The isobaric problem with the use of odd carbon fatty acyl LPLs is eliminated by the use of the d_{31}-LPL internal standards. A potential problem with the latter is that they are not completely deuterated and thus they give rise to an envelope of isotopic species. ESI-MS analysis of

the d_{31}-internal standards used in this study showed that the d_{30}/d_{31} ratio is ~1, the d_{29}/d_{31} ratio is ~0.3, and the d_{28}/d_{31} ratio is ~0.05. For this reason, we also included in our isobar analysis the d_{30} and d_{29} species for all of the internal standards. No additional isobar problems arise from these species (Table 2.3). It should be noted that if the amount of internal standard used is in vast excess over the analyte being quantified that isobar problems from partially deuterated species of d_{28} or less may arise if the two LPL's in question are not resolved by LC.

Thus, caution is advised, and it is recommended to use amounts of internal standards that are not orders of magnitude greater than the amounts of analytes being quantified. All things considered, the use of perdeuterated internal standards is preferred over those with odd carbon fatty acyl chains.

Several other points emerge. Many of the isobaric issues are resolved by the use of LC preceding mass spectrometry. Thus, LPL analysis by direct infusion of the sample into the mass spectrometer is not recommended (also because of the LPS to LPA conversion as noted above). The use of MS/MS rather than MS helps to resolve isobaric species, but the number of such resolutions is small compared to those resolved by LC. The main advantage of MS/MS over MS is to improve signal-to-noise and to distinguish LPL's from non-LPL isobaric species that may be present in the sample.

Some trends in the LC retention time of LPL were also noted. For fatty acyl LPL's, long chain species elute earlier than short chain species, and the presence of double

bonds tends to delay the chromatographic elution. For LPE and LPC species the plasmenyls elute prior to the fatty acyl LPL species with the same carbon chain number and number of double bonds (*i.e.* 18:2-plasmenyl-LPC elutes before 18:2-LPC). Comparable data for other head group LPL's was not obtained. On the other hand, the plasmanyl-LPC species tend to co-migrate with the fatty acyl LPC species with the same carbon chain number. Although we did not obtain comparable data for plasmeyl and fatty acyl LPL's with non-choline head groups, we did observed that a 16:0-plasmanyl-LPA standard co-migrated with 16:0-LPA standard. We used these LC trends to make predictions on which isobaric species can be resolved.

Of the 360 LPL masses considered, there are 182 isobars, 10 of which are unlikely to be resolved by LC or by MS/MS. Thus, the vast majority of isobaric issues are resolved by the methods described in this paper. As already noted, the above analysis treats double bond regioisomers as single species. The most convincing way to distinguish an isobaric LPL pair in which one species has a double bond as an enol ether from the other species which does not have an enol ether is to treat the sample under acidic conditions and to look for the loss of the LC/ESI-MSMS signal compared to the sample that was processed in the absence of acid. The other method, which is shown in this study to be reliable for LPE and LPC species, is to rely on the earlier LC retention time for the enol ether species (as noted above). In the case of other double bond regioisomers, for

example a LPL containing a γ-linolenoyl chain ($\Delta^{6,9,12}$-18:3) versus an α-linolenoyl chain ($\Delta^{9,12,15}$-18:3), the methods presented here will likely not allow a distinction.

LC/ESI-MSMS analysis of LPL mixtures.

Figure 2.1 shows an LC/ESI-MS/MS analysis of the standard test mixture of commercially available LPL species. Limit of quantification (defined as a signal peak height-to-noise height of ~10/1) values are given in Table 2.2 and are in the range of ~20 fmole for LPC species and ~1000 fmole for enyl-LPE species. We found that it is important to include 5 mM ammonium acetate in the LC mobile phase as the use of lower concentrations leads to significant LC peak tailing for LPA and LPS species (not shown). Note that the LPA and LPS peaks have similar peak shape as those for other LPL species (Figure 4). Results with 10 mM ammonium acetate were similar to those with 5 mM (not shown).

In the analysis of LPL species reported here we cycled through 89 SRM events during the entire period of time in which the instrument was in negative mode. We

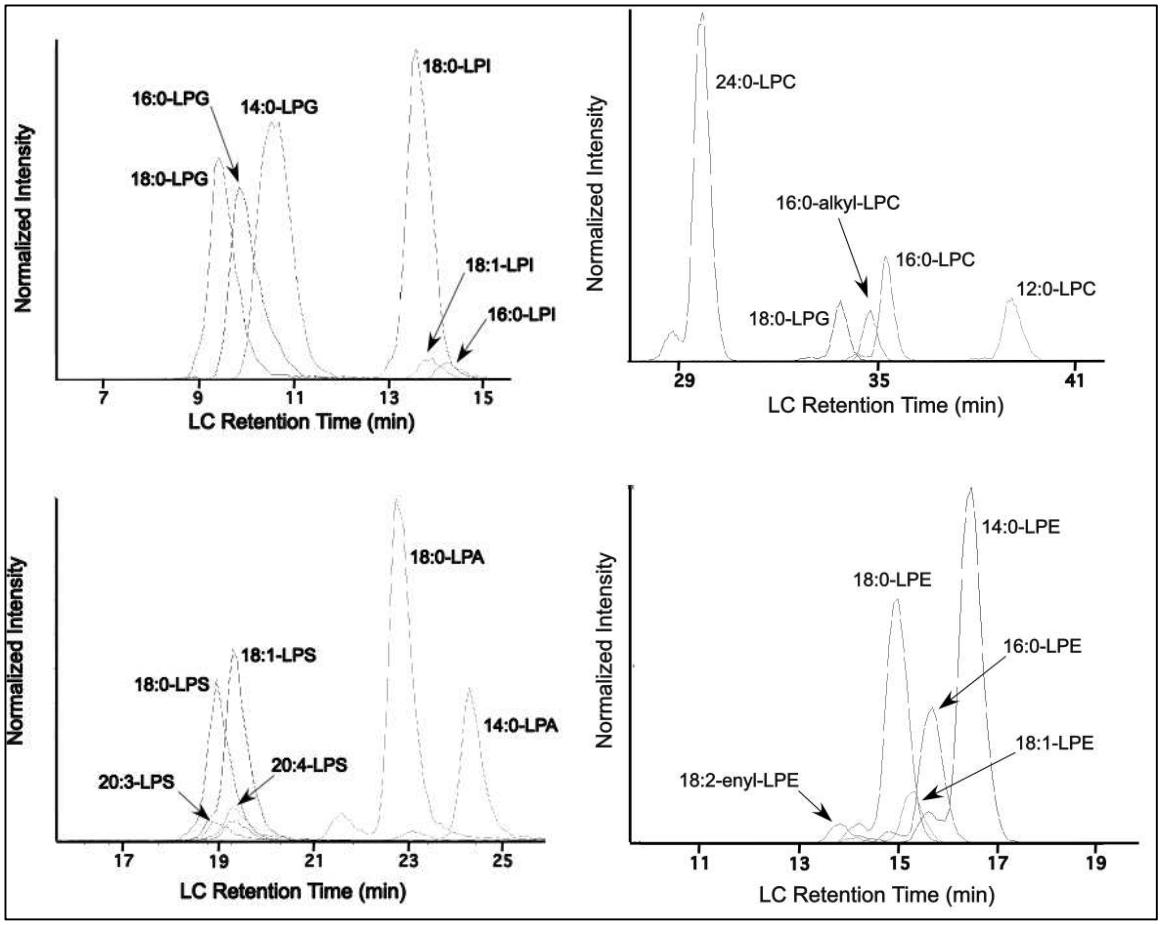


FIGURE 2.1: LC/ESI-MSMS detection of a standard mixture of LPL's. The top left trace shows negative mode detection of 14:0-LPG (9.4 pmole), 16:0-LPG (6.1 pmole), 18:0-LPG (6.4 pmole), 16:0-LPI (0.4 pmole), 18:1-LPI (0.55 pmole), and 18:0-LPI (7.9 pmole). The bottom left panel shows negative mode detection of 18:0-LPA (7.9 pmole), 14:0-LPA (3.2 pmole), 20:3-LPS (0.5 pmole), 20:4-LPA (0.5 pmole), 18:0-LPS (3.7 pmole) and 18:1-LPS (4.4 pmole). The top right panel shows positive mode detection of 24:0-LPC (1.5 pmole), 18:0-LPC (0.2 pmole), 16:0-LPC (0.4 pmole), 12:0-LPC (0.3 pmole), and 16:0-alkyl-LPC (1.0 pmole). The bottom right panel shows negative mode detection of 18:0-LPE (3.8 pmole), 18:1-LPE (0.8 pmole), 16:0-LPE (2.2 pmole), 14:0-LPE (5.8 pmole), and 18:2-enyl-LPE (2.1 pmole). The X-axis is the LC retention time (min) and the Y-axis is the ion intensities normalized to the largest peak in the group.

compared the LPL detection sensitivity under these conditions to that observed under conditions where we monitored a smaller set of single ion reactions in time windows appropriate for the elution of each LPL head group class. Results were comparable under both conditions (not shown). This is expected since each cycle of 89 ion reactions

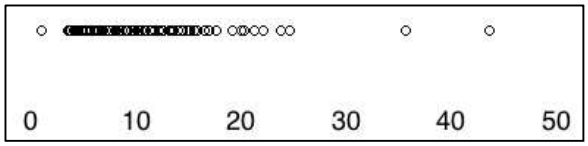


FIGURE 2.2: Distribution of coefficient of variances (CV's) for the analysis of LPL's in mouse serum. For each of the 80 LPL species listed in Table 2.4, we calculated the CV among the 4 runs (100 x (standard deviation/mean)). The CV's are displayed along the X-axis. It can be seen that most of the values are < 20%.

takes ~5 sec, and given the LC peak widths of about 1 min (Figure 2.1), there are about 12 cycles per LC peak, which is presumably sufficient to well define the peak.

We analyzed the LPL species present in mouse serum mainly to determine statistics for the quantification of LPL's using our LC/ESI-MS/MS method. Among the full set of LPL's analyzed by LC/ESI-MS/MS (116 species, see Table 2.2) 80 gave discernable peaks in the selective ion trace chromatograms (by visual inspection) and were quantified with the aid of the perdeuterated internal standards (Figure 2.4, Table 2.4). The method was carried out on four 100 μL aliquots of the same batch of mouse serum. The coefficient of variation (100 x (standard deviation/mean) were all < 20% except 5 species were in the 20-25% range, 1 was 35% and 1 was 43%. The distribution of coefficients of variation is shown as Figure 2.2. Thus, the LC/ESI-MS/MS method is highly reproducible. Also highly reproducible among the 4 runs are the LC retention times for the 80 detected LPL species (Table 2.2). The concentration of the various LPL classes in mouse serum are as follows: total LPG, 0.05 μM; total LPI, 2.5 μM; total LPE 1.1 μM; total LPS, 0.13 μM; total LPA, 5.7 μM; total LPC, 66 μM; total enyl-LPE, 0.33 μM; total enyl-LPC, 0.50 μM; total alkyl-LPC, 3.2 μM. Previously reported values for serum LPL concentrations include: 2 μM for LPA[58] and 200 μM for LPC[59].

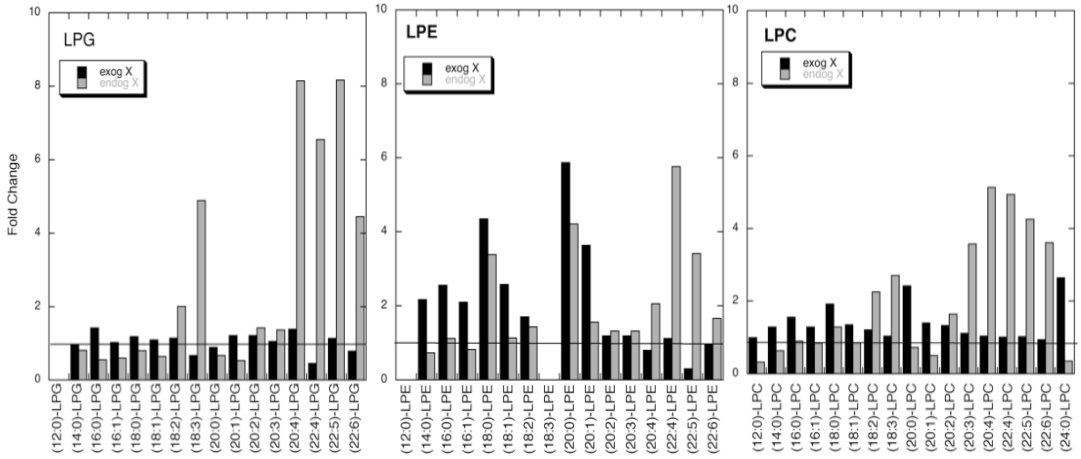


FIGURE 2.3: LPL molecular species changes in HEK293 cells in response to group X sPLA2 action. Results are shown for LPG (panel A), LPE (panel B) and LPC (panel C) species. Data for all LPL species are given in Table 2.5. Black bars give the ratio of LPL species indicated on the X-axis) measured in HEK293 cells treated exogenously for 4 hrs at 37 °C with 200 ng/mL $sPLA_2$-GX to the amount of LPL measured HEK293 cells cultured for 4 hrs at 37 °C in the absence of the PLA_2. Grey bars give the ratio of LPL species measured in HEK293 cells stably expressing $sPLA_2$-GX after culturing for 4 at 37 °C to the amount of LPL measured in non-transfected HEK293 cells after culturing for 4 hrs at 37 °C. Each LC/ESI-MS/MS analysis was carried out using one 10 cm dish of cells.

We analyzed the changes in LPL levels in HEK293 cells in response to exogenous addition of mature human $sPLA_2$–GX or in cells stably transfected with the human $sPLA_2$–GX gene (endogenously expressed enzyme). Complete results are listed in Table 2.5. Relatively large changes were seen in the levels of LPG, LPE and LPC species, and these are shown in Figure 2.3. Smaller changes in LPL levels were seen for the other head group species. In the case of LPG, only small changes were seen after treating cells with exogenously added PLA_2, but transfected cells displayed relatively large changes in a subset of LPG species (18:3-, 20:4-, 22:4-, 22:5- and 22:6-LPG) (Figure 2.3, Panel 1). Both exogenous and endogenous PLA_2 led to significant increases in specific LPE species, but the species produced were different depending on the presentation of the enzyme

(Figure 2.3, Panel 2). In particular, 22:4-, 22:5-, and 22:6-LPE species were produced only by endogenous PLA_2. LPC levels showed a similar trend as for LPE levels (Figure 2.3, Panel 3). A significant increase in 24:0-LPC was seen only with exogenous $sPLA_2$ addition (Figure 2.3, Panel 3). These data clearly show that exogenous and endogenous human $sPLA_2$–GX act at different membrane sites. This in turn is consistent with a wealth of data from our earlier study showing that endogenously produced group X enzyme acts on membranes of the secretory compartment prior to externalization from cells, whereas exogenously added enzyme likely acts on the extracellular face of the plasma membrane[32].

Section 4: Summary

We developed an improved sample extraction procedure that best prevents the acid-catalyzed breakdown of enol ether containing GPL's and LPL's compared with previously reported methods. The new method also results in high recovery of the major types of LPL species including LPA and LPI, which are generally more difficult to isolate than the more hydrophobic species. Breakdown of even 5–10% of the plasmenyl GPL's is a significant problem if one is trying to assess the presence of LPL's in a sample, as LPL's are in relatively low abundance compared with plasmenyl GPL's. It should also be pointed out that the new extraction method does result in a low level of plasmenyl GPL breakdown, thus, LPL analysis is best carried out by looking at a relative change in molecular species level as a result of a biological stimulus rather than looking

at absolute levels in a single sample. Still, relative changes in LPL's will be hard to spot if there is significant breakdown of plasmenyl GPL species; thus, the new extraction procedure is recommended in all studies of LPL abundance when using biological membranes that contain plasmenyl GPL's. Analysis of LPL's by the LC/ESI-MS/MS method described here allows for the detection of 20–1000 fmoles of molecular species using an instrument manufactured about a decade ago. With use of more updated instruments, it should be possible to extend the limit of quantification by a factor of five to ten fold. Finally, we analyzed isobaric species of *sn-1* ester and ether LPL's and showed that the use of internal standards with fatty chains with odd carbon number, i.e., 17:0 or 17:1 chains is problematic and the use of d_{31} -16:0 LPL internal standards is preferred. Also, LC is needed along with ESI-MS/MS to detect all the *sn*-1 ester and ether LPL's with a high degree of confidence of species identification. The new method was used to quantify LPL's present in mouse serum with acceptable inter-sample reproducibility. Finally, the method was used to illustrate that human sPLA$_2$-GX added exogenously to HEK293 cells acts on a different membrane site than cells expressing endogenous sPLA$_2$-GX within the cell.

TABLE 2.2: Autosampler (2795 Alliance HT LC) and ESI-MS/MS (Waters Quattro Micro) data collection parameters.

Injection type	Sequential	
Fill mode	Partial loop	
Pre-sample airy boundary	2 μL	
Post-sample air boundary	2 μL	
Post-injection wash frequency	10 cycles	
Flush time	6 sec	
Wash time	15 sec	
Secondary wash volume	600 μL	
	Negative Mode	**Positive Mode**
Capillary Voltage (kV)	(-) 2.8	(+) 3.0
Extractor (V)	3	3
RF Offset	0.3	0.3
Dwell Time (msec)	40	100
Inter-Scan Delay (msec)	10	10
Inter-Channel Delay (msec)	100	100
Source Temp (^{o}C)	130	130
Desolvation Temp (^{o}C)	450	450
Desolvation Gas (L/Hr)	1100	1100
Cone Gas (L/Hr)	25	25
Collision Cell Entrance (V)	-1	-1
Collision Cell Exit (V)	1	1

TABLE 2.3: Isobar analysis of LPA, LPE, LPG, LPI and LPS species

The table is organized as follows. The first column gives the mass at which isobaric LPL species exists. For all LPL's except the perdeuterated species we considered its parent ion mass as well as the carbon-13 satelite (M+1). For the d31-internal standards we considered the parent ion mass (d31) and the partially deuterated species (d30 and d29) as well as the carbon-13 satelite (M+1) and the additional species M+2. For example, when the [M-1] mass equals the isobaric mass, this LPL species appears in column 3. The "e" in e12:0-LPE designates and *sn*-1 ether linked fatty chain, which includes alkyl and enol ethers. We use a single designation for ethers since this table does not make a distinction between double bond regioisomers. For example, e18:1-LPC could have an enol ether or an alkyl chain with the double more distant from the ether oxygen. Analysis of LPC isobars shows that aside from double bond regioisomers, there are no isobars as long as d31-16:0-LPC and d4-alkyl-16:0-LPC are used as internal standards. If LPC species with odd carbon number fatty acyl chains are used, isobars between multiple LPC species exist. This is of course true for any particular head group; the isobars listed in Table 2.3 are between two LPL's that have different polar head groups. As already noted, all LPC species elute well after the region of LPA elution, and other head group species elute earlier than LPA species. As described in the above text, when one of the double bonds is part of an enol ether, it is possible to distinguish the species from a double bond regioisomer isobar which does not contain an enol ether.

[1]In the "Resolution of Isobars" column, "chromatography" means that the isobars are likely to be resolved by LC. "Q3" means that they are likely to be resolved by MSMS (vs MS). "calculation" means that the peak area for the putative analyte peak is significantly larger than the area calculated for the isobaric internal standard-derived peak where the latter is obtained by knowing the area of the d31 internal standard peak and the relative amounts of partially deuterated internal standard species. "Unresolved" means isobaric resolution cannot be made based on observations made in this study. "?" means no definitive statement about isobaric resolution can be made.

[2]In the "Comments on Resolution" column, "likely means the resolution of isobar statement is based on experimental trends seen with related lysophospholipid species, "experimental" means that isobaric resolution is based on experimental observations made in this study. Isobaric overlaps that are difficult to resolve are flagged by red text.

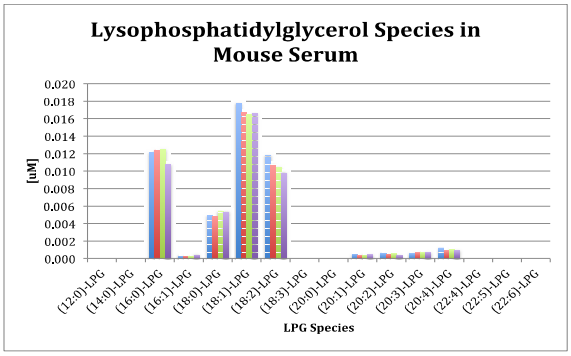
Isobaric Mass	[M-2] Isobars	[M-1] Isobars	Parent Ion Isobars	[M+1] Isobars	[M+2] Isobars	Resolution of Isobars	Comments on Resolution
382			e12:0-LPE	14:0-LPA		Chromatography	**Likely**
396			12:0-LPE	e16:0-LPA		Chromatography	**Likely**
410			e14:0-LPE	16:0-LPA		Chromatography	**Likely**
423			e18:0-LPA, 17:0-LPA			Unresolved	
424			14:0-LPE	e18:0-LPA		Chromatography	**Likely**
			14:0-LPE	17:0-LPA		Chromatography	**Likely**
				e18:0-LPA, 17:0-LPA		Unresolved	
427			12:0-LPG	e12:0-LPS		Chromatography	**Likely**
436			e16:1-LPE	18:1-LPA		Chromatography	**Likely**
437			18:0-LPA	e16:1-LPE		Chromatography	**Experimental**
438			e16:0-LPE	18:0-LPA		Chromatography	**Likely**
	d31-16:0-LPA			18:0-LPA		calculation	**Experimental**
	d31-16:0-LPA		e16:0-LPE			Chromatography	**Likely**
439		d31-16:0-LPA		e16:0-LPE		Chromatography	**Likely**
440			d31-16:0-LPA, 12:0-LPS			Chromatography	**Likely**
441			e14:0-LPG	d31-16:0-LPA		Chromatography	**Likely**
			e14:0-LPG	12:0-LPS		Chromatography	**Likely**
				d31-16:0-LPA, 12:0-LPS		Chromatography	**Likely**
442				e14:0-LPG	d31-16:0-LPA	Chromatography	**Likely**
450			16:1-LPE	e20:1-LPA		Q3/Chromatography	**Likely**
451			e20:0-LPA	16:1-LPE		Chromatography	**Likely**
452			16:0-LPE	e20:0-LPA		Chromatography	**Likely**
455			14:0-LPG	e14:0-LPS		Chromatography	**Likely**
460			e18:3-LPG	20:3-LPA		Chromatography	**Likely**
461			20:2-LPA	e18:3-LPE		Chromatography	**Likely**
462			e18:2-LPE	20:2-LPA		Chromatography	**Likely**
463			20:1-LPA	e18:2-LPE		Chromatography	**Likely**
464			e18:1-LPE	20:1-LPA		Chromatography	**Likely**
465			20:0-LPA	e18:1-LPE		Chromatography	**Likely**

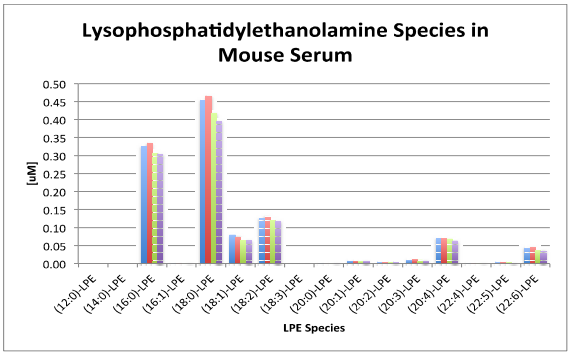
Isobaric Mass	[M-2] Isobars	[M-1] Isobars	Parent Ion Isobars	[M+1] Isobars	[M+2] Isobars	Resolution of Isobars	Comments on Resolution
466			e18:0-LPE	20:0-LPA		Chromatography	**Likely**
467			e22:6-LPA, e16:1-LPG			Chromatography	**Likely**
			e22:6-LPA	e18:0-LPE		Chromatography	**Likely**
			e16:1-LPG	e18:0-LPE		Chromatography	**Likely**
468			14:0-LPS	e16:1-LPG		Chromatography	**Likely**
			14:0-LPS	e22:6-LPA		Chromatography	**Likely**
				e22:6-LPA, e16:1-LPG		Chromatography	**Likely**
469			e22:5-LPA, e16:0-LPG			Chromatography	**Likely**
			e22:5-LPA	14:0-LPS		Chromatography	**Likely**
			e16:0-LPG	14:0-LPS		Chromatography	**Likely**
470				e16:0-LPG, e22:5-LPA		Chromatography	**Likely**
476			18:2-LPE, e19:2-LPE			Unresolved	**Experimental**
477				18:2-LPE, e19:2-LPE		Unresolved	**Experimental**
480			e16:1-LPS, 18:0-LPE			Chromatography	**Likely**
481			22:6-LPA, 16:1-LPG			Chromatography	**Likely**
			22:6-LPA	e16:1-LPS		Chromatography	**Likely**
			22:6-LPA	18:0-LPE		Chromatography	**Experimental**
			16:1-LPG	e16:1-LPS		Chromatography	**Likely**
			16:1-LPG	18:0-LPE		Q3/Chromatography	**Experimental**
				e16:1-LPS, 18:0-LPE		Chromatography	**Likely**
	d31-16:0-LPE		22:6-LPA			Chromatography	**Likely**
	d31-16:0-LPE		16:1-LPG			Chromatography	**Likely**
	d31-16:0-LPE			e16:1-LPS		Chromatography	**Likely**
	d31-16:0-LPE			18:0-LPE		calculation	**Likely**
482			e16:0-LPS	22:6-LPA		Chromatography	**Likely**
			e16:0-LPS	16:1-LPG		Chromatography	**Likely**
				22:6-LPA, 16:1-LPG		Chromatography	**Likely**
		d31-16:0-LPE	e16:0-LPS				
		d31-16:0-LPE		22:6-LPA		Chromatography	**Likely**
		d31-16:0-LPE		16:1-LPG		Q3/Chromatography	**Likely**
483			22:5-LPA, d31-16:0-LPE			Chromatography	**Experimental**
			22:5-LPA, 16:0-LPG			Chromatography	**Likely**
			16:0-LPG, d31-16:0-LPE			Q3/Chromatography	**Likely**
484				22:5-LPA, d31 16:0-LPE		Chromatography	**Likely**
				16:0-LPG, d31 16:0-LPE		Q3/Chromatography	**Likely**
				22:5-LPA, 16:0-LPG		Chromatography	**Likely**
486			e20:4-LPE	22:4-LPA		Chromatography	**Likely**
491			e18:3-LPG	e20:2-LPE		Chromatography	**Likely**
492			e20:1-LPE	e18:3-LPG		Chromatography	**Likely**
493			e18:2-LPG	e20:1-LPE		Chromatography	**Likely**
494			16:1-LPS, e20:0-LPE			Chromatography	**Likely**
			16:1-LPS	e18:2-LPG		Chromatography	**Likely**
			e20:0-LPE	e18:2-LPG		Chromatography	**Likely**
495			e18:1-LPG, 17:1-LPG			Unresolved	
			e18:1-LPG	16:1-LPS		Chromatography	**Likely**
			e18:1-LPG	e20:0-LPE		Chromatography	**Likely**
			17:1-LPG	16:1-LPS		Chromatography	**Likely**
			17:1-LPG	e20:0-LPE		Chromatography	**Likely**
				16:1-LPS, e20:0-LPE		Chromatography	**Likely**

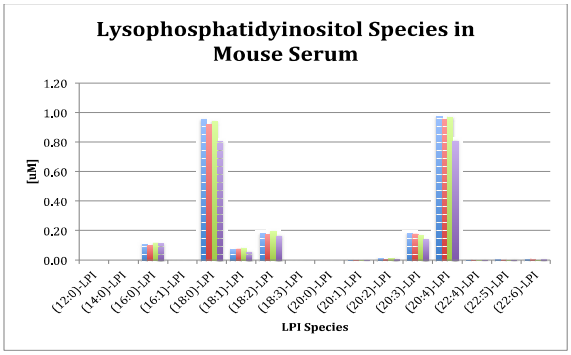
Isobaric Mass	[M-2] Isobars	[M-1] Isobars	Parent Ion Isobars	[M+1] Isobars	[M+2] Isobars	Resolution of Isobars	Comments on Resolution
496			16:0-LPS	e18:1-LPG		Chromatography	**Likely**
			16:0-LPS	17:1-LPG		Chromatography	**Experimental**
				e18:1-LPG, 17:1-LPG		Unresolved	
497			e18:0-LPG	16:0-LPS		Chromatography	**Likely**
501			e12:0-LPI	20:4-LPE		Chromatography	**Likely**
502			20:3-LPE	e12:0-LPI		Chromatography	**Likely**
504			e18:3-LPS, 20:2-LPE			Chromatography	**Likely**
505			18:3-LPG	e18:3-LPS		Chromatography	**Likely**
			18:3-LPG	20:2-LPE		Q3/Chromatography	**Experimental**
				e18:3-LPS, 20:2-LPE		Chromatography	**Likely**
506			e18:2-LPS, 20:1-LPE			Chromatography	**Likely**
			e18:2-LPS	18:3-LPG		Chromatography	**Likely**
			20:1-LPE	18:3-LPG		Q3/Chromatography	**Experimental**
507			18:2-LPG	e18:2-LPS		Chromatography	**Likely**
			18:2-LPG	20:1-LPE		Q3/Chromatography	**Experimental**
				e18:2-LPS, 20:1-LPE		Chromatography	**Likely**
508			e18:1-LPS, 20:0-LPE			Chromatography	**Likely**
			e18:1-LPS, 17:1-LPS			Unresolved	
			20:0-LPE, 17:1-LPS			Chromatography	**Likely**
			e18:1-LPS	18:2-LPG		Chromatography	**Likely**
			20:0-LPE	18:2-LPG		Q3/Chromatography	**Experimental**
			17:1-LPS	18:2-LPG		Chromatography	**Likely**
509			18:1-LPG	e18:1-LPS		Chromatography	**Likely**
			18:1-LPG	20:0-LPE		Q3/Chromatography	**Experimental**
			18:1-LPG	17:1-LPS		Chromatography	**Experimental**
				17:1-LPS, e18:1-LPS		Unresolved	
				17:1-LPS, 20:0-LPE		Chromatography	**Likely**
				e18:1-LPS, 20:0-LPE		Chromatography	**Likely**
510			e18:0-LPS, e22:6-LPE			Chromatography	**Likely**
			e18:0-LPS	18:1-LPG		Chromatography	**Likely**
			e22:6-LPE	18:1-LPG		Q3/Chromatography	**Likely**
511			18:0-LPG	e18:0-LPS		Chromatography	**Likely**
			18:0-LPG	e22:6-LPE		Chromatography	**Likely**
				e18:0-LPS, e22:6-LPE		Chromatography	**Likely**
512			e22:5-LPE	18:0-LPG		Chromatography	**Likely**
	d31-16:0-LPG		e22:5-LPE			Chromatography	**Likely**
	d31-16:0-LPG			18:0-LPG		calculation	**Likely**
513		d31-16:0-LPG		e22:5-LPE		Chromatography	**Likely**
514			d31-16:0-LPG, e22:4-LPE			Chromatography	**Likely**
515			12:0-LPI	d31-16:0-LPG		Q3/Chromatography	**Likely**
			12:0-LPI	e22:4-LPE		Q3	**Likely**
				d31-16:0-LPG, e22:4-LPE		Q3/Chromatography	**Likely**
516				12:0-LPI	d31-16:0-LPG	Q3/Chromatography	**Likely**
518			18:3-LPS	e20:4-LPG		Chromatography	**Likely**
519			e20:3-LPG	18:3-LPS		Chromatography	**Likely**
520			18:2-LPS	e20:3-LPG		Chromatography	**Likely**
521			e20:2-LPG	18:2-LPS		Chromatography	**Likely**
522			18:1-LPS	e20:2-LPG		Chromatography	**Likely**
523			e20:1-LPG	18:1-LPS		Chromatography	**Likely**
524			18:0-LPS, 22:6-LPE			Chromatography	**Experimental**
			18:0-LPS	e20:1-LPG		Chromatography	**Likely**
			22:6-LPE	e20:1-LPG		Chromatography	**Likely**

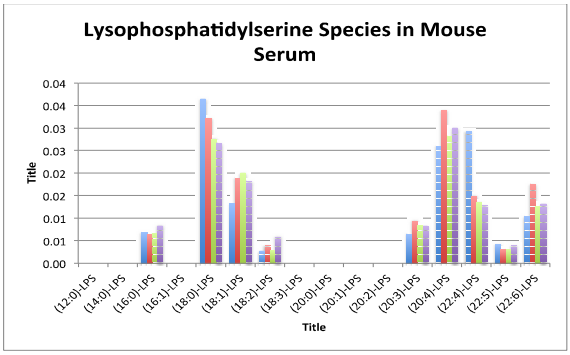
Isobaric Mass	[M-2] Isobars	[M-1] Isobars	Parent Ion Isobars	[M+1] Isobars	[M+2] Isobars	Resolution of Isobars	Comments on Resolution
525			e20:0-LPG	18:0-LPS		Chromatography	**Likely**
			e20:0-LPG	22:6-LPE		Chromatography	**Likely**
	d31-16:0-LPS		e20:0-LPG			Chromatography	**Likely**
				18:0-LPS, 22:6-LPE		Chromatography	**Experimental**
	d31-16:0-LPS			18:0-LPS		calculation	**Experimental**
	d31-16:0-LPS			22:6-LPE		Chromatography	**Experimental**
526			22:5-LPE	e20:0-LPG		Chromatography	**Likely**
		d31-16:0-LPS	22:5-LPE			Chromatography	**Experimental**
		d31-16:0-LPS		e20:0-LPG		Chromatography	**Likely**
527			d31-16:0-LPS	22:5-LPE		Chromatography	**Experimental**
528			22:4-LPE	d31-16:0-LPS		Chromatography	**Experimental**
529			e14:0-LPI	22:4-LPE		Chromatography	**Likely**
			e14:0-LPI		d31-16:0-LPS	Chromatography	**Likely**
				22:4-LPE	d31-16:0-LPS	Chromatography	**Experimental**
530			e20:4-LPS	e14:0-LPI		Chromatography	**Likely**
531			20:4-LPG	e20:4-LPS		Chromatography	**Likely**
532			e20:3-LPS	20:4-LPG		Chromatography	**Likely**
533			20:3-LPG	e20:3-LPS		Chromatography	**Likely**
534			e20:2-LPS	20:3-LPG		Chromatography	**Likely**
535			20:2-LPG	e20:2-LPS		Chromatography	**Likely**
536			e20:1-LPS	20:2-LPG		Chromatography	**Likely**
537			20:1-LPG	e20:1-LPS		Chromatography	**Likely**
538			e20:0-LPS	20:1-LPG		Chromatography	**Likely**
539			20:0-LPG	e20:0-LPS		Chromatography	**Likely**
543			e22:5-LPG, 14:0-LPI			Chromatography,Q3	**Likely**
544			20:4-LPS	e22:5-LPG		Chromatography	**Likely**
			20:4-LPS	14:0-LPI		Chromatography	**Likely**
				e22:5-LPG, 14:0-LPI		Chromatography,Q3	**Likely**
545			e22:4-LPG	20:4-LPS		Chromatography	**Likely**
546			20:3-LPS	e22:4-LPG		Chromatography	**Likely**
555			22:6-LPG, e16:1-LPI			Chromatography,Q3	**Likely**
			22:6-LPG	e22:6-LPS		Chromatography	**Likely**
			e16:1-LPI	e22:6-LPS		Chromatography	**Likely**
556			e22:5-LPS	e16:1-LPI		Chromatography	**Likely**
			e22:5-LPS	22:6-LPG		Chromatography	**Likely**
				e16:1-LPI, 22:6-LPG		Q3	**Likely**
557			22:5-LPG, e16:0-LPI			Chromatography,Q3	**Likely**
			22:5-LPG	e22:5-LPS		Chromatography	**Likely**
			e16:0-LPI	e22:5-LPS		Chromatography	**Likely**
558			e22:4-LPS	e16:0-LPI		Chromatography	**Likely**
			e22:4-LPS	22:5-LPG		Chromatography	**Likely**
				e16:0-LPI, 22:5-LPG		Q3	**Likely**
559			22:4-LPG	e22:4-LPS		Chromatography	**Likely**
569			16:1-LPI	22:6-LPS		Chromatography	**Experimental**
570			22:5-LPS	16:1-LPI		Chromatography	**Likely**
571			16:0-LPI	22:5-LPS		Chromatography	**Experimental**
572			22:4-LPS	16:0-LPI		Chromatography	**Experimental**
583			17:1-LPI, e18:1-LPI			Unresolved	
584				17:1-LPI, e18:1-LPI		Unresolved	

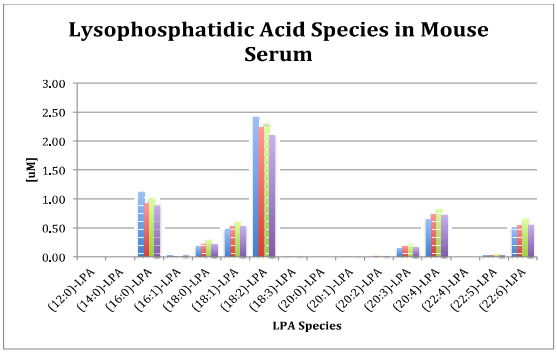
FIGURE 2.4: Summary of the concentration of LPL's in mouse serum. Numbers are given in micromolar (μM)

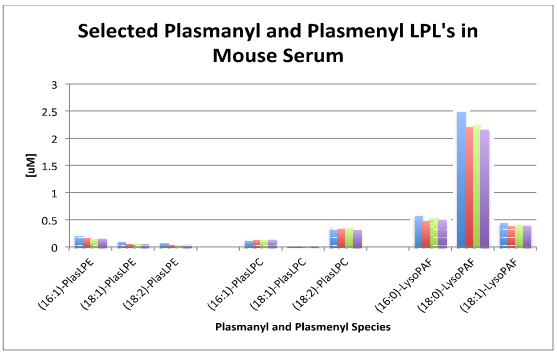












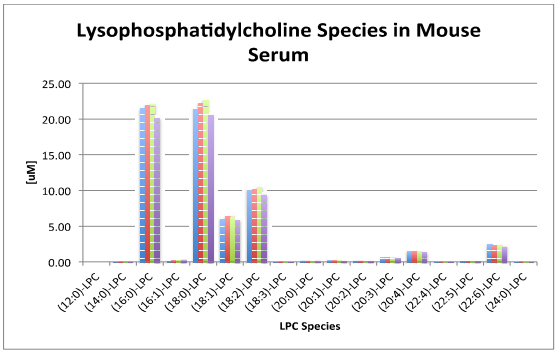


TABLE 2.4: Analysis of LPL's in mouse serum. Runs 1-4 are independent experiments prepared with 100 µL of the same batch of mouse serum. Values are given as pmole/100 µL serum

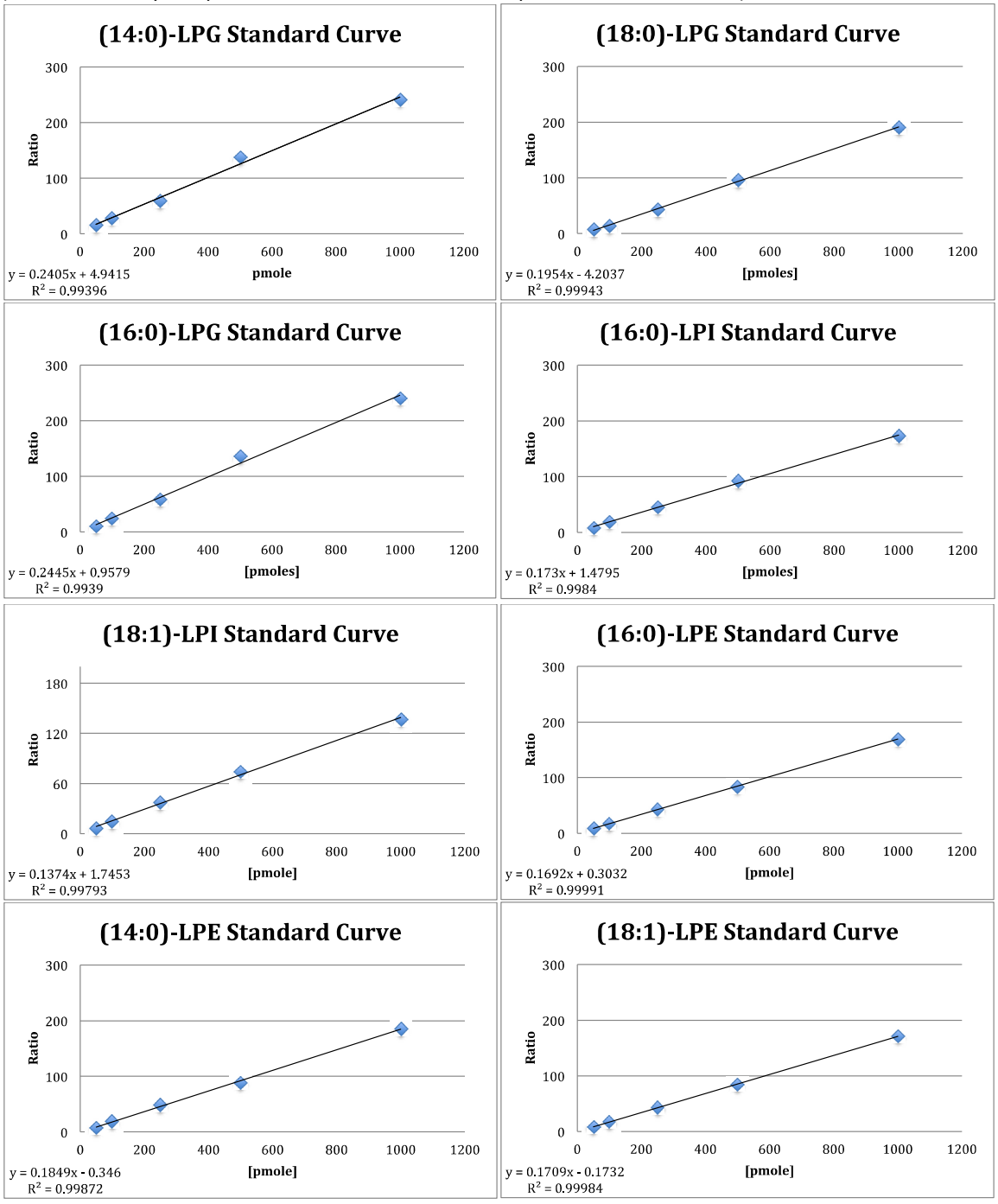
	Serum 1	Serum 2	Serum 3	Serum 4			Serum 1	Serum 2	Serum 3	Serum 4
(12:0)-LPG						(12:0)-LPS				
(14:0)-LPG						(14:0)-LPS				
(16:0)-LPG	1.2	1.3	1.3	1.1		(16:0)-LPS	0.7	0.7	0.7	0.8
(16:1)-LPG	0.0	0.0	0.0	0.1		(16:1)-LPS				
(18:0)-LPG	0.5	0.5	0.6	0.5		(18:0)-LPS	3.7	3.2	2.8	2.7
(18:1)-LPG	1.8	1.7	1.7	1.7		(18:1)-LPS	1.4	1.9	2.0	1.8
(18:2)-LPG	1.2	1.1	1.1	1.0		(18:2)-LPS	0.3	0.4	0.3	0.6
(18:3)-LPG						(18:3)-LPS				
(20:0)-LPG						(20:0)-LPS				
(20:1)-LPG	0.1	0.0	0.1	0.1		(20:1)-LPS				
(20:2)-LPG	0.1	0.1	0.1	0.1		(20:2)-LPS				
(20:3)-LPG	0.1	0.1	0.1	0.1		(20:3)-LPS	0.7	1.0	0.9	0.8
(20:4)-LPG	0.1	0.1	0.1	0.1		(20:4)-LPS	2.6	3.4	2.8	3.0
(22:4)-LPG						(22:4)-LPS	2.9	1.5	1.4	1.3
(22:5)-LPG						(22:5)-LPS	0.4	0.3	0.3	0.4
(22:6)-LPG						(22:6)-LPS	1.1	1.8	1.3	1.3
	Serum 1	**Serum 2**	**Serum 3**	**Serum 4**			**Serum 1**	**Serum 2**	**Serum 3**	**Serum 4**
(12:0)-LPI						(12:0)-LPA				
(14:0)-LPI						(14:0)-LPA				
(16:0)-LPI	11.7	11.0	11.9	12.2		(16:0)-LPA	112.5	94.1	102.2	91.8
(16:1)-LPI						(16:1)-LPA	4.0	2.8	3.0	3.6
(18:0)-LPI	96.1	92.8	94.6	81.5		(18:0)-LPA	20.1	23.2	29.9	24.0
(18:1)-LPI	7.9	8.1	8.4	6.4		(18:1)-LPA	49.5	54.6	61.4	53.9
(18:2)-LPI	18.6	18.3	19.9	17.1		(18:2)-LPA	243.7	225.4	231.2	211.2
(18:3)-LPI						(18:3)-LPA	1.3	1.1	1.3	1.5
(20:0)-LPI						(20:0)-LPA				
(20:1)-LPI	0.4	0.4	0.4	0.5		(20:1)-LPA	0.4	0.5	0.7	0.5
(20:2)-LPI	1.6	1.5	2.1	1.5		(20:2)-LPA	1.5	1.9	1.9	1.8
(20:3)-LPI	18.9	18.0	17.6	15.0		(20:3)-LPA	17.1	19.1	22.8	18.1
(20:4)-LPI	98.1	96.6	97.3	81.5		(20:4)-LPA	67.5	76.6	83.5	73.0
(22:4)-LPI	0.6	0.6	0.4	0.6		(22:4)-LPA	0.4	0.4	0.5	0.5
(22:5)-LPI	1.0	0.8	0.9	0.8		(22:5)-LPA	4.5	4.8	5.5	5.1
(22:6)-LPI	1.4	1.0	0.9	1.0		(22:6)-LPA	52.4	55.8	66.2	56.4
	Serum 1	**Serum 2**	**Serum 3**	**Serum 4**			**Serum 1**	**Serum 2**	**Serum 3**	**Serum 4**
(12:0)-LPE						(12:0)-LPC				
(14:0)-LPE						(14:0)-LPC	5.9	7.3	9.5	7.9
(16:0)-LPE	32.8	33.8	31.0	30.6		(16:0)-LPC	2168.2	2207.7	2222.1	2027.1
(16:1)-LPE	0.3	0.3	0.2	0.2		(16:1)-LPC	27.9	32.5	38.6	34.9
(18:0)-LPE	45.7	46.7	42.1	39.7		(18:0)-LPC	2155.0	2233.5	2275.7	2061.4
(18:1)-LPE	8.2	7.8	6.8	6.7		(18:1)-LPC	620.4	647.9	646.3	596.0
(18:2)-LPE	12.9	13.3	12.4	11.9		(18:2)-LPC	1022.6	1034.2	1058.5	939.7
(18:3)-LPE						(18:3)-LPC	4.8	5.5	6.4	5.9
(20:0)-LPE	0.3	0.2	0.2	0.3		(20:0)-LPC	19.0	18.4	17.8	16.4
(20:1)-LPE	1.1	1.1	0.8	0.8		(20:1)-LPC	29.3	30.1	29.8	26.8
(20:2)-LPE	0.5	0.5	0.6	0.5		(20:2)-LPC	24.3	24.9	25.4	23.4
(20:3)-LPE	1.4	1.5	1.3	1.1		(20:3)-LPC	74.7	76.4	76.2	69.8
(20:4)-LPE	7.4	7.2	6.9	6.4		(20:4)-LPC	155.8	161.3	162.2	149.8
(22:4)-LPE	0.3	0.3	0.3	0.2		(22:4)-LPC	2.6	2.6	2.4	2.3
(22:5)-LPE	0.5	0.6	0.5	0.5		(22:5)-LPC	27.4	27.5	27.0	25.5
(22:6)-LPE	4.6	4.8	4.0	3.8		(22:6)-LPC	256.3	253.2	243.1	224.8
						(24:0)-LPC	4.8	4.2	4.0	4.0
	Serum 1	**Serum 2**	**Serum 3**	**Serum 4**						
(16:1)-PlasLPE	22.1	18.3	16.5	16.7						
(18:1)-PlasLPE	11.4	7.9	7.4	7.1						
(18:2)-PlasLPE	8.3	5.8	4.9	5.4						
(16:1)-PlasLPC	13.3	14.2	14.6	13.3						
(18:1)-PlasLPC	1.6	1.6	1.6	1.6						
(18:2)-PlasLPC	35.0	34.9	36.4	33.0						
(16:0)-LysoPAF	57.5	49.1	54.5	51.8						
(18:0)-LysoPAF	250.2	221.9	225.5	216.0						
(18:1)-LysoPAF	44.6	40.1	42.0	41.0						

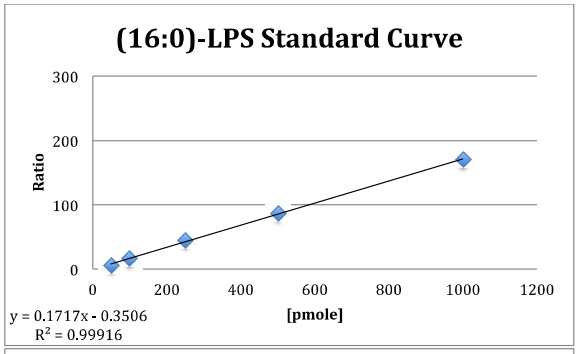
TABLE 2.5: LPL molecular species changes in HEK293 cells in response to human $sPLA_2$-GX action.
Analysis was carried out using one 10 cm dish of cells and results are reported in picomoles.
[1]HEK293 cells cultured for 4 hrs at 37 °C in the absence of the PLA_2.
[2]HEK293 cells treated exogenously for 4 hrs at 37 °C with 200 ng/mL $sPLA_2$-GX
[3]HEK293 cells stably expressing $sPLA_2$-GX after culturing for 4 at 37 °C

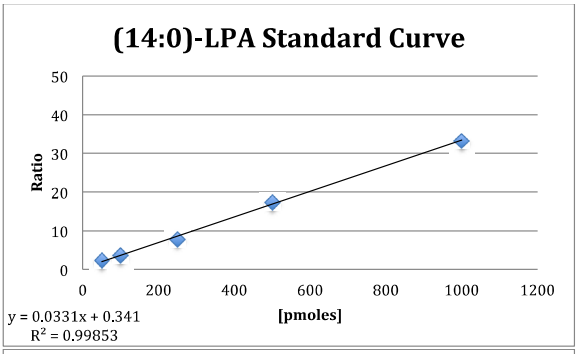
	WT HEK[1]	WT HEK[1]		WT HEK (+) 200 ng/ml hGX[2]	WT HEK (+) 200 ng/ml hGX[2]		pre-pro-hGX overexpressed3	pre-pro-hGX overexpressed (B)
(12:0)-LPG								
(14:0)-LPG								
(16:0)-LPG	3.8	3.8		5.8	5.1		2.4	2.3
(16:1)-LPG	0.7	0.7		0.7	0.7		0.5	0.4
(18:0)-LPG	4.7	4.3		5.2	5.5		3.9	3.6
(18:1)-LPG	24.6	22.7		25.8	25.8		17.1	15.1
(18:2)-LPG	0.6	0.5		0.6	0.6		1.2	1.0
(18:3)-LPG	0.0	0.0		0.0	0.0		0.1	0.1
(20:0)-LPG	0.1	0.1		0.1	0.1		0.1	0.1
(20:1)-LPG	0.9	1.0		1.2	1.1		0.5	0.5
(20:2)-LPG	0.4	0.4		0.5	0.5		0.7	0.5
(20:3)-LPG	0.5	0.5		0.4	0.5		0.7	0.6
(20:4)-LPG	0.1	0.1		0.1	0.1		0.6	0.5
(22:4)-LPG	0.1	0.1		0.0	0.1		0.4	0.3
(22:5)-LPG	0.1	0.1		0.1	0.1		1.1	0.7
(22:6)-LPG	0.2	0.2		0.1	0.2		0.8	0.7
(12:0)-LPI								
(14:0)-LPI								
(16:0)-LPI	3.6	2.9		3.7	3.0		0.8	0.7
(16:1)-LPI	0.3	0.3		0.4	0.3		0.2	0.0
(18:0)-LPI	44.9	38.9		40.3	37.7		9.4	9.0
(18:1)-LPI	8.5	7.3		4.5	5.5		1.1	1.3
(18:2)-LPI	0.7	0.5		0.4	0.4		0.5	0.4
(18:3)-LPI								
(20:0)-LPI								
(20:1)-LPI	0.7	0.7		0.3	0.5		0.0	0.0
(20:2)-LPI	2.1	1.5		1.2	1.3		0.0	0.0
(20:3)-LPI	1.1	0.8		0.6	0.8		0.6	0.9
(20:4)-LPI	2.4	1.5		1.2	1.4		2.4	2.6
(22:4)-LPI								
(22:5)-LPI								
(22:6)-LPI								
(12:0)-LPE								
(14:0)-LPE	0.5	0.4		0.9	1.0		0.4	0.3
(16:0)-LPE	13.3	13.2		33.3	34.7		17.5	15.2
(16:1)-LPE	1.5	1.3		2.7	3.3		1.1	0.9
(18:0)-LPE	13.3	12.9		55.5	57.3		48.7	45.8
(18:1)-LPE	13.5	12.9		33.3	34.9		16.9	14.9
(18:2)-LPE	0.6	0.7		1.1	1.1		1.1	0.9
(18:3)-LPE								
(20:0)-LPE	0.3	0.3		1.9	1.6		1.2	1.3
(20:1)-LPE	1.1	1.0		3.8	3.7		1.8	1.6
(20:2)-LPE	0.2	0.1		0.4	0.3		0.3	0.3
(20:3)-LPE	0.2	0.2		0.2	0.3		0.3	0.3
(20:4)-LPE	0.5	0.7		0.5	0.5		1.5	1.2
(22:4)-LPE	0.1	0.2		0.1	0.2		0.8	0.7
(22:5)-LPE	0.1	0.1		0.0	0.1		0.2	0.3
(22:6)-LPE	0.1	0.1		0.1	0.1		0.1	0.1
(12:0)-LPS								
(14:0)-LPS								
(16:0)-LPS	4.3	3.2		5.6	5.6		0.4	0.5
(16:1)-LPS	0.3	0.4		0.3	0.3		0.0	0.0
(18:0)-LPS	23.3	26.2		30.8	32.2		8.4	10.0
(18:1)-LPS	6.0	5.6		6.5	6.1		1.7	2.1
(18:2)-LPS								
(18:3)-LPS	0.6	1.0		0.9	0.7		0.1	0.1
(20:0)-LPS	2.2	2.9		2.5	3.3		0.5	0.7
(20:1)-LPS	1.1	1.2		1.6	0.8		0.3	0.5
(20:2)-LPS	0.2	0.3		0.3	0.2		0.0	0.0
(20:3)-LPS	2.4	4.8		3.3	3.7		0.9	1.5

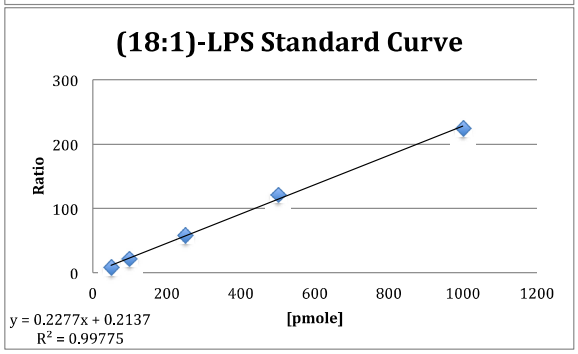
	WT HEK[1]	WT HEK[1]		WT HEK (+) 200 ng/ml hGX[2]	WT HEK (+) 200 ng/ml hGX[2]		pre-pro-hGX overexpressed3	pre-pro-hGX overexpressed (B)
(20:4)-LPS	0.6	0.9		0.5	0.6		0.3	0.2
(22:4)-LPS	0.3	0.4		0.2	0.2		0.1	0.2
(22:5)-LPS	0.2	0.2		0.2	0.1		0.1	0.0
(22:6)-LPS	0.2	0.2		0.2	0.2		0.0	0.0
(12:0)-LPA								
(14:0)-LPA								
(16:0)-LPA	0.9	0.5		0.5	0.8		0.2	0.5
(16:1)-LPA								
(18:0)-LPA	0.7	0.8		0.6	0.8		0.0	0.2
(18:1)-LPA	1.1	1.2		0.6	1.2		0.6	1.2
(18:2)-LPA								
(18:3)-LPA								
(20:0)-LPA								
(20:1)-LPA								
(20:2)-LPA								
(20:3)-LPA								
(20:4)-LPA								
(22:4)-LPA								
(22:5)-LPA								
(22:6)-LPA								
(12:0)-LPC	0.5	0.7		0.6	0.6		0.2	0.2
(14:0)-LPC	23.5	22.7		31.8	27.9		16.8	16.5
(16:0)-LPC	294.0	259.6		456.7	407.1		281.1	286.5
(16:1)-LPC	18.3	18.8		25.9	22.0		17.6	17.9
(18:0)-LPC	60.9	69.2		138.6	111.1		79.8	92.5
(18:1)-LPC	102.6	107.2		149.3	133.2		92.1	99.8
(18:2)-LPC	2.3	2.8		3.2	3.1		6.8	6.1
(18:3)-LPC	0.1	0.1		0.1	0.1		0.4	0.3
(20:0)-LPC	3.0	4.0		9.0	8.1		1.8	2.8
(20:1)-LPC	17.2	27.1		31.1	31.0		9.4	11.8
(20:2)-LPC	1.1	1.9		2.0	2.0		2.5	2.6
(20:3)-LPC	0.5	0.7		0.7	0.7		2.1	2.3
(20:4)-LPC	0.7	1.0		0.8	0.9		4.5	4.0
(22:4)-LPC	0.4	0.8		0.6	0.7		2.5	2.4
(22:5)-LPC	0.3	0.3		0.3	0.3		0.9	1.0
(22:6)-LPC	0.3	0.3		0.2	0.3		0.9	1.0
(24:0)-LPC	2.4	2.9		8.2	6.0		0.7	1.1
(16:1)-PlasLPE	3.1	2.8		6.6	5.6		2.3	1.9
(18:1)-PlasLPE	2.8	2.5		5.2	4.7		2.8	2.3
(18:2)-PlasLPE	0.8	0.6		1.8	1.6		0.7	0.5
(16:1)-PlasLPC	7.0	7.2		11.7	8.2		4.3	4.5
(18:1)-PlasLPC	2.1	2.5		4.0	2.6		2.0	2.4
(18:2)-PlasLPC	1.3	1.4		2.4	1.7		1.4	1.6
(16:0)-LysoPAF	17.9	16.7		20.1	19.6		3.4	4.0
(18:0)-LysoPAF	10.6	11.4		14.5	15.5		8.8	9.4
(18:1)-LysoPAF	6.6	6.5		7.9	6.9		2.6	2.9

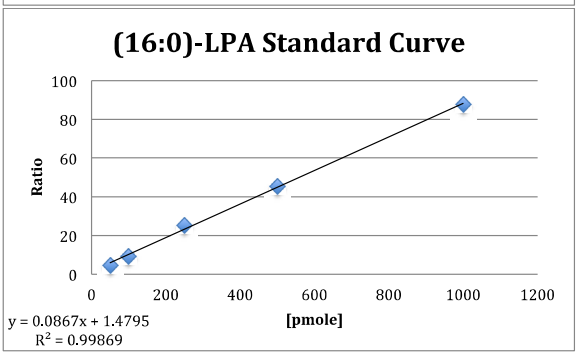
FIGURE 2.5: Standard curves for commercially available LPL's. The Y-axes gives the area of the peak in the selected ion trace chromagram (arbitray units) and the X-axes gives the total pmole of analytes injected (based on callibration of lysophospholipid stocl solutions using inorganic phosphorous analysis) (note: each analyte is present in the stock solution in equi-molar concentration).

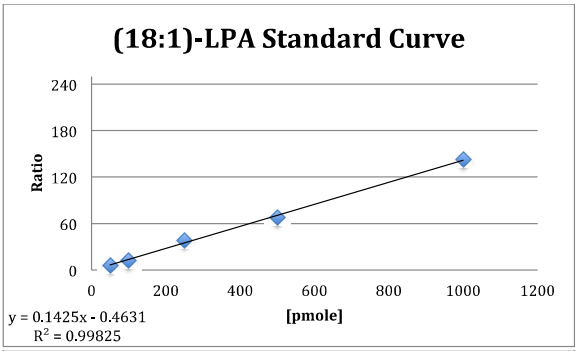


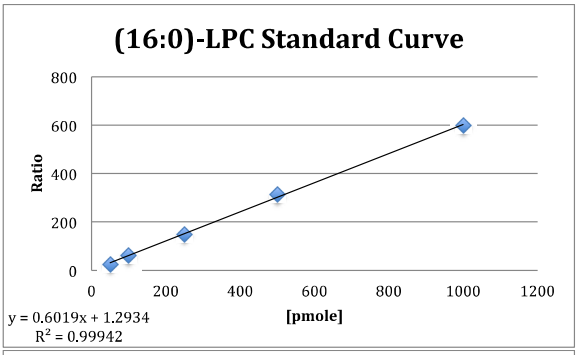

(16:0)-LPS Standard Curve
Ratio
[pmole]
y = 0.1717x - 0.3506
R² = 0.99916

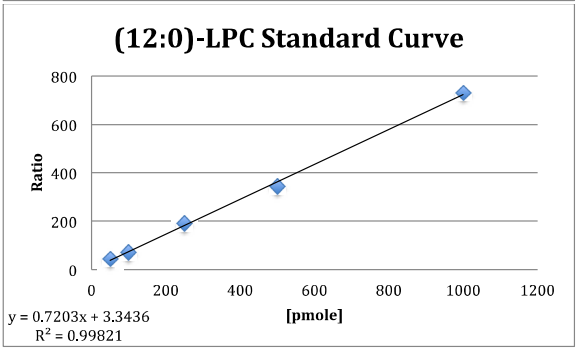

(14:0)-LPA Standard Curve
Ratio
[pmoles]
y = 0.0331x + 0.341
R² = 0.99853

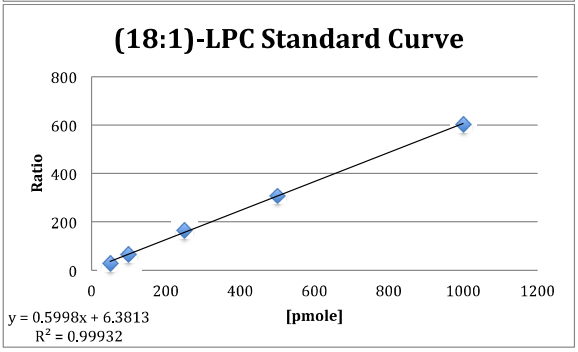

(18:1)-LPS Standard Curve
Ratio
[pmole]
y = 0.2277x + 0.2137
R² = 0.99775

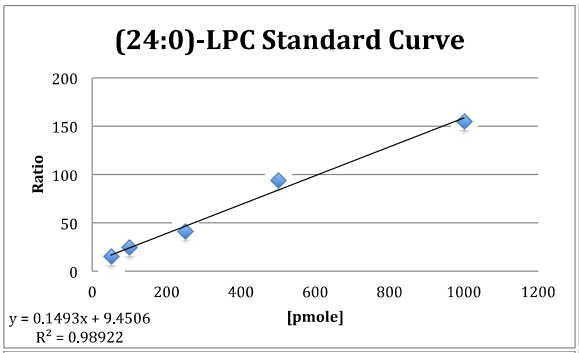

(16:0)-LPA Standard Curve
Ratio
[pmole]
y = 0.0867x + 1.4795
R² = 0.99869

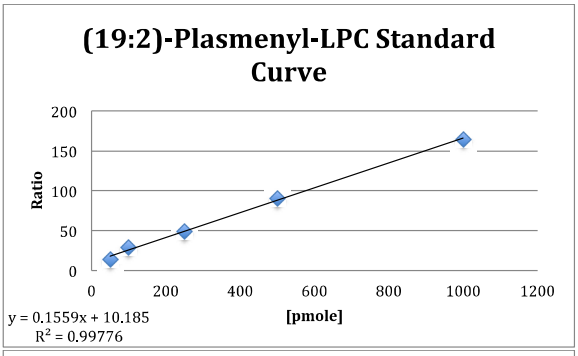

(18:1)-LPA Standard Curve
Ratio
[pmole]
y = 0.1425x - 0.4631
R² = 0.99825

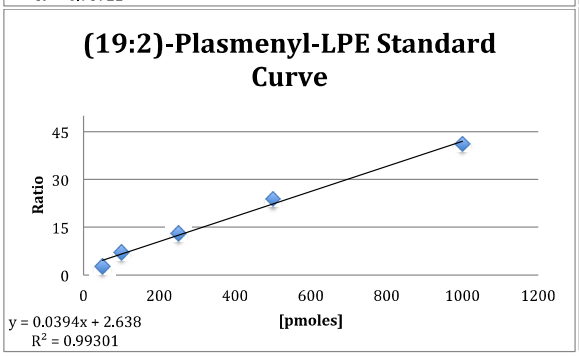

(16:0)-LPC Standard Curve
Ratio
[pmole]
y = 0.6019x + 1.2934
R² = 0.99942

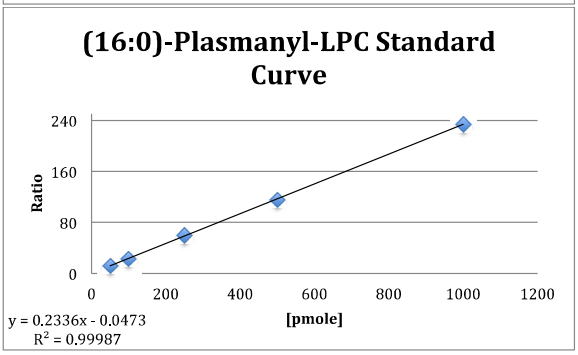

(12:0)-LPC Standard Curve
Ratio
[pmole]
y = 0.7203x + 3.3436
R² = 0.99821


(18:1)-LPC Standard Curve
Ratio
[pmole]
y = 0.5998x + 6.3813
R² = 0.99932


(24:0)-LPC Standard Curve
Ratio
200
150
100
50
0
0
200
400
600
800
1000
1200
[pmole]
y = 0.1493x + 9.4506
R² = 0.98922


(19:2)-Plasmenyl-LPC Standard Curve
Ratio
200
150
100
50
0
0
200
400
600
800
1000
1200
[pmole]
y = 0.1559x + 10.185
R² = 0.99776


(19:2)-Plasmenyl-LPE Standard Curve
Ratio
45
30
15
0
0
200
400
600
800
1000
1200
[pmoles]
y = 0.0394x + 2.638
R² = 0.99301


(16:0)-Plasmanyl-LPC Standard Curve
Ratio
240
160
80
0
0
200
400
600
800
1000
1200
[pmole]
y = 0.2336x - 0.0473
R² = 0.99987

Section 5 : Addendum to Chapter 2

In an effort to increase the utility of our lipid mediator assay, we added MRM transitions for sphingosine-1-phosphate (S1P), 16:0 PAF, and 18:0 PAF. The S1P transition used was +380→ +264 *m/z* (Cone Voltage +20 V/Collision Energy 24 eV) and the transitions used for 16:0 PAF and 18:0 PAF were 524 → 184 and 552 → 184 *m/z*, respectively (Cone Voltage +30 V/Collision Energy 30 eV). In the course of assay validation, we discovered an isobaric overlap between 16:0 PAF and 18:0 LPC that was not addressed in our original isobar analysis. In order to resolve these isobaric peaks, it was necessary to change the column operating temperature to 40° C, the flow rate to 0.3 mL/min, and alter the elution gradient to maximize resolution between species with the choline head group. The following solvent program was used: 0-5 min, 40-50% linear B gradient (0.3 mL/min); 5-40 min, 50-75% linear B gradient (0.3 mL/min); 40-40.2 min, 75-90% linear B gradient (0.3 mL/min); 40.2-46 min, 90% B (0.3 mL/min) 46-46.2 90-40% linear B gradient (0.3 mL/min); 46.2-54 min, 40% B (0.3 mL/min). Transitions for LPG, LPI, LPE, LPS, and LPA are monitored in negative mode for the first 26 minutes of the LC program and S1P, LPC, Lyso-PAF, and PAF are monitored in positive mode for final 28 minutes. The retention times for all species in negative mode remained relatively unchanged. However, the revised gradient now extends the elution profile of the species monitored in positive mode from 7 to 12 minutes. Under this new

chromatography protocol, S1P elutes at 31.4 minutes, 24:0, 16:0 PAF, 18:0, 16:0, and 12:0 LPC elutes at 41.7, 44.2, 46.1, 47.3, and 49.9 minutes, respectively. Unless otherwise noted, all other analytical parameters were unaltered.

Chapter 3

Improved Sensitivity Mass Spectrometric Detection of Eicosanoids by Charge Reversal Derivatization

Section 1: Introduction

Liquid chromatography coupled to electrospray ionization tandem mass spectrometry (LC/ESI-MS/MS) has emerged as a powerful method to detect oxygenated derivatives of fatty acids including eicosanoids (for example,[22, 60]). With these methods it is possible to analyze a large collection of eicosanoids in a single LC/ESI-MS/MS run. These lipid mediators are detected by single reaction monitoring (SRM) in which precursor ions are isolated in the first stage of the mass spectrometer followed by collision-induced dissociation to give fragment ions, which are detected after an additional stage of mass spectrometer isolation. The current limit of quantification for these analytes is in the ~10-20 pg range. This sensitivity level is appropriate for studies with cultured cells *in vitro* or with relatively large tissue samples, but it is not sufficient for studies with smaller volume samples such as joint synovial fluid or bronchoalveolar lavage fluid from experimental rodents. Given the importance of oxygenated fatty acid derivatives in numerous medically important processes such as inflammation and resolution of inflammation, we sought to improve the LC/ESI-MS/MS sensitivity of detection of these lipid mediators using a widely available analytical platform.

For reasons that are not well understood, cations generally form gaseous ions better than anions in the electrospray ionization source of the mass spectrometer. Additionally, for underivatized carboxylic acids it is required to add a weak organic acid to the chromatographic mobile phase, i.e. formic acid, so that the carboxylic acid is kept in its protonated state, which allows it to be retained on the reverse-phase column to ensure chromatographic separation. However, the presence of the weak acid offsets the formation of carboxylate anions in the electrospray source because the weak acid carries most of the anionic charge in the electrospray droplets, and thus formation of analyte anions is suppressed. We reasoned that conversion of the carboxylic acid to a fixed-charge cationic derivative would lead to improved detection sensitivity by ESI-MS/MS. Charge-reversal derivatization of carboxylic acids with quaternary amines has been explored in previous work (for example,[61]). However, these reagents utilize organic cations that tend to fragment by collision-induced dissociation near the cationic site. Fragmentation in the derivatization tag is not desirable because analytes that form isobaric precursor ions and that co-migrate on the LC column will not be distinguished in the mass spectrometer if they give rise to the same detected fragment ion. This loss of analytical specificity is a serious problem when analyzing complex biological samples. Fragmentation in the analyte portion rather than in the tag portion also reduces chemical noise, which also enhances sensitivity of detection.

In this study we report the design and synthesis of a new cationic tag and show that it can be quantitatively attached via an amide linkage to the carboxyl group of eicosanoids by a simple derivatization procedure. We then show that the derivatized eicosanoids can be analyzed by LC/ESI-MS/MS with limits of quantifications that are well below those reported for underivatized eicosanoids.

Section 2: Methods

Synthesis of AMPP

Pyridine (40 mmole, 3.2 mL) was dissolved in 46 mL absolute ethanol followed by the addition of 1-chloro-2,4-dinitrobenzene (40 mmole, 8.2 g, Aldrich). The mixture was heated with a reflux condenser at 98°C for 16 hrs under nitrogen. After cooling, ethanol was removed by rotary evaporation, and the crude product was recrystallized by dissolving in a minimal amount of hot ethanol and allowing the solution to slowly cool to room temperature. The product *N*-2,4 dinitrophenyl pyridinium chloride was isolated as a yellow solid in 62% yield, and its identity was confirmed by melting point analysis (189-191°C observed, 189-190°C reported[62]). *N*-2,4 Dinitrophenyl pyridinium chloride (16.8 mmoles, 4.76 g) was dissolved in 70 mL of ethanol:pyridine (3:1). 4-[(*N*-Boc) -amino-methyl] aniline (33.6 mmoles, 7.56 g, Aldrich) was added, and the reaction mixture was heated under a reflux condenser at 98 °C under nitrogen for 3 hr. After cooling, 700 mL water was added to precipitate 2,4-dinitroaniline. After filtration, the filtrate was concentrated to dryness by rotary evaporation, and the product was isolated as a brown

oil. This oil was treated with 112 mL 25% (v/v) trifluoroacetic acid in dichloromethane for 30 min at room temperature. The mixture was concentrated by rotary evaporation, and the solid was triturated twice with benzene to remove excess trifluoroacetic acid. The mixture was again concentrated by rotary evaporation. The residue was dissolved in a minimal amount of heated ethanol, the solution was allowed to cool for ~5 min and then diethyl ether was added with swirling until the solution started to cloud up. The mixture was transferred to the freezer (-20 °C) and left overnight. The mixture was allowed to warm to room temperature and then decanted. The obtained mother liquor was treated with additional diethyl ether as above to give additional AMPP solid. The solids were combined and triturated with diethyl ether. The solid was dried under vacuum to give 3.30 g of AMPP as a brown solid, 59% yield. ^{1}H-NMR (300 MHz, D_6-DMSO) 9.34 (d, 2H), 8.81 (t, 1H), 8.53 (broad, 3H), 8.33 (t, 2H), 7.95 (d, 2H), 7.80 (d,2H), 4.22 (s, 2H). The estimated purity of AMPP is > 95 %.

Preparation of eicosanoid stock solutions

The following eicosanoid standards from Cayman Chemicals were used (PGE_2, PGD_2, $PGF_{2\alpha}$, 6-Keto-$PGF_{1\alpha}$, TxB_2, 5(S)-HETE, 8(S)-HETE, 11(S)-HETE, 12(S)-HETE, 15(S)-HETE, LTB_4, arachidonic acid, d_4-PGE_2, d_4-PGD_2, d_4-$PGF_{2\alpha}$, d_4-6-Keto-$PGF_{1\alpha}$, d_4-TXB_2, d_8-5(S)-HETE, d_4-LTB_4, d_8-arachidonic acid). Stock solutions of eicosanoids were prepared at concentration of 100 pg/μl in absolute ethanol and stored at -80°C under Ar in teflon septum, screw cap vials. Serial dilutions of the stock solutions were made in absolute

ethanol for standard curve and extraction analysis. Internal standards were diluted to a working stock of 5 pg/μl in absolute ethanol.

Preparation of samples prior to derivatization with AMPP

3.2.a Standard curves.

Each sample contained 50 pg of each internal standard and various amounts of non-isotopic eicosanoids (added from the stock solutions described above) transferred to a glass auto-sampler vial insert (Agilent Cat. 5183-2085). Solvent was removed with a stream of nitrogen, and the residue was derivatized with AMPP as described below.

3.2.b Mouse serum

Analysis of endogenous eicosanoids in serum was carried out with commercial mouse serum (Atlantic Biologicals Cat. S18110). One, Five, or Ten μL of serum was placed in a glass auto-sampler vial insert. Two volumes of methanol (LC/MS, JT Baker Cat. 9863-01) containing 50 pg of each internal standard were added. The vial insert was mixed on a vortex mixer for ~10 sec. The concentration of methanol was lowered to 10% (v/v) by addition of purified water (Milli-Q, Millipore Corp.), and the samples were loaded via a glass Pasteur pipet on to a solid phase extraction cartridge (10 mg Oasis-HLB, Waters Cat. 186000383). The cartridges were previously washed with 1 mL of methanol and then 2 x 0.75 mL purified water:methanol (95:5, v/v). After sample loading, the sample tube was rinsed with 200 μL of purified water:methanol (95:5, v/v), and this was added to the cartridge. The cartridge was washed with 2 x 1 mL purified

water:methanol (95:5, v/v). Additional solvent was forced out of the cartridge solid phase by applying medium pressure N_2 (house N_2 passed through a 0.2 micron cartridge filter) for a few seconds. Column eluant receiver vials (Waters Total Recovery auto-sampler vials, Waters Cat. 186002805) were placed under the cartridges. The cartridges were then eluted with methanol (1 mL). All cartridge steps were carried out using a vacuum manifold (Waters Cat. WAT200606) attached to a water aspirator. Solvent was removed by placing the receiver vials in a centrifugal evaporator (Speed-Vac). These processed samples were derivatized with AMPP (see below) without storage.

3.2.c Lung epithelial cells

The University of Washington Institutional Review Board approved the studies involving human subjects, and written informed consent was obtained from all participants. Primary bronchial epithelial cells were isolated from a volunteer with asthma during bronchoscopy using a nylon cytology brush of cells from subsegmental airways. To establish primary culture, the epithelial cells were seeded into a culture vessel coated with type 1 collagen in bronchial epithelial basal media (BEBM, Lonza, Allendale, NJ) supplemented with bovine pituitary extract, insulin, hydrocortisone, gentamicin, amphotericin B, fluconazole, retinoic acid, transferrin, triiodothyronine, epinephrine, and human recombinant epidermal growth factor (serum-free BEGM) and maintained at 37°C in a humidified incubator. After expansion *in vitro*, passage 2 epithelial cells were grown to >90% confluence on a 12-well plate. The medium was

changed to 200 μL Hanks balanced salt solution, and the cells were treated with either calcium ionophore (A23187, 10 μM in DMSO) or a DMSO-containing control solution for 20 min. at 37°C. The synthesis of eicosanoids was stopped by the addition of 4 volumes of ice-cold methanol with 0.2% formic acid, and samples were stored at -80 °C until processed. The number of epithelial cells was 5.0 x 10^5 cells per well. The studies were performed in duplicate.

Frozen samples were thawed on ice, 50 pg of each internal standard was added, and Milli-Q water was added to bring the methanol to 10% (v/v). The samples were processed by solid-phase extraction (Oasis-HLB) as described for mouse serum samples.

3.2.d Rat 3Y1 cells

3Y1 cells were a gift from Dr. H. Kuwata (Department of Health Chemistry, School of Pharmaceutical Sciences, Showa University). 3Y1 cells were maintained in complete medium consisting of Dulbecco's Modified Eagle Medium (DMEM) with low glucose (Invitrogen Cat. 11885-084) containing 10% heat inactivated, fetal bovine serum (FBS) (Invitrogen Cat. 16140), 100 units/ml penicillin and 100 μg/ml streptomycin (Invitrogen Cat. 15140) in plastic tissue culture dishes (Nunc Cat.172958) in a humidified atmosphere of 5% CO_2 at 37ºC. Passage of cells was performed using 0.25% Trypsin/EDTA (Invitrogen Cat. 25200-056).

For PGE_2 analysis, 3Y1 cells were plated at 5 x 10^4 cells/well in a 24-well plate (Nunc Cat. 142475) in 1 ml complete medium and incubated overnight. The medium

was then replaced with DMEM containing 2% FBS. After 24 hour incubation, the medium was removed from each well and replaced with 1 ml DMEM containing 2% FBS and the cytosolic phospholipase A_2-α inhibitor Wyeth-2 (Compound 10 from[63]) or DMSO vehicle control (final concentration in each well did not exceed 0.1% (v/v)). Cells were incubated for 20 min. at room temperature. Mouse interleukin-1β (1 ng/well) and human tumor necrosis factor-α (1 ng/well) (R & D Systems Cat. 401-ML and 210-TA) were both added to each well in 10 μl DMEM containing 2% FBS (negative control wells received only 10 μl DMEM containing 2% FBS). Cells were incubated for 48 hours at 37ºC in a humidified atmosphere of 5% CO_2. The supernatant was then carefully removed from each well and transferred into a glass test tube and placed on ice for immediate analysis. PGE_2 levels were measured both by enzyme immunoassay kit (Cayman Chemical Cat. 500141) according to manufacturer's instructions using 50 μL of medium above the cells. A sample of medium (50 μL) was also analyzed by LC/ESI-MS/MS as follows. To the medium was added 2 volumes of methanol containing 50 pg of each internal standard, methanol was reduced to 10% v/v by addition of Milli-Q water, and samples were submitted to solid-phase extraction using Oasis-HLB cartridges as described for mouse serum samples.

Derivatization with AMPP

To the residue in the Waters Total Recovery auto-sampler vial was added 10 μL

of ice-cold ACN (JT Baker Cat. 9017-03): DMF (Sigma Cat. 227056) (4:1, v:v). Then 10 μL of ice-cold 1 M EDCI (TCI America Cat. D1601) in Milli-Q water was added. The vial was briefly mixed on a vortex mixer and placed on ice while other samples were processed as above. To each vial was added 20 μL of 5 mM HOBt (Pierce Cat. 24460)/15mM AMPP in ACN. The vials were mixed briefly on a vortex mixer, capped, and placed in a 60°C incubator for 30 min. The cap was replaced with a split-septum screw cap (Agilent Cat. 5185-5824) for auto-injection onto the LC/ESI-MS/MS. Samples were analyzed on the same day. Samples were kept in the auto-sampler rack at 4 °C while queued for injection.

LC/ESI-MS/MS analysis

Some studies were carried out with a Waters Quattro Micro triple quadrupole mass spectrometer, a 2795 Alliance HT LC/auto-sampler system and the QuanLynx software package. Chromatography was carried out with a C18 reverse-phase column (Ascentis Express C18, 2.1 x 150 mm, 2.7 μm, Supelco Cat. 53825-U). Solvent A is 95% H_2O/5 % ACN/1% acetic acid, and solvent B is ACN/1% acetic acid. The solvent program is (linear gradients): 0-1.0 min, 95-78% A; 1.0-7.0 min, 78–74 %A; 7.0-7.1 min, 74-55% A; 7.1-12.1 min, 55-40% A; 12.1-13.0 min, 40-0% A; 13.0-15.0 min, 0% A; 15.0-15.1 min, 0-95% A; 15.1-20.1 min, 95% A. The flow rate is 0.25 mL/min.

Similarly, some studies were carried out with a Waters Quattro Premier triple quadrupole mass spectrometer interfaced to an Acquity UPLC. Solvent A is 100% water (Fisher Optima Grade Cat. L-13780)/0.1% formic acid (Fluka Cat. 94318), and solvent B is ACN (Fisher Optima Grade Cat. L-14338)/0.1% formic acid. The same LC column was used but with a modified solvent program (linear gradients): 0-1.0 min, 95% A; 1.0-2.0 min, 95% - 85% A; 2.0-2.1 min, 85% - 74% A; 2.1-6.0 min, 74% - 71% A; 6.0-6.1 min, 71% - 56% A; 6.1-10.0, 56% A, 10.0 – 14.0, 56% - 0% A; 14.0 – 14.1, 0% - 95% A; 14.1 – 18.0 min, 95% A. Tables 3.5 and 3.6 the give the auto-sampler and ESI-MS/MS data collection parameters for the Waters Quattro Micro triple quadrupole and the Waters Quattro Premier triple quadrupole mass spectrometers, respectively. For comparison purposes, we also carried out LC/ESI-MS/MS analysis of underivatized eicosanoids in negative ion mode. The same LC column, solvent A and B, and flow rate was used as for the AMPP amides. The solvent program was slightly modified as follows: For the Waters Quattro Micro we used 0-1.0 min, 95-63% A; 1.0-7.0 min, 63%A; 7.0-7.1 min, 63-38% A; 7.1-12.1 min, 38-23% A; 12.1-13.0 min, 23-0% A; 13.0-15.0 min, 0% A; 15.0-15.1 min, 0-95% A; 15.1-20.1 min, 95% A; For the Waters Quattro Premier we used 0-1.0 min, 95% A; 1.0-2.0 min, 95% - 85% A; 2.0-2.1 min, 85% - 59% A; 2.1-6.0 min, 59% A; 6.0-6.1 min, 59% - 38% A; 6.1 11, 38% - 23% A, 11 – 11.1, 23% - 0% A; 11.1 – 14, 0% A: 14.0 – 14.1, 0% - 95% A; 14.1 – 19.0 min, 95% A. Values of m/z for precursor and product ions were as published[64], and cone voltages and collision energies were optimized for each

instrument and for each analyte in the usual way (values not shown but similar to those published[64]).

TABLE 3.1: Extraction yields, liquid chromatography retention times, and tandem mass spectrometry parameters for eicosanoid AMPP amide molecular species.

Eicosanoid	Extr. yield (%)	LC ret. time (min)[2]	AMPP Amide Limit of quant. (pg)/ (CV)[3]	Limit of quant. in neg. mode (pg)[4]	Precursor ion[5] (*m*/*z*)	Fragment ion[5] (*m*/*z*)	Cone voltage[6] (V)	Collision energy[6] (eV)
6-keto-$PGF_{1\alpha}$	102/87	5.4/4.1	5/0.3 (6.8)	110/10	537	239	65/80	55/55
$PGF_{2\beta\alpha}$	64/100	6.7/5.2	5/0.5 (9.1)	110/7	521	239	60/75	43/52
PGE_2	67/74	6.8/5.3	5/0.3 (5.5)	100/7	519	239	60/75	40/45
PGD_2	63/67	7.2/5.7	5/0.6 (7.5)	120/7	519	307	60/75	40/48
TxB_2	86/86	6.2/4.6	5/0.2 (2.3)	90/4	537	337	65/70	43/42
LTB_4	42/63	9.8/7.7	5/0.5 (10.3)	80/7	503	323	50/60	35/35
5(S)-HETE	42/65	10.4/9.7	5/0.4 (10.4)	120/10	487	283	55/65	37/34
8(S)-HETE	40/75	10.3/9.1	5/0.2 (6.7)	120/10	487	295	55/65	37/40
11(S)-HETE	31/66	10.2/8.8	5/0.3 (8.9)	80/5	487	335	55/65	32/30
12(S)-HETE	69/62	10.2/8.9	10/0.9 (6.6)	140/10	487	347	55/65	35/35
15(S)-HETE	35/53	10.1/8.5	5/0.4 (11.1)	200/10	487	387	55/65	33/34
Arachidonic acid	73/113	11.7/12.4	10/1 (5.6)	no data	471	239	55/65	40/50
D_4-6-keto-$PGF_{1\alpha}$		5.4/4.1			541	241	65/80	55/55
d_4-$PGF_{2\beta\alpha}$		6.7/5.2			525	241	60/75	43/52
d_4-PGE_2		6.8/5.3			523	241	60/75	40/45
d_4-PGD_2		7.1/5.6			523	311	60/75	40/48
d_4-TxB_2		6.2/4.6			541	341	65/70	43/42
d_4-LTB_4		9.8/7.7			507	325	50/60	35/35
d_8-5(S)-HETE		10.4/9.6			495	284	55/65	37/34
d_8-Arachidonic acid		11.7/12.4			479	239	55/65	40/50

[1]The first number is for the Waters Oasis HLB cartridge, and the second number is for the Phenomenex Strata-X cartridge.
[2]The first number is for the Waters Quattro Micro, and the second number is for the Waters Quattro Premier.
[3]LOQ values are for eicosanoid AMPP amides in positive mode. The first number is for the Waters Quattro Micro, and the second number is for the Waters Quattro Premier. The values in parentheses are the CVs based on 6 independent 15 μ1 injections of 0.075 pg/μ1 on the Waters Quattro Premier (see main text).
[4]LOQ values are for underivatized eicosanoids analyzed by LC/ESI-MS/MS in negative mode. The first number is for the Waters Quattro Micro, and the second number is for the Waters Quattro Premier.
[5]*m*/*z* Values listed are calculated monoisotopic values. The actual values used are derived from instrument tuning, which is instrument dependent.
[6]Cone voltages and collision energies were optimized for each analyte. These numbers are instrument dependent. The first number is for the Waters Quattro Micro instrument, and the second number is for the Waters Quattro Premier instrument.

Eicosanoid recovery studies

We measured the recovery of eicosanoids following the sample workup procedure given above. Recovery studies were done using either 30 mg Strata-X (Phenomenex Cat. 8B-S100-TAK-S) or 10 mg Oasis-HLB (Waters Cat. 186000383) cartridges with 50 pg or 5 pg of each eicosanoid in phosphate buffered saline. For these recovery studies, 50 pg of each internal standard was added to samples just prior to derivatization with AMPP (i.e. post-solid phase extraction). Recoveries were obtained by comparing the LC/ESI-MS/MS peak integrals to those obtained from a sample of eicosanoids that were derivatized with AMPP and injected directly onto the LC column without sample processing. Recovery yields are given in Table 3.1. The peak areas for the internal standards were similar in all samples studied (not shown) showing that the eicosanoid recoveries were similar regardless of sample matrix.

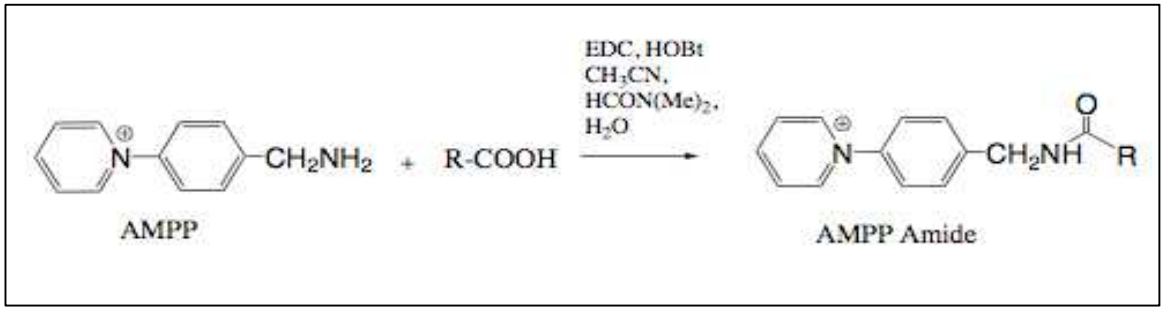


FIGURE 3.1: Structure of AMPP and an AMPP amide along with the reagents used for derivatization.

Section 3: Results and Discussion

Design and preparation of AMPP amides

Our goal was to develop a simple derivatization procedure to convert the carboxylic acid terminus of eicosanoids to a cationic group so that mass spectrometry could be carried out in positive mode. The tag should be designed so that fragmentation occurs in the analyte portion rather than in the tag portion so that the power of tandem mass spectrometry can be used for analytical specificity and sensitivity. Our computational analysis of substituted *N*-pyridinium methylamino derivatives[65] indicated that these had only moderate dissociation energies for loss of pyridine and other single bond cleavages in the linker, and thus might not be suitable for our purposes, which require fragmentation in the fatty acyl chain. Therefore, the charge tag was redesigned to strengthen the pyridinium N-C bond by inserting a phenyl ring as a linker. The phenyl ring also serves to enhance the derivative's interaction with the LC reverse phase column, which is necessarily used to minimize any matrix effects during ESI-MS/MS analysis. Density functional theory calculations (B3LYP/6-31G*) indicated that homolytic cleavage of the benzylic CH_2-N bond in the charge tag was a high-energy process that required > 350 kJ mol-1 of dissociation energy and was deemed not to out compete fragmentations in the fatty acyl chain (Figure 3.3). A side reaction that could not be evaluated with the model system shown in Figure 3.3 is elimination of 4-(*N*-

pyridyl)benzylamine, which gives rise to the *m*/*z* 183 marker fragment ion. An amide linkage of the charge tag to the analytic carboxylic acid was preferred over an ester since the former are generally more resistant to fragmentation in the mass spectrometer[66]. The final feature of the design of AMPP is its ease of synthesis in pure form.

We developed a simple synthesis of highly pure *N*-(4-aminomethylphenyl)-pyridinium (AMPP, Figure 3.2) and used it as a new derivatization reagent. We developed a simple method to convert the carboxyl group of lipid mediators to the AMPP amide using a well-known carbodiimide coupling reagent. Coupling conditions were optimized to give near quantitative formation of the AMPP amide. The was shown by converting the fluorescent fatty acid 10-pyrene-decanoic acid into its AMPP amide and examining the reaction mixture by fluorimetric HPLC and ESI-MS. No remaining 10-pyrenedecanoic acid was detected, and the AMPP amide was formed in >95% yield with <1% N-acyl urea formation (a common side product in carbodiimide-promoted couplings) (data not shown). Derivatization is carried out using

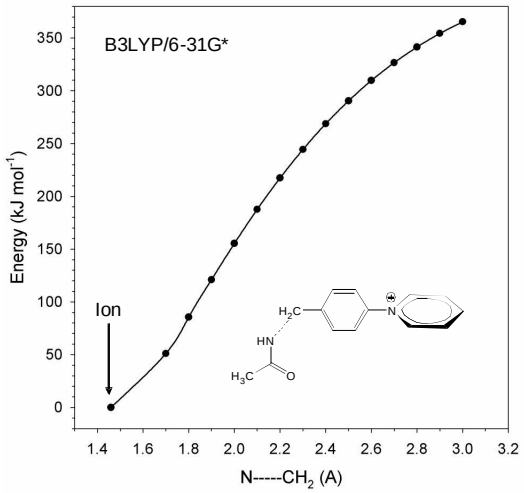
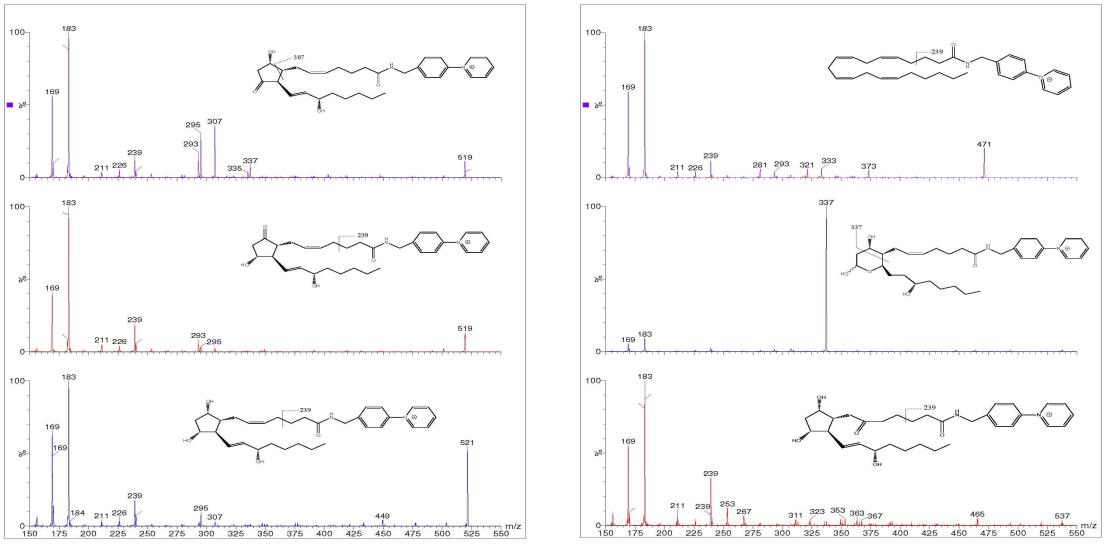


FIGURE 3.2: B3LYP/6-31G* calculated potential energy profile for the N—CH_2 benzylic bond dissociation in the charge tag. See text for further discussion.

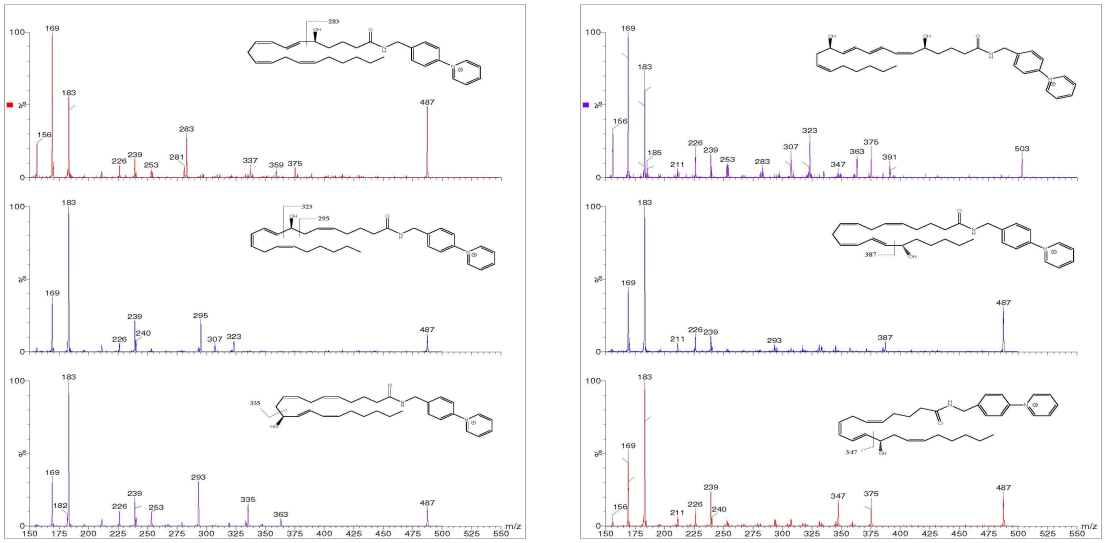
a single reagent cocktail in a small vial heated at 60°C for 30 min without the need for anhydrous or anaerobic conditions.

FIGURE 3.3: Fragment ion spectra of eicosanoid AMPP amides. (A) PGD_2, PGE_2, $PGF_{2\alpha\alpha}$; (B) arachidonic acid, TxB_2, 6-keto-$PGF_{1\,\alpha}$; (C) 5(*S*)-, 8(*S*)-, 11(*S*)-HETE; (D) LTB_4, 15(*S*)- and 12(*S*)-HETE.

A B



C D



LC/ESI-MSMS analysis of eicosanoid AMPP amides

In this study we focused on representative eicosanoids that do not contain peptides such as cysteinyl LT's. The analytes studied are PGD_2, PGE_2 and $PGF_{2\alpha}$, 6-keto-$PGF_{1\alpha}$ (the spontaneous breakdown product from prostacyclin, PGI_2), TxB_2 (the spontaneous breakdown product from TxA_2), LTB_4, 5(*S*)-HETE), 8(*S*)-HETE, 11(*S*)-HETE, 12(*S*)-HETE and 15(*S*)-HETE, and AA. ESI-MS/MS analysis with fragment ion scanning of AMPP amides of the analytes is shown in Figures 3.2 A-D. In all spectra, some cleavage of the AMPP tag occurs giving rise to the peaks at *m*/*z* = 169 and 183. To best ensure analytical specificity, we quantified the eicosanoids using a fragment in the analyte portion rather than in the AMPP tag. For PGD_2, we used the *m*/*z* = 307 fragment, which is likely due to cross-ring cleavage of the cyclopentanone ring and represents the most abundant non-tag fragment ion (Figure 3.4A). For PGE_2 and $PGF_{2\alpha}$, we used *m*/*z* = 239 due to cleavage between C3 and C4 (Figure 3.4A). For AA and 6-keto-$PGF_{1\alpha}$, we used *m*/*z* = 239, again due to C3-C4 cleavage (Figure 3.4B). The major non-tag fragment for TxB_2 is *m*/*z* = 337 due to cross-ring cleavage (Figure 3.4B). For all HETE species, we could identify a unique fragment ion (see Table 3.1) to avoid cross contamination of MS/MS signals due to partially unresolved LC peaks (Figure 3.4C, 3.4D). Finally, for LTB_4, we chose *m*/*z* = 323, which is the most abundant non-tag fragment ion but has a non-obvious origin.

Figure 3A

Figure 3B

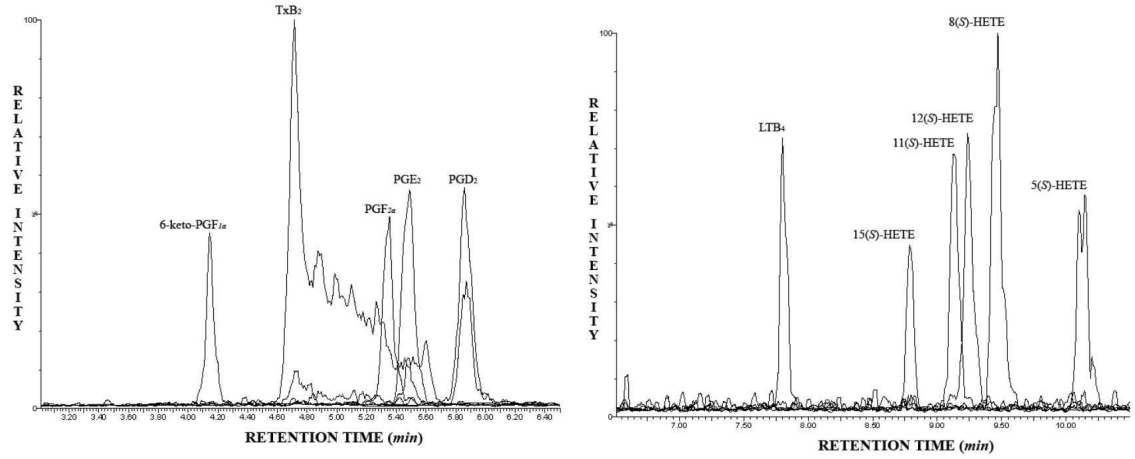


FIGURE 3.4: LC/ESI-MSMS traces of eicosanoids after workup from a solution in phosphate buffered saline. (A) Early eluting eicosanoids; (B) Latter eluting eicosanoids.

Next we studied a mixture of eicosanoids in phosphate buffered saline and optimized pre-ESI-MSMS sample workup and LC/ESI-MS/MS conditions. Critical for a successful method with ultra-sensitive analyte detection is high yield recovery of analytes from the sample prior to LC/ESI-MS/MS analysis. We found that solid phase extraction with a rapidly wettable matrix (Oasis HLB cartridges, Waters Inc. or Strata-X cartridges, Phenomenex) combined with analyte elution with methanol gave high yield recovery of all eicosanoids analyzed (Table 3.1). The data in Table 3.1 is based on 50 pg of each analyte submitted to recovery studies. When the same recovery studies were carried out with 5 pg of eicosanoid, results were essentially identical (data not shown). Inferior recoveries were obtained using elution of the solid phase cartridges with

acidified methanol or if the sample was subjected to liquid-liquid extraction or protein precipitation using various solvents (Not shown). Figure 3.5A and 3.5B shows a typical LC/ESI-MS/MS run of an eicosanoid mixture. All of the analytes examined elute from the LC column in less than 11 min. All HETEs except 11(*S*)- and 12(*S*)- are baseline resolved. The partial overlap of 11(*S*)- and 12(*S*)-HETEs is not a concern because completely selective fragment ions are being monitored. The LC elution profile and peak shape for both the derivatized and underivatized analytes (not shown) are similar. This shows that the presence of the quaternary ammonium group of the AMPP tag has no negative effect on the LC. TxB_2 gives rise to the typical broad peak shape due to interconversion between the two hemiacetal isomers. Also similar to underivatized analysis, the fragments used to monitor PGD_2 and PGE_2 (isobars of each other) are not completely unique to each species, but baseline LC resolution of these two eicosanoids resolves the issue. The same is true for the isobaric pair TxB_2 and 6-keto-$PGF_{1\alpha}$.

To ensure high yield conversion of eicosanoids to AMPP amides with minimal formation of *N*-acyl-ureas, we used a large excess of derivatization reagents. The AMPP tag and the EDCI coupling reagent elute in the void volume (not shown), and the HOBt elutes in the large time window between PGD_2 and LTB_4 (not shown). In subsequent studies, we discovered that the use of HOAt was equally as effective as HOBt in the formation of AMPP amides. The advantage of HOAt is that it elutes before any of the analyzed eicosanoids and thus simplifies the solvent bypass parameters required to

avoid source contamination with the large excess of derivitization reagents. With consideration for these parameters, the removal of these reagents is not necessary prior to LC/ESI-MS/MS.

Standard curve analysis was performed starting below the limit of quantification up to two orders of magnitude above this limit. In all cases, the mass spectrometry response was linear from the limit of quantification up to the highest amount analyzed (19 pg on-column for the Waters Quattro Micro and 5-10 pg on-column for the Waters Quattro Premier). We define limit of quantification as the amount of eicosanoid AMPP amide needed to give an ESI-MS/MS signal that is 10-fold the noise (as determined using the Waters MassLynx software). Limit of quantification for all eicosanoid AMPP amides are listed in Table 3.1. The values using the Waters Quattro Micro are 5 pg for all eicosanoids except 12(*S*)-HETE (10 pg) and AA (10 pg). With the Waters Quattro Premier the values are 0.2-0.5 pg for all eicosanoids except 12(*S*)-HETE (0.9 pg) and AA (1 pg). We also determined limit of quantification of underivatized eicosanoids analyzed by LC/ESI-MS/MS in negative ion mode. Values are shown in Table 3.1 for the Waters Quattro Micro and the Waters Quattro Premier. The new method using AMPP amides is found to be 10- to 20- fold more sensitive on both

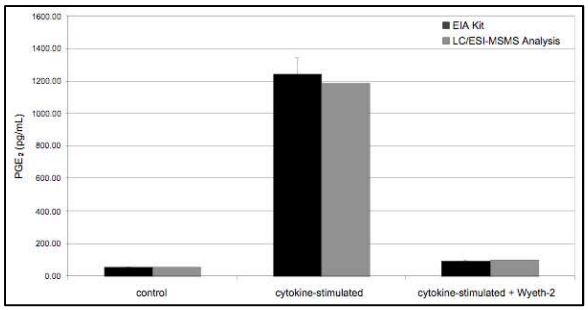


FIGURE 3.5: AMPP LC/ESI-MS/MS method cross-validation with commercial EIA kit.

instruments. This constitutes a significant improvement in detection sensitivity of eicosanoids.

To validate the above stated estimates of the limit of quantification, we injected eicosanoids standard mixtures 6 times on the Waters Quattro Premier, where each analyte was injected at roughly twice the estimated limit of quantification. Values of CV for analyte to internal standard peak ratios for each analyte are listed in Table 3.1. These CV's validate our estimates for the limits of quantification by demonstrating that eicosanoid analysis can be performed with reasonable reproducibility proximal to these stated values.

Next, we more thoroughly investigated the reproducibility of the AMPP derivatization method for eicosanoid analysis. The results are summarized in Table 3.2. Three repetitive LC/ESI-MS/MS analyses of an identical sample (19 pg on-column levels of each eicosanoid) gave coefficients of variation in the range of 2.4 to 12.7 % range. We also prepared 3 independent mixtures of eicosanoids (50 pg each) in phosphate buffered saline, submitted each to sample work-up and analyzed each by LC-ESI-MS/MS (19 pg on-column) (Table

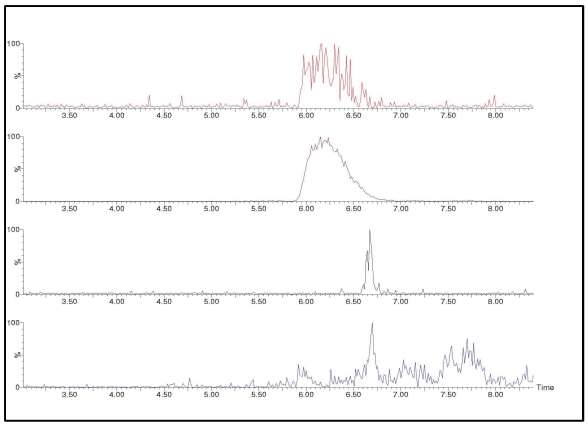


FIGURE 3.6: Selected ion traces for LC/ESI-MSMS analysis of eicosanoids in mouse serum. Panel 1 is for d_4-TxB_2, panel 2 is for TxB_2, panel 3 is for d_4-$PGF_{2\alpha}$, and panel 4 is $PGF_{2\alpha}$.

3.2). Coefficients of variation ranged from 2.8 to 28.2 %. We also analyzed 3 independent serum aliquots (10 μL), and the coefficient of variation ranged from 3.7 to 13.7 %.

TABLE 3.2: Coefficient of variation (%) for LC/ESI-MSMS analysis of eicosanoid AMPP amides.

	Intra-sample[1]	Inter-sample (10 μL PBS)[2]	Inter-sample (10 μL Serum)[3]
6-keto-$PGF_{1\alpha}$	4.9	16.9	not detected
TxB_2	2.4	3.0	3.7
$PGF_{2\alpha}$	8.1	6.5	6.4
PGE_2	8.0	9.2	not detected
PGD_2	4.5	8.3	not detected
LTB_4	7.3	17.2	7.3
5(*S*)-HETE	3.3	2.8	6.4
8(*S*)-HETE	6.7	20.3	13.7
11(*S*)-HETE	5.5	12.2	8.8
12(*S*)-HETE	5.2	10.7	6.3
15(*S*)-HETE	4.0	5.8	12.4
Arachidonic acid	12.7	28.2	7.9

[1]Coefficient of variation for the analysis of the same sample of 1.25 pg/μl of eicosanoid standards injected 3 times onto the LC/ESI-MSMS.
[2]Coefficient of variation for the analysis of 3 independent samples of 1.25 pg/μl of eicosanoid standards. (50 pg of standards spiked into phosphate buffered saline and worked up as described in Methods section for LC/ESI-MSMS.)
[3]Coefficient of variation for 3 separate serum samples spiked with internal standards only.

TABLE 3.3: Eicosanoid levels (pg/μl) in mouse serum.[1]

Serum (μL)	TxB_2	$PGF_{2\alpha}$	LTB_4	5(*S*)-HETE	8(*S*)-HETE	11(*S*)-HETE	12(*S*)-HETE	15(*S*)-HETE	Arachidonic acid
1	46	15	198	748	393	437	11345	240	28623
1	49	11	340	1075	545	646	17840	703	23246
5	43	13	174	792	490	350	14116	617	14900
5	43	11	169	986	469	350	16512	672	16631
10	51	9	255	971	586	536	15108	749	12200
10	39	13	248	958	593	416	14487	732	15476

[1]Eicosanoids not listed in the table were not detected

We then analyzed the set of endogenous eicosanoids present in mouse serum in order to test the AMPP derivatization method on a complex biological sample. Representative LC/ESI-MS/MS traces are shown in Figure 3.7 for a relatively high abundant serum eicosanoid (TxB_2) and a relatively low abundant eicosanoid ($PGF_{2\alpha}$).

Eicosanoids levels are shown in Table 3.3 for multiple runs and with different volumes of serum analyzed.

As another example of low-level eicosanoid analysis in a complex biological matrix, we also analyzed eicosanoid formation in calcium ionophore stimulated primary bronchial epithelial cells. Results are summarized in Table 3.4. Finally, we cross-validated the AMPP method with a commercially available antibody-based assay kit. We analyzed PGE_2 production by Rat 3Y1 cells and compared the results obtained via LC/ESI-MSMS analysis of AMPP amides with those obtained from EIA kit. Results are summarized in Figure 3.6 and show that there is strong agreement between the two methods.

TABLE 3.4: Eicosanoid levels (pg/ml) from primary human bronchial cells[1].

	Non-stimulated	(+) Ca ionophore
TxB_2	4	7
$PGF_{2\alpha}$	170	300
PGE_2	105	195
PGD_2	25	22
11(*S*)-HETE	5	19
Arachidonic acid	880	1210

[1]Eicosanoids not listed in the table were not detected. Values are for 0.47 million cells per sample stimulated in 200 µl of Hank's balanced salt solution.

Section 4: Summary

We developed a simple derivatization procedure to convert carboxylic acids to AMPP amides and showed that this significantly improves the sensitive for detection of eicosanoids by LC/ESI-MSMS. Antibody-based quantifications of eicosanoids have a limit of quantification around 1 pg, and the method requires that each analyte be quantified

in a single assay well. Thus, if 12 eicosanoids are to be analyzed, one requires a sample containing ~12 pg of each species. The AMPP amide method disclosed in the current study can detect all 12 eicosanoid species in a single sample containing ~0.3-1 pg of each eicosanoid and is thus more than an order of magnitude more sensitive than antibody based detection. Previously reported LC/ESI-MS/MS detection of underivatized eicosanoids in negative ion mode provide limit of quantification in 10 pg range[22, 60] (see also our data in Table 3.1), and thus our method is more than an order of magnitude more sensitive than these methods. We are currently studying the use of AMPP to improve the detection sensitivity for other oxygenated fatty acids including cysteinyl-leukotrienes, lipoxins, resolvins and protectans. Analysis of the full spectrum of fatty acids should be feasible based on the results with AA reported in this study. This new method based on AMPP amides should find widespread use in the quantification of lipid mediator levels where sample supply is limited.

TABLE 3.5: Autosampler (2795 Alliance HT LC) and ESI-MS/MS (Waters Quattro Micro) data collection parameters.

Injection type	Sequential	
Fill mode	Partial loop	
Pre-sample airy boundary	2 μL	
Post-sample air boundary	2 μL	
Post-injection wash frequency	10 cycles	
Flush time	6 sec	
Wash time	15 sec	
Secondary wash volume	600 μL	
	Negative Mode	**Positive Mode**
Capillary Voltage (kV)	(-) 2.8	(+) 3.5
Extractor (V)	3	3
RF Offset	0.2	0.2
Dwell Time (msec)	50	50
Inter-Scan Delay (msec)	10	10
Inter-Channel Delay (msec)	100	100
Source Temp (^{o}C)	130	130
Desolvation Temp (^{o}C)	500	500
Desolvation Gas (L/Hr)	1100	1100
Cone Gas (L/Hr)	25	25
Collision Cell Entrance (V)	-2	-2
Collision Cell Exit (V)	1	1

TABLE 3.6: Autosampler (Water ACQUITY UPLC) and ESI-MS/MS (Waters Quattro Premier) data collection parameters.

Injection type	Sequential
Fill mode	Partial loop with needle overfill
Weak wash volume (H_2O)	600 μL
Strong wash volume (50:50 ACN:MeOH)	200 μL
Pre-Aspirate air gap	Automatic
Post-Aspirate air gap	Automatic
Syringe draw rate	Automatic
Needle placement	Automatic

	Negative Mode	**Positive Mode**
Capillary Voltage (kV)	-2.8	+3.25
Extractor (V)	5	5
RF Offset	0.0	0.0
Dwell Time (msec)	50	50
Inter-Scan Delay (msec)	5	5
Inter-Channel Delay (msec)	10	10
Source Temp (^oC)	130	130
Desolvation Temp (^oC)	450	450
Desolvation Gas (L/Hr)	900	900
Cone Gas (L/Hr)	0	0
Collision Cell Entrance (V)	-5	-5
Collision Cell Exit (V)	0	0

Section 5 : Addendum to Chapter 3

3.5.a Method parameters for Waters Xevo TQ/Acquity UPLC

The AMPP derivitization method for eicosanoids was adapted for a recently acquired Waters Xevo TQ triple quadrupole mass spectrometer interfaced to an Acquity UPLC. The MassLynx 4.1 software package was used for data collection and analysis. Chromatography was carried out with a C18 reverse-phase column (Waters Acquity UPLC BEH Shield RP18, 2.1 x 100 mm, 1.7 μm, Cat. # 186002854). Solvent A is 100% water (Fisher Optima Grade Cat. # L-13780)/0.1% formic acid (Fisher Optima Grade Cat. # A117-50), and solvent B is ACN (Fisher Optima Grade Cat. # L-14338)/0.1% formic acid. The solvent program is (linear gradients): 0-0.25 min, 95% A; 0.25-0.26 min, 95% - 92.5% A; 0.26-1.25 min, 92.5% - 90.5% A; 1.25-1.3 min, 90.5% - 75% A; 1.3-2.8 min, 75% A; 2.8-2.9 min, 75% – 60% A; 2.9-4.5 min, 60% - 55% A; 4.5-5 min, 55% - 1% A; 5-7 min, 1% A; 7-7.1 min, 1% – 95% A; 7.1-10 min, 95% A. The flow rate is 0.4 mL/min and column temperature is 45 ^{o}C. Tables 3.7 and 3.8 summarize the auto-sampler and ESI-MS/MS parameters for AMPP amide data collection on the Waters Xevo TQ mass spectrometer coupled to a Waters Acquity UPLC.

Similarly, we adapted our LC/ESI-MS/MS assay of underivatized eicosanoids in negative ion mode for use on the Waters Xevo TQ instrument. The same LC column, solvent A and B, column temperature, and flow rate was used as for the AMPP amides.

The solvent program was slightly modified as follows: 0-0.25 min, 95% A; 0.25-0.3 min, 95% - 85% A; 0.3-1.3 min, 85% - 79% A; 1.3-1.35 min, 79% - 65% A; 1.35-2.95 min, 65% - 50% A; 2.95-3 min, 50% - 40% A; 3-5 min, 40% - 34% A; 5-5.05 min, 34% - 1% A; 5.05-6.95 min, 1% A; 6.95-7 min, 1% - 95% A; 7-10 min, 95% A. Total time between injections is 10 minutes. Values of m/z for precursor and product ions were as published[64], and cone voltages and collision energies were optimized for each instrument and for each analyte in the usual way. Tables 3.7 and 3.8 summarize the auto-sampler and ESI-MS/MS parameters for underivatized eicosanoid data collection in negative ionization mode on the Waters Xevo TQ and Acquity UPLC instruments.

TABLE 3.7 : Autosampler (Acquity UPLC) and ESI-MS/MS (Waters Xevo TQ) data collection parameters for underivatized and AMPP amide eicosanoids.

Injection type	Sequential
Load ahead	Disabled
Pre-aspirate air gap	Automatic
Pre-aspirate air gap	Automatic
Weak Wash Solvent	0.1% Formic Acid/5% ACN in H_2O
Weak wash volume	1000 μL
Strong wash solvent	0.1 % Formic acid in CAN
Stron wash volume	1000 μL

	Negative Mode	**Positive Mode**
Capillary Voltage (kV)	(-) 1.0	(+) 0.5
Extractor (V)	3	3
Aperture	0.1	0.1
Gain	1	1
Dwell Time (msec)	50	50
Inter-Scan Delay (msec)	10	10
Inter-Channel Delay (msec)	100	100
Source Temp (^oC)	150	150
Desolvation Temp (^oC)	600	600
Desolvation Gas (L/Hr)	1000	1000
Cone Gas (L/Hr)	25	25
Collision Gas Flow (mL/min)	0.15	0.15
Collision Cell Entrance (V)	0.5	0.5
Collision Cell Exit (V)	0.5	0.5

TABLE 3.8: Liquid chromatography retention times (Waters Acquity UPLC) and tandem mass spectrometry parameters for eicosanoid AMPP amide molecular species (Waters Xevo TQ).

Eicosanoid	Notes	LC retention time (min)[1]	AMPP-amide SRM[4] (*m/z*)	UD Eicosanoid SRM[4] (*m/z*)	Cone voltage[5] (V)	Collision energy[5] (eV)
Tetranor-PGFM	$[M]^{2+}$ AMPP	1.48	332->239	329->311	42/18	30/14
Tetranor-PGDM	$[M\text{-}H_2O]^{2+}$ AMPP $[M]^{2+}$ AMPP	1.71	322->239 331->239	327->309 327->309	42/20 42/20	33/12 33/12
PGDM	$[M]^{2+}$ AMPP $[M\text{-}H_2O]^{+}$ AMPP Underivatized LC lactone	2.18	331->239 477->349	309->265	42/20	32/13
Tetranor-PGEM	$[M]^{2+}$ AMPP	1.57	331->239	327->309	40/25	30/12
2,3-Dinor-6-Keto-$PGF_1\alpha$	Underivatized LC lactone	2.29	509->239 509->437	341->135 341->135	72/35 72/35	55/25 45/25
2,3-Dinor-11B-$PGF_1\alpha$		2.43	493-449	325->145	62/24	33/12
2,3-Dinor-TXB_2		2.38	509->309	341->167	55/25	40/12
11-Dehydro-TXB_2		3.28	535->447	367->305	60/28	35/16
12-HHTrE		3.88	447->239	279->163	46/25	42/15
6-keto-$PGF_1\alpha$		2.40	537->239	369->163	66/36	52/28
11β-$PGF_1\alpha$		2.84	521->447	353->193	64/35	44/24
$PGF_{2\beta}\alpha$		3.17	521->239	353->193	65/35	48/24
PGE_2		3.22	519->239	351->271	65/21	40/17
PGD_2		3.47	519->307	351->271	70/17	48/17
TxB_2		2.75	537->337 537->337	369->169 369->195	65/22 65/22	43/16 43/16
LTB_4		3.83	503->323	335->195	52/32	36/16
5(S)-HETE		4.70	487->283	319->115	60/26	40/15
8(S)-HETE		4.53	487->323	319->155	60/28	34/16
11(S)-HETE		4.43	487->335	319->167	62/28	34/16
12(S)-HETE		4.45	487->375	319->179	60/28	35/15
15(S)-HETE		4.30	487->387	319->175	60/26	34/14
Tetranor-12-HETE		3.84	433->253	265->109	50/25	36/12
D6-Tetranor-PGDM	$[M\text{-}H_2O]^{2+}$ AMPP $[M]^{2+}$ AMPP	1.66	334-239	333->315	42/20	33/15
D4-PGDM	$[M]^{2+}$ AMPP $[M\text{-}H_2O]^{+}$ AMPP Underivatized LC lactone	2.17	333->242 481->349	313->265	42/20	32/13
D6-Tetranor-PGEM	$[M]^{2+}$ AMPP	1.56	334->239	333->315	40/18	30/13
D9-2,3-Dinor-6-Keto-$PGF_1\alpha$	Underivatized LC lactone	2.28	518->239 518->446	350->135 350->161	72/35 72/35	55/25 45/23
D4-11-Dehydro-TXB_2		3.26	539->451	371->309	58/28	36/16
D_4-6-keto-$PGF_1\alpha$		2.40	541->241	373->167	70/35	60/28
D4-11β-$PGF_1\alpha$		2.84	525->241	357->197	60/34	46/25
D4-$PGF_{2\beta}\alpha$		3.14	525->241	357->197	65/34	48/25

Eicosanoid	Notes	LC retention time (min)[1]	AMPP-amide SRM[4] (*m/z*)	UD Eicosanoid SRM[4] (*m/z*)	Cone voltage[5] (V)	Collision energy[5] (eV)
D9-PGE_2		3.18	528->239	360->280	65/20	46/17
D9-PGD_2		3.41	528->307	360->280	70/18	48/18
D4-TxB_2		2.74	541->341 541->341	373->173 373->199	65/21 65/21	43/19 43/17
D4-LTB_4		3.85	507->325	339->197	50/32	35/16
D8-5(S)-HETE		4.68	495->284	327->116	60/25	40/16
D8-12(S)-HETE		4.43	495->381	327->184	60/27	35/15
D8-15(S)-HETE		4.28	495->394	327->226	60/26	35/14

[1]The first number is for the AMPP amide eicosanoid assay, and the second number is for the underivatized eicosanoid assay.
[2]LOQ values are for eicosanoid AMPP amides in positive mode.
[3]LOQ values are for underivatized eicosanoids analyzed by LC/ESI-MS/MS in negative mode.
[4]*m/z* Values listed are calculated monoisotopic values. The actual values used are derived from instrument tuning, which is instrument dependent.
[5]Cone voltages and collision energies were optimized for each analyte. These numbers are instrument dependent. The first number is for eicosanoid AMPP amide analysis in positive ion mode, and the second number is for underivatized eicosanoid analysis in negative ion mode.

3.5.b Substitution of HOBt with HOAt

During the course of transferring the AMPP amide method to the Waters Xevo TQ instrument, it occurred to us that we might be able eliminate any potential ion suppression and ion source contamination issues introduced by the excess of derivitization reagents by substituting HOAt for the previously used HOBt. We reasoned that HOAt was comparably more polar than HOBt and would thus elute off the LC column earlier and increase the separation between the latest eluting of the coupling reagents (EDC1 and uncoupled AMPP elute in the void volume) from the earliest eluting of the eicosanoids. Using the LC gradient detailed in section 3.5.a, we analyzed the MS full scan elution profile of all the AMPP method's amide coupling reagents. As expected, unreacted AMPP and EDCI elute in the void volume and HOAt elutes prior to HOBt.

Thus, All coupling reagents elute significantly ahead of the most polar of the eicosanoids. When used in conjunction with proper divert valve settings, MS/MS analysis of AMPP amides should be free of any potential ion suppression or source contamination issues that might be introduced by the use of excess AMPP amide derivitization reagents. All other method parameters were left unchanged and AMPP amide yields were deemed equivalent (data not shown).

3.5.c Eicosanoids from sPLA$_2$ incubations of platelet derived microparticles

Isolation of human platelets, generation of platelet microparticles, and subsequent sPLA$_2$ enzymatic incubations were performed by Dr. Luc Boudreau in the laboratory of Dr. Eric Boilard at Centre de Recherche du CHU de Quebec. Human blood was drawn from healthy donor with citrate as anticoagulant. Human platelets were prepared as previously described[67]. Briefly, blood was centrifuge at 180 x *g* for 10 min at RT. Platelet-rich plasma was then centrifuge at 400 x *g* at RT to remove contaminant red blood cells and supernatant was centrifuge at 1300 x *g* for 5 min at RT to obtain the platelet pellet. Platelets were resuspended in 200 μl of Tyrode Buffer pH 6.5 (134 mM NaCl, 2.9 mM KCl, 0.34 mM Na_2HPO_4, 12 mM $NaHCO_3$, 20 mM HEPES, 1mM $MgCl_2$, 5 mM glucose and 0.5 mg/ml BSA) and then transferred into Tyrode Buffer pH 7.4 at a concentration of 1 x 10^8 cells/ml.

For the preparation of platelet microparticles, 5 mM of $CaCl_2$ and 0.5 μg/ml of collagen was added to the platelet cell suspension. Platelets were stimulated overnight

and 20 mM of EDTA was added the following day to quench the stimulation. The suspension was then centrifuge at 2000 x *g* for 10 min at RT to remove remaining platelets and supernatant was then centrifuge at 16 000 x *g* for 90 min at 18°C to pellet platelet microparticles. Platelet microparticles were resuspended in Tyrode Buffer pH 7.4 (without BSA) at a concentration of 2 x 10^5 microparticles/ml supplemented with 5 mM $CaCl_2$.

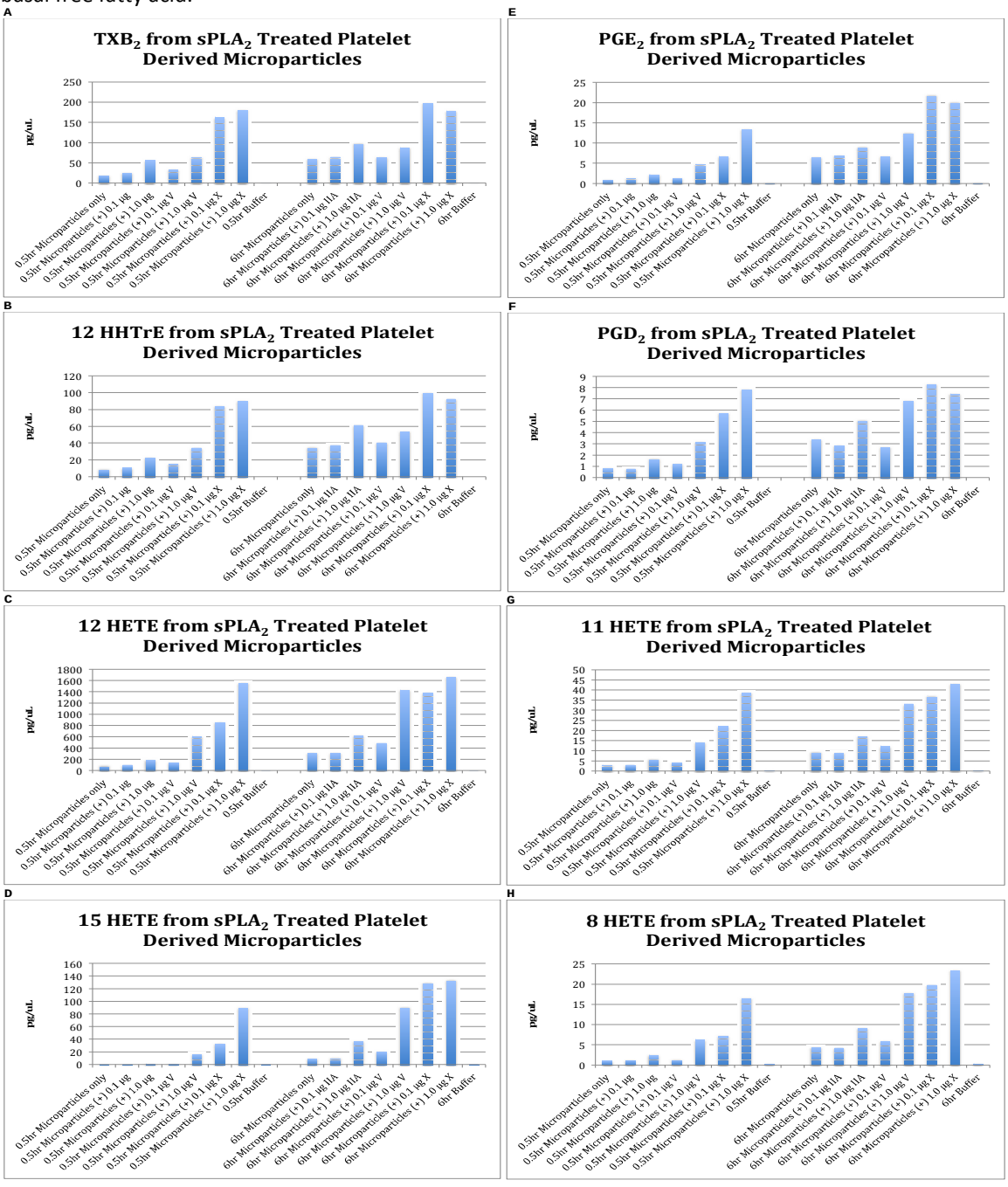
TABLE 3.9: Eicosanoid levels (pg/µl) in $sPLA_2$ enzymatic incubations of platelet derived microparticles

	TxB_2	$PGF_{2\alpha}$	PGE_2	PGD_2	8(*S*)-HETE	11(*S*)-HETE	12(*S*)-HETE	15(*S*)-HETE	12-HHTrE
0.5hr Microparticles only	20.6	0.5	1.1	0.9	1.2	3.2	99.0	1.0	9.5
0.5hr Microparticles (+) 0.1 µg IIA	26.5	0.5	1.5	0.8	1.4	3.1	103.2	1.1	11.5
0.5hr Microparticles (+) 1.0 µg IIA	58.2	0.7	2.2	1.7	2.5	6.2	196.6	2.2	23.7
0.5hr Microparticles (+) 0.1 µg V	35.0	1.0	1.5	1.3	1.4	4.5	150.6	1.8	16.4
0.5hr Microparticles (+) 1.0 µg V	66.7	2.3	5.0	3.2	6.4	14.4	620.0	17.5	34.5
0.5hr Microparticles (+) 0.1 µg X	164.0	2.9	6.8	5.8	7.3	22.4	864.5	33.7	84.6
0.5hr Microparticles (+) 1.0 µg X	182.7	3.2	13.5	7.9	16.7	38.9	1566.8	90.9	91.3
0.5hr Buffer only	0.0	0.0	0.3	0.0	0.5	0.4	0.5	0.2	0.0
6 hr Microparticles only	60.9	2.5	6.7	3.4	4.6	9.7	324.9	10.2	35.3
6hr Microparticles (+) 0.1 µg IIA	66.0	2.4	7.1	2.9	4.4	9.3	331.4	11.2	37.8
6hr Microparticles (+) 1.0 µg IIA	99.1	2.8	9.1	5.1	9.3	17.6	630.4	38.3	61.9
6hr Microparticles (+) 0.1 µg V	66.3	2.3	6.9	2.8	6.0	12.6	493.0	21.7	41.4
6hr Microparticles (+) 1.0 µg V	89.1	4.1	12.6	6.9	18.0	33.2	1447.6	91.0	54.8
6hr Microparticles (+) 0.1 µg X	200.5	6.8	21.9	8.4	19.8	37.4	1396.6	130.0	100.4
6hr Microparticles (+) 1.0 µg X	179.4	5.1	20.3	7.5	23.5	43.5	1681.1	134.0	93.2
6 hr Buffer only	0.0	0.0	0.3	0.0	0.5	0.4	0.4	0.2	0.0

[1] Significant changes were not observed for eicosanoids omitted from the table.

Platelet microparticles were incubated at 37°C in presence of 0.1 μg/ml and 1 μg/ml of recombinant $sPLA_2$-IIA, $sPLA_2$-V or $sPLA_2$-X for 30 min and 6 h. Platelet microparticles were also incubated in absence of $sPLA_2$ to determine the content of basal free fatty acid. Following incubation, each reaction was quenched via the addition of 20 mM of EGTA.

FIGURE: 3.7 Eicosanoids generated from platelet derived microparticles. Microparticles were incubated at 37°C in presence of 0.1 µg/ml and 1 µg/ml of recombinant $sPLA_2$-IIA, $sPLA_2$-V or $sPLA_2$-X for 30 min and 6 hours. Platelet microparticles were also incubated in absence of $sPLA_2$ to determine the content of basal free fatty acid.



Chapter 4

Improved Sensitivity Mass Spectrometric Detection of Fatty Acids by Charge Reversal Derivatization

Section 1: Introduction

The analysis of fatty acids (FA's) is of considerable importance to both the clinical and biomedical research communities at large. From the clinical perspective, perturbations of FA metabolism have important physiological implications for a variety of medical conditions such as obesity, cardiovascular disease, and diabetes mellitus[68]. Attention from the biomedical community is largely derived from the observation that some FA's, in particular the non-esterified fractions of polyunsaturated species such as arachidonic acid (AA) and docosohexaenoic acid (DHA), have distinct roles as precursors to important lipid signaling molecules[44, 69]. Given their diverse biological roles and implication in a host of pathological conditions, considerable effort is dedicated to the development of methodologies to reliably and accurately assess FA composition and metabolism in a host of biological contexts. To meet these ends, tandem mass spectrometry (MS/MS) has emerged as the premier analytical platform due to its sensitivity, specificity, and ability to be directly coupled to chromatography systems[23].

Early quantitation methods for free FA's typically relied on gas chromatography (GC) coupled to a mass spectrometer (MS) via either electron impact or flame ionization

sources. The advantages of GC include high specificity, sensitivity, and good reproducibility[70]. Resolution of fatty acids by GC requires prior derivatization to increase their volatility and thermal stability. Historically, this has typically been accomplished by esterification of the carboxyl moiety to its respective methyl[71], trimethylsilyl[72], or pentafluorobenzyl ester[73]. The utility of these GC methods was greatly enhanced through the development of novel ionization sources and tandem MS/MS instrumentation capable of selected reaction monitoring (SRM) experiments. SRM detects fragmentation products of specific chemical species at the exclusion of potential interference from chemical noise and co-eluting compounds with identical masses. The analytical specificity of these experiments enables the direct quantitative analysis of species from very complex biological mixtures. Although useful, these methods are still limited by dynamic range limitations and compound volatility considerations[74]. Additionally, their derivitization procedures have the potential to introduce unwanted variability via oxidation or isomerization of some FA's and can ultimately mask some lipid structural information.

In an effort to address the shortcomings of GC-MS methodologies, protocols utilizing liquid chromatography (LC) were developed to analyze FA's in their non-derivatized, free carboxylate form[75]. The relatively recent development of "softer" ionization techniques such as electrospray ionization (ESI) and atmospheric pressure chemical ionization (APCI) has permitted the coupling of LC to MS detectors and enabled

the direct analysis of FA carboxylate anions. However, a major obstacle to this technique is a FA's less than ideal fragmentation behavior via collision-induced dissociation (CID). Under low-energy (< 100 eV) CID conditions typical to most commercial instruments, fragmentation of the featureless backbone of a saturated FA is minimal. Furthermore, the most prominent fragments originate from the loss of CO_2 (−44 *amu's*) and elimination of water (−18 *amu's*) from the carboxylic acid group, neither of which are specific enough for reliable quantitation in complex matrices. Unsaturated FA's do undergo, to some extent, fragmentations that are specific to their structure. However, the intensities of these fragmentations are relatively weak and result in SRM measurements of poor sensitivity. Another major limitation of this approach is related to a FA's relative ionization efficiency and the manner in which the ions are analyzed. For compounds that contain free carboxylates such as FA's, ionization is best achieved in negative ion mode under basic pH conditions where the carboxylate is ionized[75]. Unfortunately, optimal LC chromatographic resolution is facilitated by acidic pH conditions where ionization of the carboxylate is suppressed. Post-column addition of base could potentially alleviate this problem at the expense of the method's simplicity and sensitivity.

One group recently reported a LC-ESI-MS/MS method of FA analysis in plasma using post-column infusion of a barium ion solution[76]. The formation of positively charged adduct ions promotes diagnostic fragmentation reactions of unsaturated FA

species with enhanced SRM detection sensitivity. Other cation reagents, including alkaline earth metals and copper ions, also proved suitable for enhanced sensitivity for FA analysis in the SRM mode[77]. An alternative strategy for enhanced sensitivity is to improve the ionization efficiency of FA's via specific derivatization with reagents that introduce either readily chargeable or fixed charge groups such as tertiary or quaternary amines, respectively. Many derivatives of this nature have been reported including: pyrolidides[78], picolinyl esters[79], dimethyloxazolines[79c, 79d, 80], benzofurazans[81], pyridiniums[61c, 82], and cholines[61a]. The advantages of these derivatives include improved MS sensitivity and reproducible chromatography profiles. Again, as with the GC derivatization procedures, a major limitation of these methodologies is the relatively harsh conditions usually required for their synthesis, which may result in unwanted oxidation, isomerization, or degradation of some FA's. This limitation could potentially be addressed by the development of robust derivatization procedures that require milder conditions. Another major limitation is the tendency of these derivatives to fragment via CID in immediate proximity to the chargeable/cationic site. Fragmentation in the derivatization tag is undesirable due to the fact that analytes that form isobaric precursor ions and co-elute during LC will not be distinguished in the mass spectrometer if they give rise to the same detected fragment ion, essentially eliminating any advantage a MS/MS experiment has over a MS one. This loss of specificity poses serious analytical issues when analyzing complex biological samples.

We recently reported a straightforward LC-ESI-MS/MS derivitization procedure for the targeted lipidomic analysis of eicosanoids via stable isotope dilution[83]. Our methodology employed a simple solid-phase extraction procedure of eicosanoids from a variety of biological matrices followed by a mild, quantitative derivatization step with fixed-charge reagent. The resulting derivatives can be directly submitted to LC-ESI-MS/MS and display robust fragmentations in their analyte segments, making them attractive candidates for high-sensitivity/specificity SRM experiments. Here we utilize a similar approach, with the exception of an alternative extraction method, to monitor the free FA profile of mouse serum as well as platelet-derived microparticle/mitochondria samples treated *in vitro* with members of the secreted phospholipase A_2 ($sPLA_2$) family of enzymes. We developed and validated a stable isotope dilution LC-ESI-MS/MS method that is able to detect and quantify over 30 saturated and unsaturated FA's in a single chromatographic run.

Section 2 : Materials and Methods

Preparation of reagents and materials for fatty acid analysis

4.2.a Synthesis of AMPP

N-(4-aminomethylphenyl)-pyridinium (AMPP) was synthesized in-house as described previously[83]. Subsequent to our lead publication, the AMPP reagent was made commercially available by Cayman Chemical Company (Cat. # 710000) under the product name AMP+ Mass Spectrometry Kit.

4.2.b Pre-derivitization work-up of glassware, solvents, and reagents

All glassware used for extraction and pre-LC-ESI-MS/MS work-up was baked overnight in a high temperature oven at 450°C to remove any residual fatty acid contamination. Similarly, isooctane (Sigma Chromasolv Plus Cat. # 650439), DMF (Sigma Cat. # 227056), Milli-Q water, and ACN (Fisher Optima Grade Cat. # L-14338) were of the highest available purity and distilled in-house (DMF distilled under vacuum) with an oven baked (450 ^{o}C, overnight) distillation apparatus into oven baked glass-stoppered flasks. Finally, EDCI (TCI America Cat. # D1601), HOAt (Sigma Cat. # 44545-2), and AMPP were triturated with distilled isooctane to remove any residual fatty acid contamination.

Preparation of fatty acid stock solutions

The following fatty acid standards from Cayman Chemicals were used (D_{14}-Palmitoleic acid, D_{14}-α-Linolenic acid, D_4-Linoleic acid, D_5-Eicosapentaenoic acid, D_8-Arachidonic acid, D_{17}-Oleic acid, D_6-Dihomo-γ-Linolenic, D_5-Docosohexaenoic acid, Stearidonic acid, and Arachidonic acid (ω-3). D_{31} Palmitic acid and D_{35} Stearic acid are from Sigma-Aldrich. GLC-463 standard (Nu-Check Prep. Inc.), containing 52 distinct molecular FA species, was used for the rest of the calibration standards. Stock solutions of fatty acids were prepared at concentration of 25-100 pg/μl in absolute ethanol and stored at -80°C under Ar in, 1.5 mL amber vials (Agilent Cat. # 5182-0716) with PTFE/silicone septum screw caps (Agilent Cat. # 5185-5838). Serial dilutions of the stock solutions were made in absolute ethanol for standard curve and extraction recovery

analysis. Internal standards were diluted to a working stock of 100 pg/µl in absolute ethanol.

Preparation of samples prior to derivatization with AMPP

4.2.a Standard curves.

Each sample contained 1 ng of each internal standard and various amounts of non-isotopic fatty acids (added from serial dilutions of the stock solution described above) transferred to a glass auto-sampler vial (Waters Total Recovery Screw Cap Vial cat. # 186002805). Solvent was removed with a stream of nitrogen, and the residue was derivatized with AMPP as described below.

4.2.b Preparation of recombinant $sPLA_2$'s

Recombinant $sPLA_2$ enzymes were generous gifts from Farideh Ghomaschi and Alan Singer and were prepared as previously described[25].

4.2.c Preparation of platelet derived microparticles

Isolation of human platelets and generation of platelet microparticles was performed by Dr. Luc Boudreau in the laboratory of Dr. Eric Boilard at Centre de Recherche du CHU de Quebec. Experimental details are detailed in the addendum to Chapter 3.

4.2.d Isolation of mitochondria

Isolation of mitochondria was performed by Dr. Luc Boudreau in the laboratory of Dr. Eric Boilard at Centre de Recherche du CHU de Quebec. Mitochondria were

isolated from mouse liver of C57BL/6 (The Jackson Laboratory Strain # 000664) mice with the Q-proteome mitochondria isolation kit (QIAgen) according to the manufacturer's protocol. All centrifugation steps were performed at 4°C. The resulting mitochondria pellet was resuspended in Tyrode's Buffer pH 7.4, labeled with anti-VDAC-FITC (Biorbyt), counted by flow cytometry on a BD Bioscience CANTO II and finally resuspended at 2 x 10^5 mitochondria/μl in Tyrode's Buffer pH 7.4 (without BSA) supplemented with 5 mM $CaCl_2$.

4.2.e Incubation of mitochondria and platelet derived microparticles in presence of $sPLA_2$.

Enzymatic incubations of mitochondria and platelet microparticles with selected $sPLA_2$'s were performed by Dr. Luc Boudreau in the laboratory of Dr. Eric Boilard at Centre de Recherche du CHU de Quebec.Mitochondria and platelet microparticles were incubated at 37°C in presence of 0.1 μg/ml and 1 μg/ml of recombinant $sPLA_2$-IIA, $sPLA_2$-V or $sPLA_2$-X for 30 min and 6 h. Platelet microparticles and mitochondria were also incubated in absence of $sPLA_2$ to determine the content of basal free fatty acid. Following incubation, the reaction was stopped with the addition of 20 mM of EGTA.

4.2.f Extraction of fatty acids from platelet derived microparticles treated with $sPLA_2$'s.

Frozen $sPLA_2$ incubations of microparticle samples were thawed on ice. An aliquot of 25 μL was transferred to a 12 X 75 mm glass culture tube (Fisher cat. # 14-961-26). To each sample, 50 μL of absolute ethanol containing 1 ng of each internal

standard was added. The samples were subsequently processed by liquid-liquid extraction as described in [84]. Briefly, each 75 μL sample was diluted to 125 μL distilled Milli-Q water. Aliquots of 250 μl of methanol (Fisher Optima Grade Cat. # A456-4) and 12.5 μl of 1N HCl were added to each sample. A bi-phasic solution was then formed via addition of 750 μl of isooctane. This solution was vortexed for 60 sec and the phases were separated by centrifugation at 3000 rpm for 60 seconds. The upper isooctane phase was removed via oven baked glass pasteur pipet and transferred to an oven baked Waters Total Recovery vial. The remaining aqueous phase was extracted once more with an additional 750 μl of isooctane. The combined isooctane phases were evaporated to dryness under a stream of filtered N_2 and derivatized with AMPP as described below.

4.2.g Extraction of fatty acids from platelet derived mitochondrion treated with sPLA$_2$'s.

Frozen sPLA$_2$ incubations of mitochondria samples were thawed on ice. An aliquot of 25 μL was transferred to a 12 X 75 mm glass culture tube and 50 μL of absolute ethanol containing 1 ng of each internal standard was added. Samples were subsequently extracted as detailed above for the microparticle samples.

4.2.h Extraction of fatty acids from mouse serum

Analysis of endogenous eicosanoids in serum was carried out with commercial mouse serum (Atlantic Biologicals catalog # S18110). A 10 μL aliquot of serum was transferred to a 12 X 75 mm glass culture tube. To each culture tube, 50 μL of absolute

ethanol containing 1 ng of each internal standard was added and the samples were extracted as detailed for microparticle analysis.

Table 4.1: Liquid chromatography retention times and tandem mass spectrometry parameters for analysis of fatty acid AMPP amide molecular species.

Fatty Acid Molecular Species	LC retention time (min)[1]	Retention Window[2]	Internal Standard	Precursor ion[3] (*m/z*)	Fragment ion[3] (*m/z*)	Cone Voltage[4] (V)	Collision Energy[4] (eV)
Dodecenoic (*11*-**12:1**)	4.37	**1**	**A**	365	239	56	42
Lauric (**12:0**)	4.96	**1**	**A**	367	239	60	44
Myristoleic (*9Z*-**14:1**)	5.35	**1**	**A**	393	239	58	44
Myristic (**14:0**)	6.04	**1**	**A**	395	239	62	47
Palmitoleic (*9Z*-**16:1**)	6.34	**1**	**A**	421	239	60	47
Palmitoleic (9*E*-**16:1**)	6.5	**1**	**A**	421	239	60	47
Palmitic (**16:0**)	7.02	**1**	**B**	423	239	65	49
Stearidonic (*6Z,9Z,12Z,15Z*-**18:4**)	5.8	**1**	**A**	443	239	64	42
α-Linolenic (*9Z,12Z,15Z*-**18:3**)	6.21	**1**	**C**	445	239	64	46
					337	64	38
γ-Linolenic (*6Z,9Z,12Z*-**18:3**)	6.29	**1**	**C**	445	239	64	45
					347	64	38
Linoleic (*9Z,12Z*-**18:2**)	6.7	**1**	**D**	447	239	65	48
Linoleic (*9E,12E*-**18:2**)	6.96	**1**	**D**	447	239	65	48
Oleic (*9Z*-**18:1**)	7.26	**1**	**E**	449	239	64	45
Petroselinic (*6Z*-**18:1**)	7.26	**1**	**E**	449	239	64	45
Vaccenic (*11Z*-**18:1**)	7.26	**1**	**E**	449	239	64	45
Stearic (**18:0**)	7.91	**2**	**G**	451	239	66	45
Eicosapentaenoic (*5Z,8Z,11Z,14Z,17Z*-**20:5**)	6.26	**1**	**F**	469	239	62	42
Arachidonic (*5Z,8Z,11Z,14Z*-**20:4**)	6.73	**1**	**H**	471	239	70	50
					373	70	40
ω3-Arachidonic (*8Z,11Z,14Z,17Z*-**20:4**)	6.6	**1**	**H**	471	239	70	50
					363	70	40
Eicosatrienoic (*11Z,14Z,17Z*-**20:3**)	7.07	**1**	**I**	473	239	70	50
					365	70	40
Dihomo-γ-Linolenic (*8Z,11Z,14Z*-**20:3**)	7.07	**1**	**I**	473	239	70	50
					375	70	38
Eicosadienoic (*11Z,14Z*-**20:2**)	7.53	**1**	**E**	475	239	65	52
5-Eicosenoic (*5Z*-**20:1**)	8.29	**2**	**G**	477	239	70	50
8-Eicosenoic (*8Z*-**20:1**)	8.15	**2**	**G**	477	239	70	50
11-Eicosenoic (*11Z*-**20:1**)	8.08	**2**	**G**	477	239	70	50
Arachidic (**20:0**)	8.74	**2**	**G**	479	239	66	55
Docosohexaenoic (4Z,7Z,10Z,13Z,16Z,19Z-**22:6**)	6.74	**1**	**J**	495	239	64	36
Docosopentaenoic (*7Z,10Z,13Z,16Z,19Z*-**22:5**)	6.98	**1**	**J**	497	239	65	55
Docosopentaenoic (*4Z,7Z,10Z,13Z,16Z*-**22:5**)	6.98	**1**	**J**	497	239	65	55
Docosotetraenoic (*7Z,10Z,13Z,16Z*-**22:4**)	7.41	**1**	**J**	499	239	65	55
Docosotrienoic (*13Z,16Z,19Z*-**22:3**)	7.88	**2**	**G**	501	239	65	55

Fatty Acid Molecular Species	LC retention time (min)[1]	Retention Window[2]	Internal Standard	Precursor ion[3] (*m/z*)	Fragment ion[3] (*m/z*)	Cone Voltage[4] (V)	Collision Energy[4] (eV)
Docosodienoic (*13Z,16Z*-**22:2**)	8.33	**2**	**G**	503	239	65	55
Erucic (*13Z*-**22:1**)	8.85	**2**	**G**	505	239	65	55
Behenic (**22:0**)	9.51	**2**	**G**	507	239	65	55
Nervonic (*15Z*-**24:1**)	9.59	**2**	**G**	533	239	70	60
Lignoceric (**24:0**)	10.22	**2**	**G**	535	239	65	55
Internal Standards							
(A) D14 Palmitoleic (*9Z*-**16:1**)	6.3	**1**	**A**	435	242	60	47
(B) D31 Palmitic (**16:0**)	6.92	**1**	**B**	455	242	65	55
(C) D14 a-Linolenic (*9Z,12Z,15Z*-**18:3**)	6.17	**1**	**C**	459	242	64	48
(D) D4 Linoleic (*9Z,12Z*-**18:2**)	6.75	**1**	**D**	451	239	68	44
(E) D17 Oleic (*9Z*-**18:1**)	7.28	**1**	**E**	466	239	68	48
(F) D5 Eicosapentaenoic (*5Z,8Z,11Z,14Z,17Z*-**20:5**)	6.31	**1**	**F**	474	239	62	43
(G) D35 Stearic (**18:0**)	7.81	**2**	**G**	487	242	65	58
(H) D8 Arachidonic (*5Z,8Z,11Z,14Z*-**20:4**)	6.77	**1**	**H**	479	239	65	45
(I) D6 Dihomo-g-Linolenic (*8Z,11Z,14Z*-**20:3**)	7.04	**1**	**I**	479	239	70	46
(J) D5 Docosohexaenoic (*4Z,7Z,10Z,13Z,16Z,19Z*-**22:6**)	6.73	**1**	**J**	501	239	64	36

[1]Retention times listed are derived from the LC protocol detailed in the Materials/Methods section.
[2]Data for retention window 1 was collected from minutes 4.0 to 7.65. Data for retention window 2 was collected from minutes 7.65 to 10.
[3]*m/z* Values listed are calculated monoisotopic values. The actual center mass values used are derived from instrument tuning, which is instrument dependent.
[4]Cone voltages and collision energies were optimized for each analyte. These numbers are instrument dependent.

Derivatization with AMPP

To the residue in the oven baked Waters Total Recovery auto-sampler vial was added 10 μL of ice-cold ACN/DMF (4:1, v:v). Then 10 μL of ice-cold 1M EDCI in distilled Milli-Q water (freshly prepared daily) was added. The vial was briefly mixed on a vortex mixer and placed on ice while other samples were processed as above. To each vial was added 20 μL of 5 mM HOAt/15mM AMPP in distilled acetonitrile (Stored at -20°C and warmed to 65°C immediately prior to use). The vials were mixed briefly on a vortex

mixer, capped with a split-septum screw cap (Agilent Cat. # 5185-5824), and placed in a 60°C incubator for 30 min. Samples were analyzed on the same day and kept in the auto-sampler rack at 10 °C while queued for injection.

LC/ESI-MS/MS analysis

Studies were carried out on a Waters Xevo TQ triple quadrupole mass spectrometer interfaced to an Acquity UPLC. The MassLynx 4.1 software package was used for data collection and analysis. Chromatography was carried out with a C18 reverse-phase column (Waters Acquity UPLC BEH Shield RP18, 2.1 x 100 mm, 1.7 μm, Cat. # 186002854). Solvent A is 100% water (Fisher Optima Grade Cat. # L-13780)/0.1% formic acid (Fisher Optima Grade Cat. # A117-50), and solvent B is ACN (Fisher Optima Grade Cat. # L-14338)/0.1% formic acid. The solvent program is (linear gradients): 0-0.5 min, 90% A; 0.5-0.51 min, 90% – 80% A; 0.51-10.0 min, 80% – 30% A; 10.0-10.1 min, 30% – 0% A; 10.1-12.0 min, 0% A; 12.0-12.1 min, 0% – 90% A; 12.1-15.0 min, 90% A. The flow rate is 0.4 mL/min and column temperature is set to 45 ^{o}C. Tables 4.1 and 4.2 summarize the auto-sampler and ESI-MS/MS parameters for data collection.

TABLE 4.2: Autosampler (Waters Acquity UPLC) and ESI-MS/MS (Waters Xevo TQ) data collection parameters for underivatized and AMPP amide eicosanoids.

Injection type	Sequential
Load ahead	Disabled
Pre-aspirate air gap	Automatic
Pre-aspirate air gap	Automatic
Weak Wash Solvent	0.1% Formic Acid/5% ACN in H_2O
Weak wash volume	1000 μL
Strong wash solvent	0.1 % Formic acid in ACN
Stron wash volume	1000 μL
	Positive Mode
Capillary Voltage (kV)	(+) 0.5
Extractor (V)	3
Aperture	0.1
Gain	1
Dwell Time (msec)	50
Inter-Scan Delay (msec)	10
Inter-Channel Delay (msec)	100
Source Temp (^oC)	150
Desolvation Temp (^oC)	600
Desolvation Gas (L/Hr)	1000
Cone Gas (L/Hr)	25
Collision Gas Flow (mL/min)	0.15
Collision Cell Entrance (V)	0.5
Collision Cell Exit (V)	0.5

Section 3: Results

FIGURE 4.1: Unsaturated Fatty acid profile of $sPLA_2$-GIIA, $sPLA_2$-GV, and $sPLA_2$-GX incubations with platelet derived microparticles.

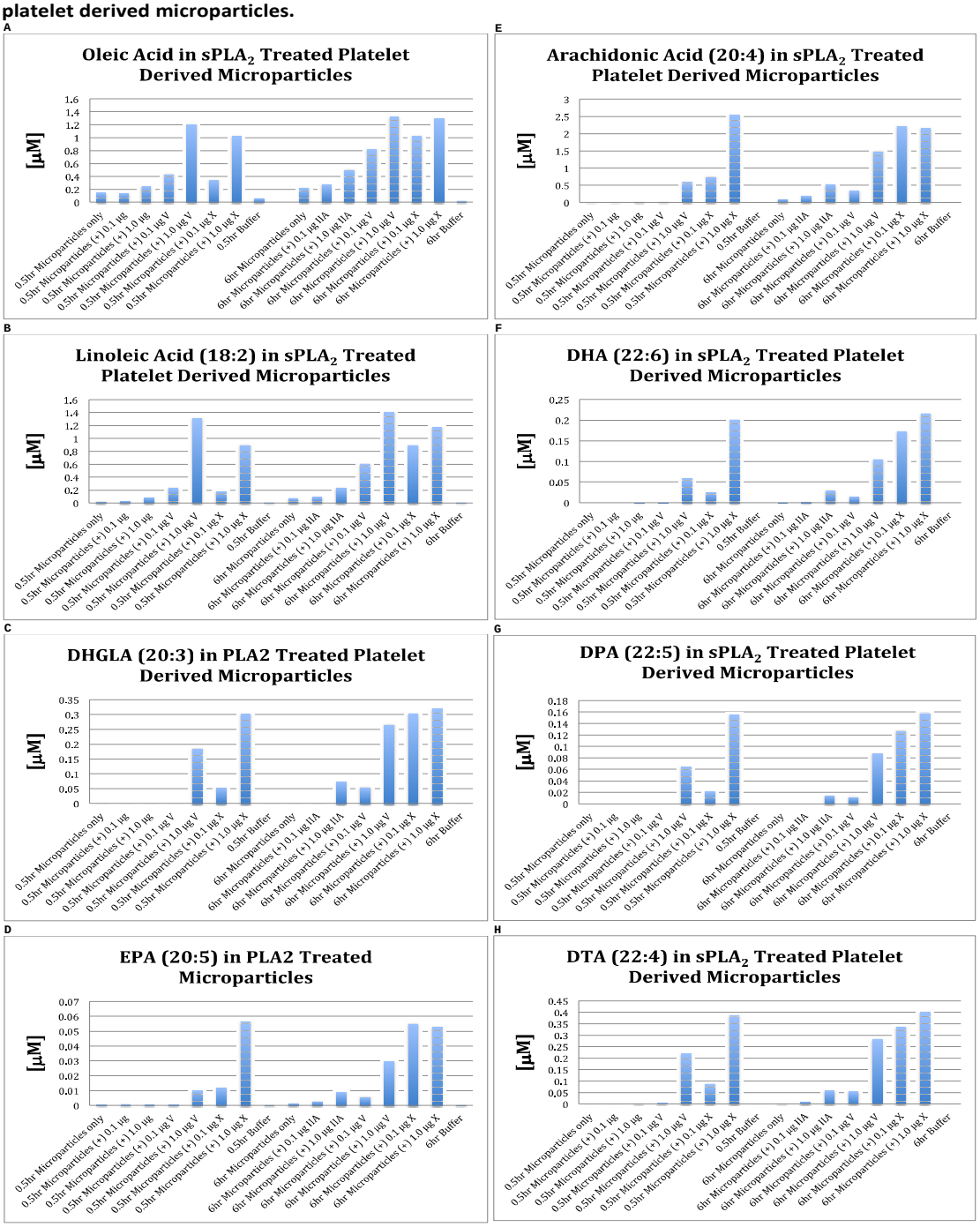


FIGURE 4.2: Unsaturated fatty acid profile of $sPLA_2$ treated mitochondria isolated from mouse liver.

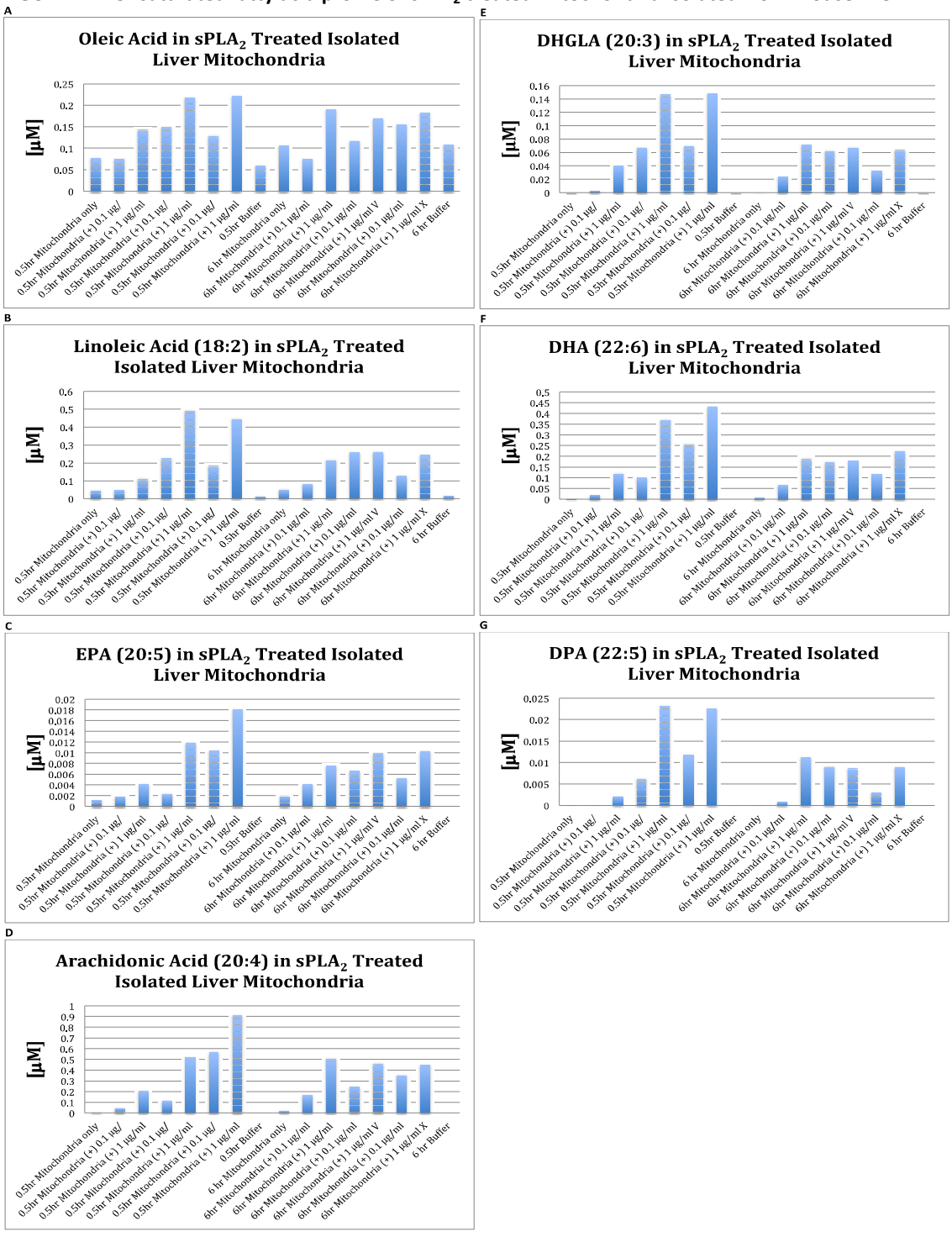
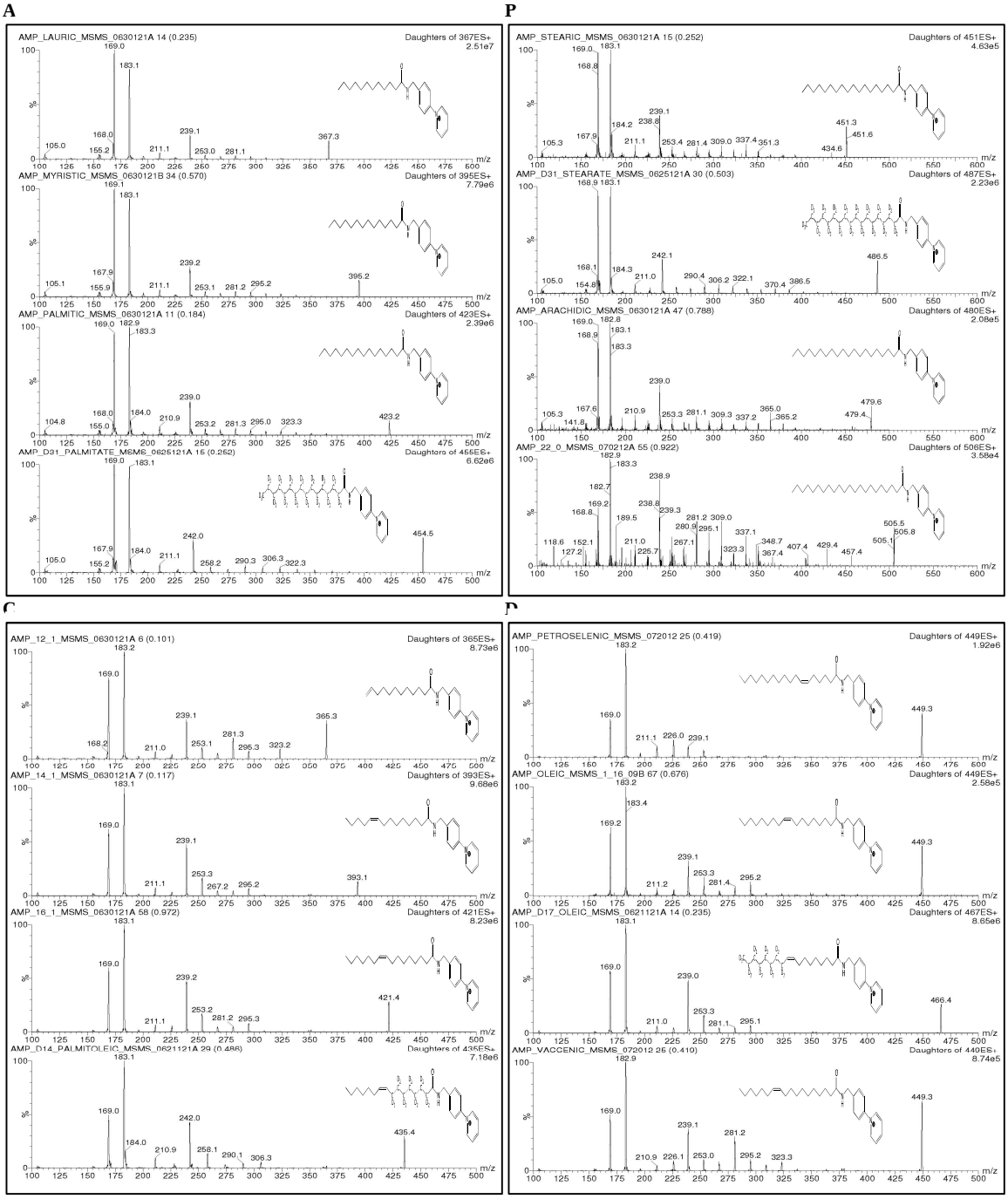
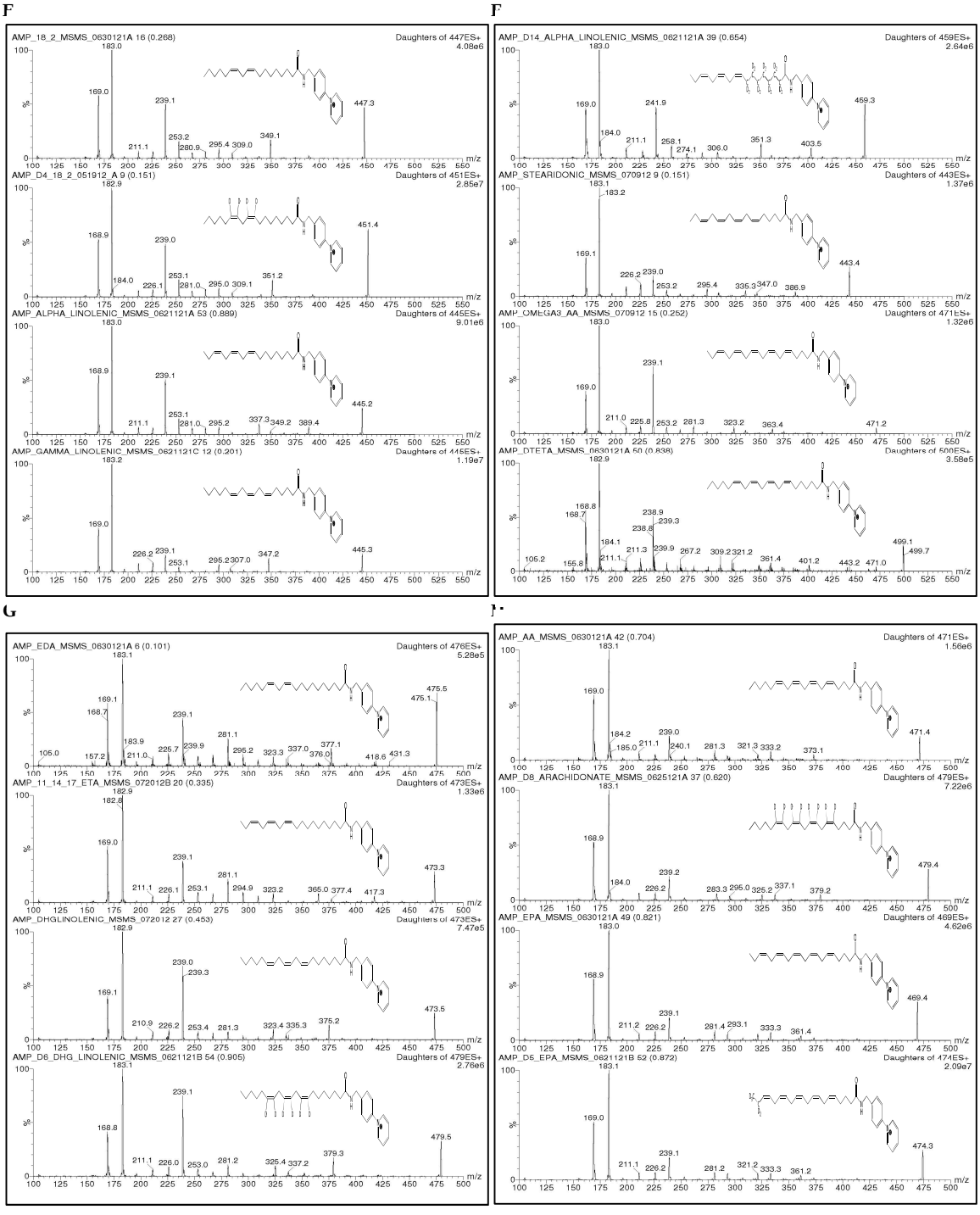


FIGURE 4.3: Fragment ion spectra of unsaturated fatty acid AMPP amides. **(A)** Lauric, Myristic, Palmitic, D_{31}-Palmitic, **(B)** Stearic, D_{35}-Stearic, Arachidic, Docosanoic, **(C)** Dodecenoic, Myristoleic, Palmitoleic, D_{14}-Palmitoleic, **(D)** Petroselenic, Oleic, D_{17}-Oleic, Vaccenic **(E)** Linoleic, D_4-Linoleic, α-Linolenic, γ-Linolenic **(F)** D_{14}-α-Linolenic, Stearidonic, ω3-Arachidonic, Docosotetraenoic **(G)** Arachidonic, D_8-Arachidonic, Eicosapentanoic, D_5-Eicosapentanoic **(H)** Eicosadienoic, Eicosatrienoic, Dihomo-γ-Linolenic, D_6-Dihomo-γ-Linolenic **(I)** ω3-Docosopentaenoic, ω6-Docosopentaenoic, Docosohexaenoic, and D_5-Docosohexaenoic.




F
AMP_18_2_MSMS_0630121A 16 (0.268)
Daughters of 447ES+
4.08e6
AMP_D4_18_2_051912_A 9 (0.151)
Daughters of 451ES+
2.85e7
AMP_ALPHA_LINOLENIC_MSMS_0621121A 53 (0.889)
Daughters of 445ES+
9.01e6
AMP_GAMMA_LINOLENIC_MSMS_0621121C 12 (0.201)
Daughters of 445ES+
1.19e7
E
AMP_D14_ALPHA_LINOLENIC_MSMS_0621121A 39 (0.654)
Daughters of 459ES+
2.64e6
AMP_STEARIDONIC_MSMS_070912 9 (0.151)
Daughters of 443ES+
1.37e6
AMP_OMEGA3_AA_MSMS_070912 15 (0.252)
Daughters of 471ES+
1.32e6
AMP_DTETA_MSMS_0630121A 50 (0.838)
Daughters of 500ES+
3.58e5
G
AMP_EDA_MSMS_0630121A 6 (0.101)
Daughters of 476ES+
5.28e5
AMP_11_14_17_ETA_MSMS_072012B 20 (0.335)
Daughters of 473ES+
1.33e6
AMP_DHGLINOLENIC_MSMS_072012 27 (0.453)
Daughters of 473ES+
7.47e5
AMP_D6_DHG_LINOLENIC_MSMS_0621121B 54 (0.905)
Daughters of 479ES+
2.76e6
H
AMP_AA_MSMS_0630121A 42 (0.704)
Daughters of 471ES+
1.56e6
AMP_D8_ARACHIDONATE_MSMS_0625121A 37 (0.620)
Daughters of 479ES+
7.22e6
AMP_EPA_MSMS_0630121A 49 (0.821)
Daughters of 469ES+
4.62e6
AMP_D5_EPA_MSMS_0621121B 52 (0.872)
Daughters of 474ES+
2.09e7
m/z

I

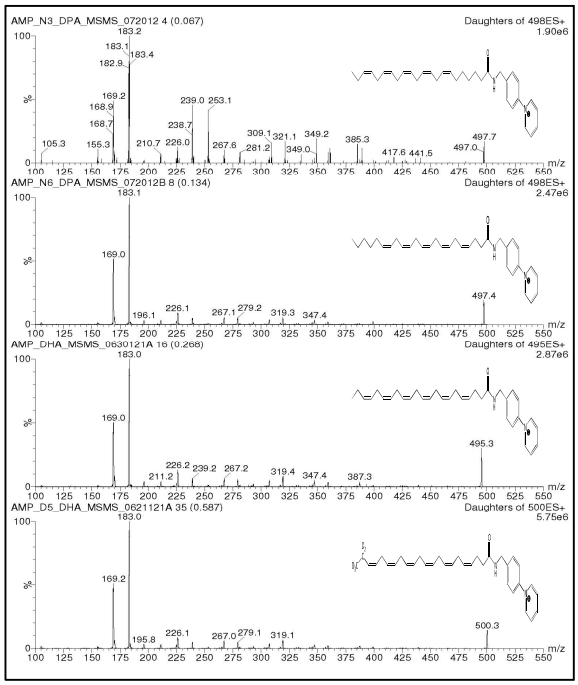

AMP_N3_DPA_MSMS_072012 4 (0.067)
Daughters of 498ES+
1.90e6
AMP_N6_DPA_MSMS_072012B 8 (0.134)
Daughters of 498ES+
2.47e6
AMP_DHA_MSMS_0630121A 16 (0.268)
Daughters of 495ES+
2.87e6
AMP_D5_DHA_MSMS_0621121A 35 (0.587)
Daughters of 500ES+
5.75e6
m/z

Table 4.3: Calculated concentrations (pg/μl) and coefficients of variation (%) for LC/ESI-MS/MS analysis of fatty acid AMPP amides in commercial mouse serum.

		Intra-sample (10 μL of Serum)[1]	Inter-sample (10 μL of Serum)[2]
Dodecenoic	6.1	15.6	14.1
Lauric	143.2	3.1	7.6
Myristoleic	12.9	1.2	5.8
Myristic	299.4	2.2	3.0
Palmitoleic	295.8	0.8	2.6
Palmitic	1286.9	1.2	5.3
Linolenic	12.5	7.6	2.7
α-LInolenic	13.1	3.0	2.7
γ-Linoleic	462.0	0.6	3.2
Oleic	2066.1	1.1	4.3
Stearic	1820.4	1.8	6.1
Eicosapentaenoic	72.0	0.9	3.7
Arachidonic	873.0	1.7	5.2
ω3-Arachidonic	24.2	4.8	5.9
Dihomo-γ-Linolenic	301.0	2.5	1.5
Eicosatrienoic	18.3	2.4	1.5
Eicosadienoic	53.9	1.7	3.8
Eicosenoic Acid	98.7	1.4	2.4
Arachidic	21.4	2.9	8.1
Docosohexaenoic	605.6	4.4	6.9
Docosopentaenoic	148.2	3.9	7.9
Docosotetraenoic	66.9	3.5	9.0
Docosotrienoic	14.5	2.4	2.7
Docosodienoic	0.8	3.1	2.7
Erucic	8.3	3.0	10.4
Behenic	7.6	1.7	5.3
Nervonic	20.6	3.5	6.0
Lignoceric	18.6	1.9	7.8

[1]Coefficient of variation for the analysis of the same sample of extracted and derivatized serum injected 5 times onto the LC/ESI-MS/MS.

[2]Coefficient of variation for the analysis of 6 independently extracted and derivatized serum samples.

Chapter 5

Comparison of the PLA_1 and PLA_2 Enzymatic Activities of a Panel of Mammalian $cPLA_2$ Isoforms

Section 1: Introduction

In this study, we utilize our recently developed LC-ESI-MS/MS method (See Chapter Two) for LPL's to analyze the PLA_1 and PLA_2 activities of human $cPLA_2$-α, human $cPLA_2$-γ, human $cPLA_2$-ε, human $cPLA_2$-δ, mouse $cPLA_2$-β, and mouse $cPLA_2$-ζ. The results presented here are part of larger analysis of the mouse $cPLA_2$-β isoform that compares the *in vitro* interfacial kinetic and binding properties of this enzyme to those of the other isoforms[85]. The five recently discovered $cPLA_2$'s were initially classified as such based on their sequence homology to $cPLA_2$-α, an enzyme with a characteristic specificity for GPL's with PUFA's esterified in the *sn-2* position. As initially discussed in Chapter One, $cPLA_2$'s are α/β lipid hydrolases that utilize serine in their active site and commonly have alterative enzymatic activities other than their namesake. This study is meant to facilitate a broader understanding of these alternative activities in the endeavor to reveal potential cellular roles for these recently discovered $cPLA_2$ isoforms.

Section 2 : Methods

Materials

The following phospholipids are from Avanti Polar Lipids, Inc. (Alabaster, AL):

POPC; POPI; POPG; POPA; POPE; and POPS. Stock solutions of GPL's were prepared in chloroform/methanol (2:1). Phospholipid concentrations in stock solutions were determined by inorganic phosphate assay using the ammonium molybdate procedure on acid-degraded samples[54]. Human cPLA2-α, human cPLA2-γ, human $cPLA_2$-ε, human $cPLA_2$-δ, mouse cPLA2-β, and mouse cPLA2-ζ (~90% pure) were prepared as described previously[41, 85-86]. All other reagents are from Sigma-Aldrich.

Kinetic Studies

Vesicles were prepared by extrusion through 0.2 μm membranes as described (1) and diluted to a final total GPL concentration of 50 μM in 80 μl of 10 mM MOPS, pH 7.2, 100 mM KCl, 0.5 mM EGTA containing either ~100 μM or no free calcium. Reactions were carried out in polypropylene microcentrifuge tubes at 37 °C for 10 min. Precise vesicle compositions and concentrations are given in the table legends.

GPL's used for studying the PLA_1 activity using mass spectrometry were purified as follows to remove trace amounts of LPL's. POPC, POPA, POPS, POPE, and POPG (5 mg) were individually injected onto a normal phase HPLC column (Varian MonoChrom 5 μm, Si, 1 X 25 cm, catalog no. A0501-250-X100) in 1:1 solvent A (30:40, v/v, *n*-hexane/isopropyl alcohol)/solvent B (43:47:10, v/v, *n*-hexane/isopropyl alcohol, 100 mM ammonium formate in water). The solvent program is as follows: 0–5 min, 25% B; 5–35 min, 25–70% B; 35–36 min, 70–99% B, 36–45 min, 99% B; 45–46 min, 99 to 25% B at 3

ml/min. A splitter was used to divert a portion of the column eluant (0.05 ml/min) to the mass spectrometer; the main stream was connected to a fraction collector. GPL and LPL molecular species were monitored by mass spectrometry as described in Chapter Two except that full scan (400–900 atomic mass units) mass spectrometry was carried out instead of tandem mass spectrometry. POPI was not purified because no LPI contaminant was detected by mass spectrometry. Reaction mixtures contained extruded phospholipid vesicles (50 μM total phospholipid) in 10 mM MOPS, pH 7.2, 100 mM KCl, 0.5 mM EGTA, and sufficient $CaCl_2$ to give ~100 μM free Ca^{2+} (monitored using Calcium GreenTM-2, Invitrogen). Reactions were started by adding 2 μg of each $cPLA_2$ and incubated for 10 min at 37 °C. Reactions were extracted for LPL analysis as described in Chapter 2 (because the sample did not contain plasmalogens, the two-stage extraction procedure was not used; rather the sample was acidified and extracted with organic solvent). The 1-palmitoyl-LPL's and the 2-oleoyl-LPL's were quantified by liquid chromatography/tandem mass spectrometry as described in Chapter Two of this thesis with the LC gradient detailed in the notes immediately following that chapter.

Section 3 : Results and Discussion

We studied the PLA_1 *versus* PLA_2 activity of recombinant $cPLA_2$ isoforms cloned from mammalian genomes. Liquid chromatography combined with electrospray tandem mass spectrometry was used to measure the amount of 1-palmitoyl-sn-glycero-

3-phosphocholine (PLA_2) and 2-oleoyl-*sn*-glycero-3-phosphocholine (PLA_1) formed during enzymatic incubations of prepared vesicles. All studies were carried out with 100 μM Ca^{2+}. and the results with POPC vesicles are summarized in Table 5.1. Mouse cPLA$_2$-β displays a PLA_1/PLA_2-specific activity ratio of 1.3 showing that it is a dual PLA_1/PLA_2 enzyme (Table 5.1, entry 1). In contrast, human cPLA$_2$-α is mainly a PLA_2, displaying a PLA_1/PLA_2 ratio of 0.1 (Table 5.1, entry 2). Human cPLA2-γ is a better PLA_2 than a PLA_1 (Table 5.1, entry 3). Human cPLA2-δ has much higher PLA_1 activity than PLA_2 activity (Table 5.1, entry 4). Again, human cPLA2-ε has very low PLA_2 activity, and its PLA_1 activity is also relatively low (Table 5.1, entry 5). The PLA1 and PLA_2 activities of mouse cPLA2-ζ are comparable (Table 5.1, entry 6).

TABLE 5.1: PLA_1 versus PLA_2 activities of cPLA$_2$s (POPC vesicles).

Enzyme	PLA_1 Specific activity (100 μM Ca^{2+}) [(nmol/min)/mg protein]	PLA_2 Specific activity (100 μM Ca^{2+}) [(nmol/min)/mg protein]	PLA_1/PLA_2 Activity Ratio
m-cPLA$_2$β	0.08	0.06	1.3
h-cPLA$_2$α	0.36	4.4	0.1
h-cPLA$_2$γ	0.02	0.10	0.2
h-cPLA$_2$δ	6.0	1.13	5.3
h-cPLA$_2$ε	0.02	0.00[1]	
h-cPLA$_2$ζ	0.13	0.84	0.15
m-cPLA$_2$ζ	0.65	1.07	0.6

[1]Although no activity was detected by mass spectrometry, h-cPLA$_2$ε has detectable PLA_2 activity when measured using the more sensitive radiometric assay (Table 1 of [85]).

We also prepared mixed phospholipid vesicles composed of 50 mol % POPC and 10 mol %each of POPG, POPA, POPE, POPS, and POPI. We monitored the formation of palmitoyl-containing *sn*-1 LPL species (PLA_2) and oleoyl-containing *sn*-2 LPL species (PLA_1), and the results are summarized in Table 5.2. Interestingly, mouse cPLA$_2$-β

preferentially utilized anionic GPL's (POPA, POPS, and POPG) over zwitterionic phospholipids (POPC and POPE) in mixed GPL vesicles, and the activity on anionic phospholipids is mainly as a PLA_2 and not as a PLA_1 (Table 5.2, entries 1–6). The activity of mouse PLA2-β on the POPC in these vesicles is mainly as a PLA_1, whereas in another study utilizing pure PAPC vesicles it displays both PLA_1 and PLA_2 activities (Table 2, entry 1 of [85]). Human cPLA2-α displays a high PLA_2/PLA_1 ratio on all GPL's in the mixed vesicles and prefers POPC (Table 5.2, entries 7–12). As for the other isoforms, human $cPLA_2$-γ displays low PLA_1 and PLA_2 activity on all GPL species (Table 5.2, entries 13–18). Human $cPLA_2$-δ displays a high PLA_1/PLA_2 ratio and hydrolyzes all of the GPL species in the mixed vesicles with comparable efficiency (Table 5.2, entries 19–24) (note the higher values for POPC hydrolysis is probably due to the fact that POPC is present at a 5-fold higher concentration than the other GPL species in these mixed GPL vesicles). Human $cPLA_2$-ε displays low PLA_1 and PLA_2 activities on all GPL species except for POPC in which it acts mainly as a PLA_1 (Table 5.2, entries 25–30). Mouse $cPLA_2$-ζ displays comparable PLA_1 and PLA_2 activities on all species except for POPI and POPG, where it shows mainly PLA_2 activity (Table 5.2, entries 31–36).

TABLE 5.2: PLA_1 versus PLA_2 activities of $cPLA_2$'s (mixed GPL vesicles).

Enzyme	Phospholipid species	PLA_1 Specific activity (100 μM Ca^{2+}) [(nmol/min)/mg protein]	PLA_2 Specific activity (100 μM Ca^{2+}) [(nmol/min)/mg protein]
m-$cPLA_2\beta$	POPC	0.13, 0.05, 0.06	0.00, 0.00, 0.00
	POPE	0.00, 0.00	0.03, 0.04
	POPS	0.00, 0.00	0.13, 0.12
	POPI	0.00, 0.00	0.03, 0.08
	POPG	0.00, 0.00	0.24, 0.14
	POPA	0.04, 0.01	0.25, 0.23
h-$cPLA_2\alpha$	POPC	0.03, 0.04	0.33, 0.27
	POPE	0.00, 0.02	0.06, 0.04
	POPS	0.00, 0.01	0.08, 0.04
	POPI	0.00, 0.00	0.07, 0.07
	POPG	0.00, 0.00	0.06, 0.02
	POPA	0.01, 0.01	0.15, 0.05
h-$cPLA_2\gamma$	POPC	0.00, 0.01	0.00, 0.03
	POPE	0.00, 0.03	0.00, 0.00
	POPS	0.00, 0.00	0.00, 0.00
	POPI	0.00, 0.00	0.00, 0.06
	POPG	0.00, 0.00	0.00, 0.00
	POPA	0.00, 0.00	0.00, 0.00
h-$cPLA_2\delta$	POPC	7.59, 5.10	1.13, 0.85
	POPE	1.4, 1.45	0.24, 0.28
	POPS	1.05, 1.25	0.16, 0.21
	POPI	0.55, 0.63	0.00, 0.10
	POPG	0.62, 0.36	0.07, 0.05
	POPA	0.54, 0.60	0.14, 0.04
h-$cPLA_2\varepsilon$	POPC	0.25, 0.26	0.00, 0.00
	POPE	0.03, 0.05	0.00, 0.01
	POPS	0.00, 0.00	0.00, 0.01
	POPI	0.00, 0.05	0.00, 0.00
	POPG	0.00, 0.00	0.00, 0.00
	POPA	0.04, 0.04	0.00, 0.00
h-$cPLA_2\zeta$	POPC	0.00, 0.08	0.06, 0.26, 0.51
	POPE	0.00, 0.07	0.02, 0.04
	POPS	0.06, 0.17	0.03, 0.06
	POPI	0.00, 0.00	0.04, 0.08
	POPG	0.00, 0.00	0.04, 0.06
	POPA	0.00, 0.00	0.00, 0.00
m-$cPLA_2\zeta$	POPC	0.48, 0.31	0.66, 0.67
	POPE	0.22, 0.24	0.23, 0.21
	POPS	0.08, 0.09	0.28, 0.22
	POPI	0.00, 0.00	0.15, 0.12
	POPG	0.07, 0.00	0.21, 0.09
	POPA	0.24, 0.14	0.28, 0.27

Chapter 6

Interfacial Binding of Bee Venom $sPLA_2$ Occurs Predominantly By a Non-Electrostatic Mechanism

Section 1: Introduction

As detailed in Chapter One, secreted phospholipases A2 ($sPLA_2$'s) are 14-18 kDa, calcium-dependent, disulfide-rich enzymes that liberate free FA's from the *sn*-2 position of GPL's[87]. These proteins are often studied as a paradigm for interfacial enzymes that act at the lipid-water interface[88]. The $sPLA_2$'s are water-soluble but must undergo a binding event to a membrane surface in order to gain access to their water-insoluble GPL substrates. Binding of the enzyme to the membrane interface is considered a distinct event from the subsequent binding of a single GPL molecule into its active site[89]. With suitable constraints on the exchange of enzyme, substrate, and products between substrate aggregates, it is possible to extract the primary rate and equilibrium constants that describe the interfacial reaction cycle[88]. Although the binding of a $sPLA_2$ to GPL-detergent mixed micelles has been attributed to the interaction of the protein with a single phospholipid[90], it is now generally accepted that the interfacial binding surface of $sPLA_2$'s involves ~10-20 amino acid residues that make contact with tens of GPL's. When a $sPLA_2$ sits on the vesicle surface, the hydrophobic amino acid side chains are thought to penetrate into the membrane bilayer just below the polar head group region[91].

Among hydrophobic amino acids, the side chain of aromatic amino acids, especially the indole of tryptophan, makes the largest contribution to the interfacial binding of a $sPLA_2$[50a, 91a, 91c, 91e, 92]. Tryptophan often occurs on trans-membrane helices near the lipid-water interface and ranks as the top amino acid in promoting the interfacial binding of peptides to membranes[93].

Electrostatic interactions between cationic lysine/arginine amino acid residues and anionic GPL head groups (GPS, GPA, GPI, GPG, and CL) have been implicated in the binding of $sPLA_2$'s to membranes enriched in anionic GPL's[91a, 94]. The notion that these electrostatic interactions are indeed the primary driving force behind $sPLA_2$ binding to anionic membranes[94b] has recently been challenged[91a, 91b, 95]. While it is likely that these basic residues do play a role in a $sPLA_2$'s preference for anionic GPL vesicles over zwitterionic ones, the question of how significant of a role remains. Furthermore, it is expected that electrostatic interactions are important for membrane association in proportion to the number of basic residues on the interfacial binding surface of $sPLA_2$'s. For example, bee venom $sPLA_2$ ($bvPLA_2$) has a net interfacial surface charge of +2 and membrane interactions that are not highly dependent on electrostatic interactions[96]. In contrast, human $sPLA_2$-GIIA has a net surface charge of +15 and has a marked preference for membranes enriched in anionic GPL's over membranes enriched in zwitterionic ones[94a].

With this in mind, our lab has previously studied the interfacial kinetics of the

$sPLA_2$ from bee venom ($bvPLA_2$) on anionic phospholipid vesicles[95]. The X-ray structure of this enzyme reveals the canonical sPLA2 ~15 Å deep active site slot, where a single GPL binds in proximity to the catalytic dyad, which is embedded in the interfacial binding surface (Figure 1 of [96]). This surface is mainly composed of hydrophobic residues. The face of the enzyme that includes the active site slot also contains six basic residues (K14, R23, R58, K85, K94, and K133) and one anionic residue (D92). It is reasonable to hypothesize that these cationic residues promote the higher affinity binding of $bvPLA_2$ to anionic versus zwitterionic membranes. However, the protein in which five of these six basic residues were mutated to the anionic residue glutamate, ($bvPLA_2$-E5, a K14E/R23E/K85E/K94E/K133E mutant), like the wild-type enzyme, bound essentially irreversibly to anionic vesicles composed of dimyristoyl phosphatidylmethanol[95]. High affinity of $bvPLA_2$-E5 to anionic vesicles was confirmed by kinetic analysis, by the fact that the enzyme follows "scooting mode kinetics" by hydrolyzing all of the GPL's in the outer monolayer of the vesicles without desorption into the aqueous phase, and by fluorimetric studies that directly measure protein-GPL binding[95].

Previous attempts to quantify the binding of $bvPLA_2$'s to vesicles of anionic phospholipids have been hindered by the high affinity that these enzymes have for vesicles enriched in anionic GPL's. Thus, only upper limit values for the dissociation constant for the enzyme from the vesicle into the aqueous phase, *K*d, have been

obtained (for example, [95]). In the present study, we examine the binding of bvPLA$_2$ and its respective interfacial binding surface mutants to mixed GPC/GPS vesicles with compositions representative of physiological membranes under conditions where accurate values of the K_d could be obtained. We also perform binding studies as a function of pH to further support our hypothesis of an electrostatic-independent interfacial binding mechanism. Our results, when considered together with finite difference Poisson-Boltzmann (FDPB) calculations performed as part of a larger study[96], provide insight into the high-affinity binding of these proteins to anionic GPL vesicles. These combined results show that electrostatic interactions between lysine and arginine residues and membranous anionic GPS molecules only contribute minimally to the overall interfacial binding energetics of bvPLA$_2$.

Section 2: Methods

Preparation of Recombinant Bee Venom PLA2's

Recombinant bv-sPLA$_2$ and associated interfacial binding surface mutant proteins were a generous gift from the efforts of Farideh Ghomaschi and were prepared as described[96].

Interfacial Binding Studies

DOetPS was prepared as described[91a]. DOPC, DOPS, DOetPC, cholesterol (CH), and egg sphingomyelin (SM) are from Avanti Polar Lipids Inc. All other reagents are from

Sigma Aldrich unless specifically noted. The concentration of GPL's in chloroform stock solutions was determined by inorganic phosphate assay after degradation with perchloric acid using the standard procedure[54]. Interfacial binding studies using sucrose-loaded, 0.1 μm liposomes were carried out as described[91a]. For studies in the presence of calcium, vesicles were extruded in 5 mM MOPS, pH 7.4, 176 mM sucrose, and the binding buffer was 5 mM MOPS, pH 7.4, 0.1 M KCl, 2 mM $CaCl_2$, 0.5 mg/mL bovine serum albumin (Gibco). Studies at pH 6.0 were carried out with Bis-Tris replacing MOPS at pH 7.0 and at pH 8.0 with HEPES replacing MOPS. For studies in the absence of calcium, vesicles were extruded in 5 mM MOPS, pH 7.4, 2 mM EGTA, 176 mM sucrose, and the binding buffer was 5 mM MOPS, pH 7.4, 0.1 M KCl, 2 mM EGTA, 0.5 mg/mL bovine serum albumin. Binding reactions, 100 μL, contained 10-500 ng of $bvPLA_2$, depending on the total lipid concentration (given in the figures) so that the lipid-to-protein ratio was at least 200 (to avoid crowding of enzyme on vesicles). The amount of $bvPLA_2$ in the supernatant after vesicles were pelleted in the ultracentrifuge was measured using the fluorimetric assay with 1-palmitoyl-2-pyrenedecanoyl phosphatidylmethanol[91a, 97]. Studies with radiolabeled CH and SM showed that these lipids and phospholipids present in the co-vesicles are recovered with similar yield after extrusion[91a].

The percent of $bvPLA_2$ remaining in the supernatant, based on enzymatic activity (100% is the amount of bvPLA2 activity in the supernatant of a sample processed as

above but in the absence of vesicles), was plotted versus the total GPL present in the binding reaction. The curve was fit to the standard equation for equilibrium dissociation: 100-([E]/[E]T)) *K*d/([L]T + *K*d), where [E] is the concentration of bvPLA$_2$ in the aqueous phase, [E]T is the concentration of total enzyme (free and vesicle bound) in the binding reaction, [L]T is the total GPL concentration in the binding reaction (expressed as total moles of phospholipid, GPS + GPC, divided by the volume of binding reaction sample), and K_d is the equilibrium constant for the dissociation of vesicle-bound enzyme into the aqueous layer. The above equation applies to the present case where the total phospholipid concentration is in large excess over the total enzyme concentration so that depletion of vesicle binding sites due to enzyme binding can be ignored. The recovery of all bvPLA2's used in the study from centrifuged samples that lacked vesicles was >80%. Thus, no correction was needed for loss of enzyme to the walls of the polyallomer tubes.

Section 3: Results

Approach to study Interfacial binding of bvPLA$_2$

Interfacial binding of bvPLA$_2$ to 0.1 μm extruded unilamellar vesicles of varying GPL composition was quantified by sedimenting vesicles and measuring the fraction of enzyme remaining in the supernatant. Vesicles are loaded with sucrose so that they can be pelleted in an ultracentrifuge[91a, 98]. Sucrose-loaded vesicles are not under osmotic

stress because of the presence of 0.1 M KCl in the binding buffer outside of the vesicles[98]. Also, the addition of 0.1 M KCl to the binding buffer brings the ionic strength to a value close to the physiological one.

It is important to use a sufficiently high lipid-to-protein ratio to ensure that enzyme is not crowded on vesicles. Otherwise interactions among proteins bound to the vesicle may complicate the meaning of K_d, and the amount of enzyme in the aqueous phase may be an overestimate due to insufficient vesicle surface available for enzyme binding. Since the binding of a typical $sPLA_2$ to vesicles prevents about 40-50 phospholipids from interacting with other $sPLA_2$'s bound on the same vesicles[89a] and because ≈50% of the total GPL is on the inner vesicle monolayer and thus, not accessible to enzyme, a lipid-to-protein ratio of at least ≈200 is required to prevent crowding of enzyme on vesicles. In the present study, we used total lipid concentrations in binding mixtures down to 1 μM. In this case, the maximum amount of $bvPLA_2$ was 10 ng to give a lipid-to-protein ratio of at least 200. It was found that inclusion of 0.5 mg/mL bovine serum albumin in the binding buffer was necessary to prevent absorption of $bvPLA_2$ to the walls of the polyallomar centrifuge tubes.

Binding of wild-type and mutant $bvPLA_2$'s to vesicles

Figure 6.1 shows initial studies of the binding of $bvPLA_2$ and $bvPLA_2$-E5 to DOetPS/DOetPC vesicles. In these experiments, saturating calcium is present in the binding buffer, and thus it is necessary to use diether GPL vesicles to prevent GPL

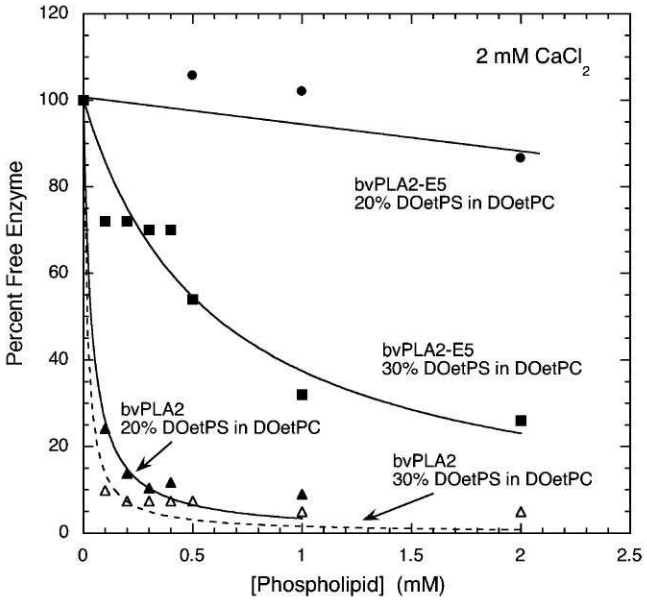


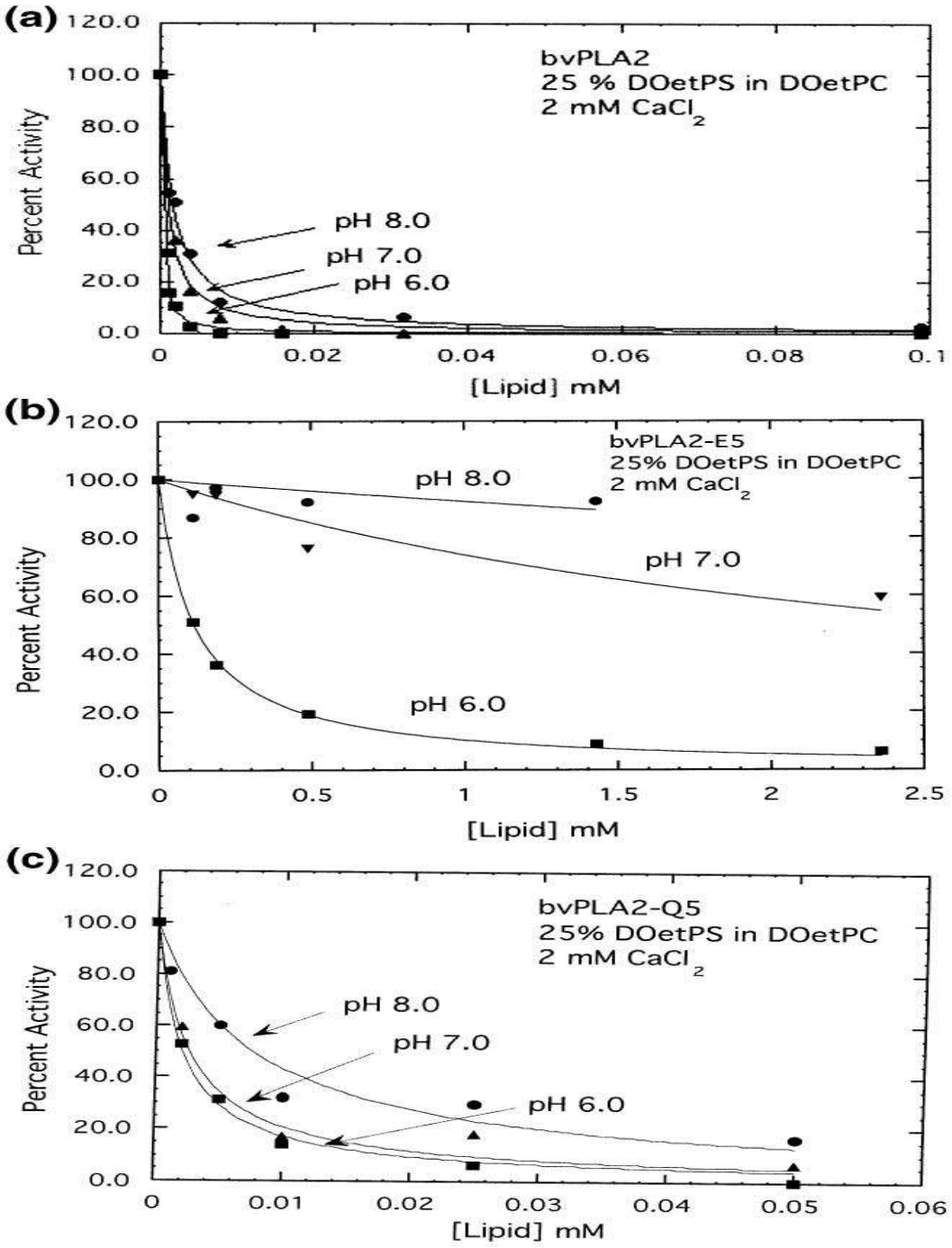
FIGURE 6.1: Binding of bvPLA$_2$ and bvPLA$_2$-E5 to DOetPS/DOet-PC vesicles. Binding buffer at pH 7.4 contained 2 mM $CaCl_2$ (see Experimental Procedures for additional details). The solid lines are the fit of the data to the binding equation given in Experimental Procedures.

hydrolysis by vesicle-bound enzyme. The binding of bvPLA$_2$ to vesicles containing 20 or 30 mol % DOetPS in DOetPC is too tight to determine the K_d accurately (*K*d < 0.05 mM). Additional studies using lower lipid concentrations were carried out as described below. For bvPLA$_2$-E5, very little binding to vesicles containing 20 mol % DOetPS in DOetPC is seen with phospholipid concentrations up to 1 mM (*K*d > 1 mM), and binding increases significantly when the amount of anionic GPL is increased to 30 mol % (*K*d = 0.3 $\pm$ 0.04 mM). Note, values of K_d are expressed in terms of the concentration of lipid in the outer monolayer of vesicles, taken as half of the total lipid concentration. Given that the interfacial binding surface of bvPLA$_2$-E5 has a high anionic character (due to the presence of five glutamates and only a single cationic residue (R58), it is remarkable that this mutant shows enhanced interfacial binding as the amount of anionic DOetPS in DOetPC vesicles is increased. These results are consistent with our earlier studies showing essentially irreversible binding of bvPLA$_2$-E5 to vesicles composed of 100 mol % of the anionic GPL dimyristoyl phosphatidylmethanol[95]. These

initial studies show that bvPLA$_2$ binds at least 20-fold more tightly than bvPLA$_2$-E5 to these GPS/GPC vesicles and that both proteins show enhanced binding to vesicles as the mole percent of GPS is increased.

To measure accurate values for K_d for bvPLA$_2$, we used 25% DOetPS in DOetPC vesicles down to a lipid concentration of 1 μM. We also determined values of *K*d at pH 6.0, 7.0, and 8.0, all in the presence of 2 mM $CaCl_2$. Binding curves for bvPLA$_2$, bvPLA$_2$-E5, and bvPLA$_2$-Q5 are shown in Figure 6.2, panels A, B, and C, respectively, and values of K_d are listed in Table 6.1. bvPLA$_2$ showed a 2-fold increase in affinity for vesicles as the pH was lowered from 8.0 to 7.0 and a 4-fold increase in affinity when the pH was lowered from 7.0 to 6.0. In contrast, the membrane association of bvPLA$_2$-E5 was significantly affected by pH. This protein did not bind to vesicles at pH 8.0 up to the maximum lipid concentration tested (2.5 mM), and binding increased 30- fold when the pH was decreased from 7.0 to 6.0. At pH 7.0, bvPLA$_2$ bound 3400-fold more tightly than bvPLA2-E5 to the 25% DOetPS/75% DOetPC vesicles, and at pH 6.0, the difference in affinity is reduced to 520-fold. bvPLA$_2$-Q5 showed a pH dependence of vesicle binding comparable to that for wild-type enzyme; interfacial binding affinity increased 2-fold in going from pH 8.0 to 7.0 and 1.5-fold increase in going from pH 7.0 to 6.0. At pH 8.0, bvPLA$_2$ binds 4-fold more tightly to vesicles than does bvPLA$_2$-Q5, at pH 7.0 the difference is 3-fold, and at pH 6.0 the difference is 10-fold.

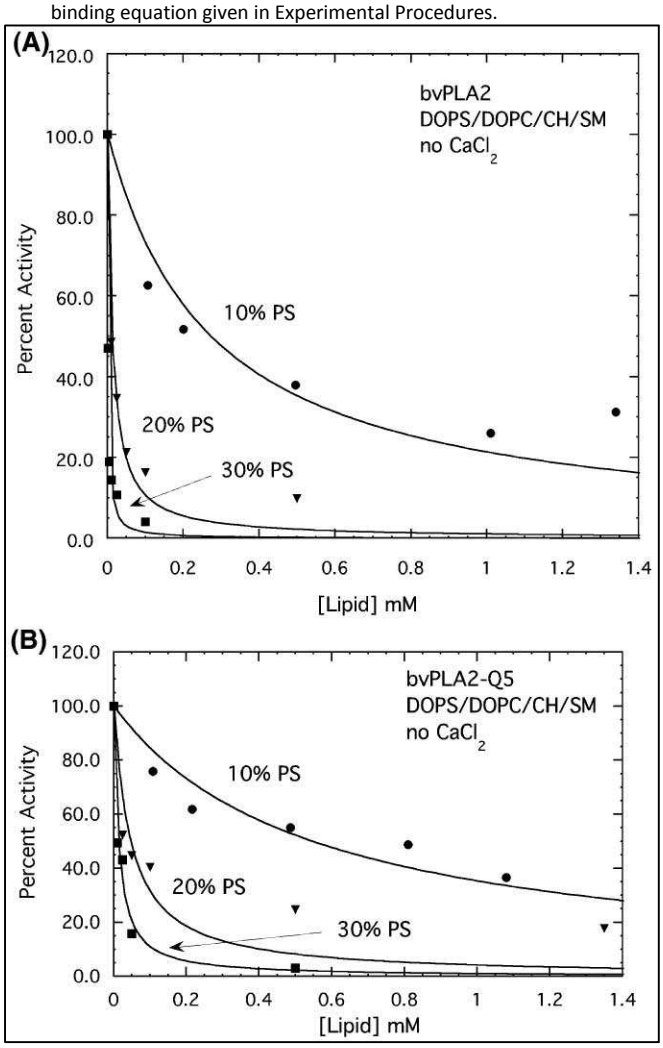
FIGURE 6.2: Binding of bvPLA$_2$'s to 25% DOetPS/75% DOetPCvesicles as a function of pH. (A) bvPLA2; (B) bv-PLA2-E5; (C) bvPLA2-Q5 with 2 mM $CaCl_2$



We studied the binding of bvPLA$_2$ and bvPLA$_2$-Q5 to GPC vesicles containing various amounts of GPS. Studies were carried out at a constant pH of 7.4. Binding was studied in the presence of $CaCl_2$ using diether GPL's or in the absence of calcium (2 mM EGTA) using diester GPL's. Since sucrose-loaded pure DOetPC vesicles do not sediment well (presumably due to leakage of sucrose), we included 30% CH and 30% SM in the vesicles. Additionally, these levels are similar to those found in mammalian cell membranes, and previous studies have shown that sucrose-loaded DOetPC/CH/SM vesicles readily pellet after ultracentrifugation[91a]. In the presence of $CaCl_2$, vesicles contained 0, 5, or 10 mol % DOetPS (Table 6.2). Since bvPLA$_2$'s bound less tightly to vesicles in the absence of calcium, we used 10, 20, and 30 mol % DOPS in DOPC/CH/SM vesicles for experiments in the absence of calcium (Table 6.2). Representative binding curves are shown in Figure 6.3 A,B, and all of the K_d values are listed in Table 6.2. bvPLA$_2$ binds 70-fold more tightly to diether GPL vesicles containing 10% PS (10% DOetPS/30% DOetPC/30% CH/30% SM) in the presence of saturating $CaCl_2$ than in the absence of $CaCl_2$, whereas bvPLA$_2$-Q5 shows a 30-fold increase in vesicle affinity in the presence of $CaCl_2$. The GPL ester carbonyl groups are not important for bvPLA$_2$ binding; in the absence of $CaCl_2$, bvPLA$_2$ and bvPLA$_2$-Q5 bind to di-ether vesicles with 10% GPS only 1.5-fold more tightly than to di-ester vesicles containing 10% GPS (Table 6.2). In the presence of $CaCl_2$, bvPLA$_2$ shows a 15-fold increase in affinity to di-ether GPL vesicles as the mole percent of GPS is increased from 0 to 10%, whereas bvPLA$_2$-Q5 shows a 10-fold

increase. In the absence of $CaCl_2$, $bvPLA_2$ shows a 130-fold increase in affinity to diester phospholipid vesicles as the mole percent OF GPS is increased from 10 to 30%, whereas $bvPLA_2$-Q5 shows a 40-fold increase.

FIGURE 6.3: Binding of $bvPLA_2$'s to DOPS/DOPC/CH/SM vesicles versus the amount of DOPS. (A) bvPLA2; (B) bv-PLA2-Q5. Binding buffer at pH 7.4 lacked $CaCl_2$ (see Experimental Procedures for additional details). The solid lines are the fit of the data to the binding equation given in Experimental Procedures.



Section 4: Discussion

In our earlier study, we found that $bvPLA_2$ and $bvPLA_2$-E5 bound tightly to vesicles composed purely of the anionic GPL dimyristoyl phosphatidylmethanol[95]. In the present study, we see that the use of GPS/GPC co-vesicles allows values of the enzyme-vesicle dissociation equilibrium constant (K_d) to increase into the measurable range. With this new data and the study of $bvPLA_2$-Q5 for the first time, we can summarize the interfacial binding trends as follows: (1) Electrostatic interactions between the five basic residues (K14, R23, K85, K94, and K133) on the face of the

protein that includes the opening to the active site slot and acidic lipids in the membrane do not constitute a major determinant of binding. This is based on the observation that bvPLA$_2$-Q5 binds only 3- to 10-fold more weakly than bvPLA$_2$ to GPS/GPC vesicles (Tables 6.1 and 6.2). This is consistent with the results from our previous EPR studies[91d], which suggest that only two of the five basic residues are within a Debye length (≈10 Å for 0.1 M KCl) of the membrane surface so that the electrostatic component to membrane association is expected to be weak. (2) Replacing the five basic residues with anionic glutamates (charge reversal) overestimates the contribution of the five basic residues to electrostatic binding to the anionic GPS/GPC vesicles. This is based on the fact that at pH 7, bvPLA$_2$-E5 binds to GPS/GPC vesicles 3000-fold more weakly than bvPLA2 and yet mutation of basic residues to charge-neutral glutamines produces only a 3-fold reduction (Table 6.1). (3) The remarkable finding that the affinity of bvPLA$_2$-E5 to anionic GPS/GPC vesicles increases as the mole percent of anionic GPS is increased is explained by the increase in the p*K*a values of a subset of the introduced glutamates when these residues transfer from bulk solution to the surface of the anionic vesicles and that the increase in p*K*a is larger as the amount of GPS in the vesicles is increased (supported by pH-dependent interfacial binding studies (Table 6.1) and calculations of p*K*a shifts (Table 3 of [96]). (4) The binding of calcium to the active site of bvPLA$_2$ increases the affinity of the enzyme for GPS/GPC vesicles by both a mass action effect (substrate binding in the active site is calcium-dependent) and an electrostatic

vesicle composition	pH	[Ca^{2+}] (mM)	K_d (μM) bvPLA$_2$	K_d (μM) bvPLA$_2$-E5	K_d (μM) bvPLA$_2$-Q5
25% $DO_{et}PS$	8.0	2	0.8 (0.1	*b*	3.8 (1
75% $DO_{et}PC$			0.9 (0.1		3.8 (1
25% $DO_{et}PS$	7.0	2	0.46 (0.05	1500 (300	1.4 (0.2
75% $DO_{et}PC$			0.49 (0.05	1700 (400	1.8 (0.3
25% $DO_{et}PS$	6.0	2	0.10 (0.01	50 (5	1.0 (0.1
75% $DO_{et}PC$			0.11 (0.02	60 (2	1.1 (0.1

[a] Shown are the estimated errors from the nonlinear regression fit of the data to the binding equation. Two independent binding analyses were carried out per condition, and values of K_d for each are listed. [b] No binding up to 2.5 mM phospholipid.

TABLE 6.1: Binding of bvPLA$_2$ to vesicles as a function of pH dependence[a]

attraction of calcium with the anionic vesicle interface. Both effects are not large. These points are discussed in more detail below.

The experimental studies presented here, with consideration of the theoretical studies from the larger study in which the current report is embedded[96], show that the active site calcium and one or two lysine residues (K14 and R23) make an electrostatic contribution to the interfacial binding of bvPLA$_2$ to anionic GPS/GPC vesicles. It is clear however, that electrostatic interactions are not the main force driving interfacial binding of bvPLA$_2$ to vesicles. This is most apparent from the observation that K_d values for bvPLA$_2$ and bvPLA$_2$-Q5 differ by 10-fold or less (Table 6.2). Thus, the five basic residues that lie on the face of bvPLA$_2$ that includes the opening to the active site slot cannot be the main anchoring mechanism for interfacial binding of this protein. This is also suggested by the relative positioning of these lysine residues in an EPR membrane-docked model (see Figure 5 of [96]). Thus, it is concluded that the large number of hydrophobic residues near the active site slot on bvPLA$_2$ contribute significantly to interfacial binding.

These studies suggest that the electrostatic attraction of the five basic residues of bvPLA$_2$ with the anionic vesicle interface is not the major force driving interfacial binding. In the case of human GIIA-sPLA$_2$, we have recently shown that this highly basic protein (23 surface lysine and argine residues) binds much more tightly to anionic GPS vesicles than to zwitterionic GPC vesicles and that the interaction with GPS vesicles results in a supramolecular aggregation involving several enzymes and vesicles[94a]. Thus high affinity of this sPLA$_2$ for anionic vesicles cannot be attributed to the electrostatic interaction of only a few lysine or arginine residues on the membrane binding surface with anionic vesicles; rather the combined effect of many basic residues distributed over the surface of the protein contributes to membrane association through electrostatic interactions. In an earlier study of the interfacial binding of venom sPLA$_2$ (*Agkistrodon pisci*V*orus pisci*V*orus*, D49 isoform) to

vesicle composition	[Ca^{2+}] (mM)	K_d (μM) bvPLA$_2$	K_d (μM) bvPLA$_2$-Q5
0% $DO_{et}PS$ 40% $DO_{et}PC$ 30% CH 30% SM	2	14 (2 14 (1	60 (7 50 (4
5% $DO_{et}PS$ 35% $DO_{et}PC$ 30% CH 30% SM	2	8 (2 8 (2	12 (2 17 (3
10% $DO_{et}PS$ 30% $DO_{et}PC$ 30% CH 30% SM	2	0.9 (0.2 1.2 (0.2	5 (0. 3 7 (0. 1
10% $DO_{et}PS$ 30% $DO_{et}PC$ 30% CH 30% SM	0	79 (8 55 (10	190 (20 190 (20
10% DOPS 30% DOPC 30% CH 30% SM	0	110 (10 130 (20	270 (50 280 (50
20% DOPS 20% DOPC 30% CH 30% SM	0	5 (1 6 (1	21 (5 23 (5
30% DOPS 10% DOPC 30% CH 30% SM	0	0.8 (0.1 1.0 (0.1	8 (2 7 (1

[a] Shown are the estimated errors from the nonlinear regression fit of the data to the binding equation. Two independent binding analyses were carried out per condition, and values of K_d for each are listed.

Table 6.2: Binding of bvPLA$_2$ to Vesicles at pH 7.4- GPS and Calcium Dependence[a]

anionic vesicles of polymerized GPG, it was suggested that K7 and K10 on the interfacial binding site of this $sPLA_2$ account for nearly half of the total interfacial binding energy[94b]. Mutation of these two basic residues to glutamates (charge reversal) led to a 500-fold increase in the value of K_d. Based on the present study with $bvPLA_2$, it seems reasonable to suggest that this charge reversal mutagenesis overestimates the electrostatic contribution of the two basic residues to interfacial binding.

Chapter 7

Interfacial Binding Studies and Sensitivity to DTT of the Secreted Phospholipases A_2

Section 1: Introduction

$sPLA_2$'s are water-soluble enzymes that must bind to the membrane interface to gain access to their highly water-insoluble GPL substrates (interfacial enzymes)[88a, 99]. Kinetic and x-ray structural studies of $sPLA_2$'s have established that they contain an interfacial recognition site that allows attachment of enzyme to the interface, which is distinct from the catalytic site where the hydrolysis of a single GPL molecule occurs. Thus, the substrate specificity of $sPLA_2$'s is dictated by the type of membrane interface to which the enzyme prefers to bind (interfacial specificity) and by the type of GPL that is accommodated in the catalytic site (catalytic site specificity). These features can be studied separately using suitable methods[100]. Interfacial binding specificity of $sPLA_2$'s has important physiological consequences. For example, human $sPLA_2$-GIIA binds several orders of magnitude more tightly to anionic GPL membranes than to an interface composed mainly of charge-neutral GPC[91a]. This may explain why the extracellular face of the plasma membrane of mammalian cells, which is rich in GPC and sphingomyelin, is normally resistant to degradation by $sPLA_2$-GIIA, and yet the GPG-rich membrane of gram-positive bacteria is readily degraded by this enzyme[35-36, 101].

In the present study, we have characterized the interfacial binding properties of the full set of mouse and human groups I, II, V, X, and XII $sPLA_2$'s (mouse/human $sPLA_2$-GIB, mouse/human $sPLA_2$-GIIA, mouse $sPLA_2$-GIIC, mouse/human $sPLA_2$-GIID, mouse/human $sPLA_2$-GIIE, mouse/human $sPLA_2$-GIIF, mouse/human $sPLA_2$-GV, mouse/human $sPLA_2$-GX, and human GXII). The group III $sPLA_2$ gene predicts a protein consisting of a central sPLA2 domain flanked by large N- and C-terminal extensions. This $sPLA_2$ was not included in the present studied because the structure of the mature protein remains to be elucidated. Mouse group XII was also omitted because its sequence is 94% identical to that of human GXII. The interfacial binding affinities of the mammalian sPLA2s for vesicles composed of zwitterionic phospholipids containing various amounts of anionic phospholipids were quantified as a prelude to interpreting the ability of these enzymes to hydrolyze the outer plasma membrane of mammalian cells.

Section 2: Methods

Materials

All GPL's are from Avanti Polar Lipids Inc. Recombinant $sPLA_2$ enzymes were generous gifts from Farideh Ghomaschi and Alan Singer and were prepared as previously described[25]. Dithiothreitol (DTT) is from EMD Millipore (Omnipur Cat. # 3860-OP). All other regents are from Sigma Aldrich.

$sPLA_2$ sensitivity to DTT

$sPLA_2$ (0.5–10 μg) was added to 100 μl of 100 mM Tris, pH 7.4. The sample was split in half, and DTT was added to one tube to give a final concentration of 10 mM. Samples were incubated at room temperature or 50 °C for the indicated times, and aliquots were assayed using a fluorometric assay with 1-palmitoyl-2-pyrenedecanoyl-*sn*-glycero-3-phosphomethanol[97]. The activity in the sample with DTT was compared with that in the sample without DTT to obtain the percent remaining activity at each time point.

Interfacial binding to vesicles

Preparation and size analysis of 0.1-μm diameter, sucrose-loaded, unilamellar vesicles of di-ether vesicles DOetPC/DOetPS was carried out as described[91a]. $sPLA_2$ binding studies were carried out in 5 mM MOPS, pH 7.4, 0.1 M KCl, 2 mM $CaCl_2$ at room temperature using the centrifugation method in which the amount of enzyme remaining in the supernatant above pelleted vesicles is quantified by enzymatic assay[91a] (pH of the binding mixture was checked after the addition of all components). Because the specific activity of the different $sPLA_2$'s varies considerably, the amount of supernatant taken and the extent of its dilution with 3% bovine serum albumin in water were chosen such that the reaction velocity measured in the assay was at least 5-fold higher than the minus $sPLA_2$ background rate[91a]. In the case of human $sPLA_2$-GIB, the buffer for binding

studies also contained 1 mg/ml bovine serum albumin to prevent loss of enzyme to the walls of the centrifuge tube.

Section 3: Results

TABLE 7.1: Remaining enzymatic activity of human and mouse sPLA$_2$'s after treatment with 10 mM DTT

sPLA$_2$	Room temperature			50 °C		
	5 min	30 min	60 min	5 min	30 min	60 min
	%	%	%	%	%	%
hGIB	100[a]	100	100	73	0	ND[b]
hGIIA	36	0	ND	ND	ND	ND
hGIID	3	0	ND	ND	ND	ND
hGIIE	100	100	100	100	55	9
hGIIF	100	98	85	40	0	ND
hGV	31	0	ND	0	ND	ND
hGX	100	100	100	100	56	16
hGXII	84	63	46	23	0	ND
mGIB	100	100	100	61	0	ND
mGIIA	13	0	ND	ND	ND	ND
mGIIC	13	0	ND	ND	ND	ND
mGIID	23	0	ND	ND	ND	ND
mGIIE	100	100	100	100	28	0
mGIIF	100	100	100	40	13	0
mGV	46	10	0	ND	ND	ND
mGX	100	97	37	89	11	0

[a] Percent remaining enzymatic activity after exposure to DTT under the indicated conditions.
[b] Not determined.

Sensitivity of mouse and human sPLA$_2$'s to DTT

There are numerous reports in the literature in which loss of PLA$_2$ activity upon treatment of the cellular extract with DTT is taken as firm evidence that the activity is caused by a sPLA$_2$. The sensitivity of the full set of mouse and human groups I, II, V, X, and XII sPLA$_2$*-+ to DTT is summarized in Table 7.1. The most DTT-sensitive sPLA$_2$'s are mouse sPLA$_2$-GIIC, human/mouse sPLA$_2$-GIIA, human/mouse sPLA$_2$-GIID, and human/mouse sPLA$_2$-GV. For these, complete loss of activity occurs in less than 30–60 min of exposure to 10 mM DTT at room temperature. The activity of human sPLA$_2$-GIB and mouse sPLA$_2$-GIB, human sPLA$_2$-GIIF and mouse sPLA$_2$-GIIF, mouse sPLA$_2$-GX, and

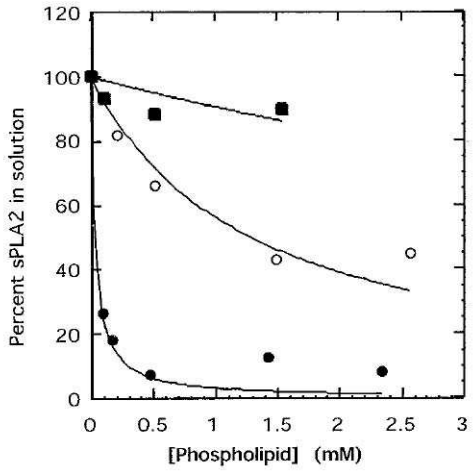


FIGURE 7.1: Interfacial binding of $sPLA_2$'s to phospholipid vesicles. Sucrose-loaded vesicles of 10% $DO_{et}PS$ in $DO_{et}PC$ were pelleted by ultracentrifugation and the percent of $sPLA_2$ remaining in the supernatant was plotted as a function of the concentration of total GPL concentration in the binding mixture for mouse $sPLA_2$-GIIC (•), human $sPLA_2$-GXII (o), and mouse $sPLA_2$-GIID (■). Independent binding studies were carried out at least three times for each $sPLA_2$.

human $sPLA_2$-GXII falls to zero but only after a 30–60-min DTT treatment at elevated temperature (50 °C). Remarkably, human $sPLA_2$-GIIE and human $sPLA_2$-GX retain measurable activity, 9 and 16%, respectively, even after treatment with 10 mM DTT for 60 min at 50 °C, and mouse $sPLA_2$-GIIE retains 28% activity after treatment with DTT for 30 min at 50 °C. In general the DTT sensitivity of each human $sPLA_2$ is similar to that for the mouse ortholog. Importantly, the data show that caution must be exercised to use thiol reduction data to establish whether a PLA_2 enzymatic activity in a cell or tissue extract is caused by an $sPLA_2$. In addition, DTT sensitivity data provided in Table 7.1 may be useful to provide information on the type of $sPLA_2$ being detected in a cell lysate.

Interfacial Binding of $sPLA_2$ to GPL vesicles

Binding of $sPLA_2$'s to vesicles is often carried out by monitoring fluorescence energy transfer from one or more tryptophan residues on or near the putative membrane binding surface of the protein and a fluorescence acceptor such as *N*-dansylphosphatidylethanol present in the interface[102]. However, not all the human and

mouse $sPLA_2$'s have tryptophans, and we have found that the energy transfer intensity varies dramatically with the GPL composition of the interface[102]. Thus, we decided to adopt the procedure of Buser *et al.*[98] in which vesicles are loaded with sucrose so that they pellet in an ultracentrifuge. The amount of $sPLA_2$ enzymatic activity remaining in the supernatant (measured with a sensitive fluorometric assay) was measured as a function of the concentration of vesicles. This method is suitable for measuring relatively weak interfacial binding of $sPLA_2$'s (for a complete discussion, see [91a]). Because we anticipated that most, if not all, of the human and mouse $sPLA_2$'s would bind weakly to GPC-rich vesicles and more tightly to GPS vesicles[103], our studies were carried out with DOetPC. Various amounts of DOetPS were added to DOetPC vesicles to determine the $sPLA_2$ binding requirement on anionic GPL. We found that sucrose-loaded DOetPC vesicles containing <10 mole % DOetPS do not pellet, and thus all vesicles contained at least 10 mole % DOetPS. Figure 7.1 shows typical interfacial binding curves (mouse $sPLA_2$-GIIC, mouse $sPLA_2$-GIID, and human $sPLA_2$-GXII binding to 10% DOetPS/DOetPC vesicles), and dissociation constants for all mouse and human $sPLA_2$'s interacting with 10% DOetPS/DOetPC and 30% DOetPS/DOetPC vesicle are given in Table 7.2 along with a summary of the other interfacial and inhibition data from the larger study from which the current report is derived[25]. Some of the enzymes (human/mouse $sPLA_2$-GIB, human/mouse $sPLA_2$-GIIA, and mouse $sPLA_2$-GIID) bind weakly or not all to GPC-rich vesicles (up to 2 mM GPL), and binding is enhanced dramatically when the amount of

anionic GPS is increased to 30 mole %. Other enzymes (mouse sPLA$_2$-GIIC, human sPLA$_2$-GIID, human sPLA$_2$-GIIF, human sPLA$_2$-GIB, mouse sPLA$_2$-GIIF, human sPLA$_2$-GV, mouse sPLA$_2$-GV, and human/mouse sPLA$_2$-GX) are able to bind to GPC-rich vesicles (K_d < 0.4 mM). For these latter sPLA$_2$'s, binding is increased when the amount of GPS is increased from 10 to 30 mole %, but the dependence on anionic DOetPS is less dramatic for human sPLA$_2$-GIIF and mouse sPLA$_2$-GIIF than for those sPLA$_2$'s that bind weaker to GPC-rich vesicles. Human sPLA$_2$-GXII shows an affinity for GPC-rich vesicles, which is intermediate between the groups of enzymes described above, and binding is increased by the addition of more DOetPS. Interestingly, human/mouse sPLA$_2$-GIIE bind weakly (K_d > 2 mM) to vesicles regardless of the mole fraction of anionic GPL.

TABLE 7.2: Interfacial kinetic and binding properties of human and mouse sPLA$_2$s

sPLA$_2$	DTT sensitivity[a]	Catalytic efficiency[b]	Vesicle preference (single phospholipid vesicles)[c]	Catalytic site phospholipid preference[d]	*sn*-2 Fatty acyl chain specificity 20:4/16:0[e]	$K_{Cat,app}$[f]	Most potent inhibitor[g]	Interfacial binding K_i[h]	Exogenous action on mammalian cells[i]
						μM		mM	
hGIB	++	+++	POPG $\gg$ POPS $\gg$ POPC	PG ~ PC ~ PA > PS > PE > PI	1.8	8 ± 3, POPG	Phosphonate-6b	~3 (30% PS/PC)	–
hGIIA	+++	+++	POPG > POPS $\gg$ POPC	PG ~ PC ~ PA > PS > PE > PI	0.8	13 ± 3, POPG	Me-Indoxam	No binding at 2 mM (10% PS/PC) ~0.02 (30% PS/PC)	–
hGIID	+++	+	POPG > POPS $\approx$ POPC	PG ~ PC ~ PE > PS > PA > PI	2.1	11 ± 3, POPG	Phosphonate-10b	0.12 (10% PS/PC) 100% bound at 0.14 mM (30% PS/PC)	–
hGIIE	+	+	POPG $\approx$ POPS $\approx$ POPC	PC > PA > PG > PE > PS > PI	0.7	112 ± 39, POPG	Me-Indoxam	No binding at 2 mM (10% PS/PC) No binding at 2 mM (30% PS/PC)	–
hGIIF	++	++	POPG $\gg$ POPS $\approx$ POPC	PG ~ PC > PE ~ PA > PS > PI	2.0	27 ± 14, POPG	MJ33 and MJ50	0.35 (10% PS/PC) 0.16 (30% PS/PC)	–
hGV	+++	++	POPG > POPS > POPC	PG ~ PC > PA > PS ~ PE > PI	0.3	1 ± 0.5, POPG 18 ± 4, POPS 225 ± 42, POPC	Me-Indoxam	0.05 (10% PS/PC) 90% bound at 0.1 mM (30% PS/PC)	++
hGX	+	++	POPC > POPG > POPS	PC > PG > PA > PE > PS > PI	2.3	1.5 ± 0.4, POPG 16 ± 4, POPS 44 ± 11, POPC	Me-Indoxam	0.13 (10% PS/PC) 0.036 (30% PS/PC)	+++
hGXII	++	+	POPG $\approx$ POPC > POPS	PC > PG ~ PA > PE > PS > PI	1.9	45 ± 13, POPG	Me-Indoxam	1.1 (10% PS/PC) 0.20 (30% PS/PC)	–
mGIB	++	+++	POPG > POPS $\gg$ POPC	PG ~ PC ~ PA > PS ~ PE > PI	1.3	8 ± 3, POPG	Phosphonate-12b	2.0 (10% PS/PC) 0.18 (30% PS/PC)	–
mGIIA	+++	+++	POPG > POPS $\gg$ POPC	PG > PC ~ PA > PE > PS > PI	0.4	4 ± 1, POPG	Me-Indoxam	No data (10% PS/PC) 100% bound at 0.1 mM (30% PS/PC)	–
mGIIC	+++	++	POPG > POPS > POPC	PG > PC ~ PA > PS > PE > PI	1.9	14 ± 4, POPG	Me-Indoxam	0.03 (10% PS/PC) 100% bound at 0.1 mM (30% PS/PC)	–
mGIID	+++	+	POPG ~ POPS > POPC	PG ~ PC ~ PS > PE ~ PA > PI	0.4	46 ± 15, POPG	DDC-1 and Me-Indoxam	<10% bound at 2 mM (10% PS/PC) 0.04 (30% PS/PC)	–
mGIIE	+	++	POPG $\approx$ POPC > POPS	PC > PG > PA > PE > PS > PI	1.0	100 ± 40, POPG	LY311727 and Me-Indoxam	No binding at 2 mM (10% PS/PC) 3 (30% PS/PC)	–
mGIIF	++	++	POPG > POPS $\approx$ POPC	PG ~ PC > PS ~ PA > PE > PI	1.7	35 ± 10, POPG	Me-Indoxam	0.04 (10% PS/PC) ~0.02 (30% PS/PC)	–
mGV	+++	++	POPG > POPS > POPC	PC > PG ~ PA > PE ~ PS > PI	0.3	1 ± 0.5, POPG 200 ± 35, POPC	Me-Indoxam	~0.02 (10% PS/PC) ~0.01 (30% PS/PC)	++
mGX	++	++	POPG $\approx$ POPS > POPC	PC > PG ~ PS ~ PA > PE > PI	2.2	48 ± 15, POPG	Me-Indoxam	0.07 (10% PS/PC) ~0.02 (30% PS/PC)	+++

[a] Actual values are in Table II.

[b] Specific activity on the most preferred of the three pure phospholipid vesicles (POPG, POPS, POPC) is ranked as +++ (140–1,030 μmol/min/mg), ++ (4–24 μmol/min/mg), and + (0.1–0.9 μmol/min/mg). Actual values are given in Table III.

[c] Ranking of specific activities on pure phospholipid vesicles.

[d] Ranked according to relative $k_{cat}{}^{*}/K_{m}{}^{*}$ values for the hydrolysis of mixed phospholipid vesicles. Actual values are given in Fig. 2, *A* and *B*.

[e] $k_{cat}{}^{*}/K_{m}{}^{*}$ for the hydrolysis of [^{14}C]SAPC divided by $k_{cat}{}^{*}/K_{m}{}^{*}$ for the hydrolysis of [^{3}H]DPPC in POPG vesicles. Estimated errors are <20% based on duplicate or triplicate analyses.

[f] Values of $K_{Cat,app}$ were determined from fitting the initial velocity for the hydrolysis of the indicated pure phospholipid vesicle as a function of the free calcium concentration to the hyperbolic equation (shown in Fig. 3 for two examples).

[g] Most potent of the 11 inhibitors shown in Fig. 3 for each sPLA$_2$ is listed. Actual potencies are shown in Table IV.

[h] Determined by the centrifugation method using sucrose-loaded vesicles (for example, see Fig. 5).

[i] For detailed values, see Fig. 6, *A–C*.

Section 4: Discussion

Examination of the interfacial binding data for all of the mouse and human $sPLA_2$'s makes apparent that some of the enzymes bind well to GPC-rich vesicles (10% DOetPS/DOetPC) but most do not. In the larger study from which the current report was extracted, it was observed that the enzymes that bound GPC rich vesicles also hydrolyzed pure POPC vesicles immediately upon addition of enzyme to the assay with no lag[25]. Conversely, those enzymes that hydrolyze POPC vesicles only after an initial lag phase bind relatively weakly to GPC-rich vesicles (compare data in Table 7.2 and Table III from [25]). This is consistent with detailed studies of porcine and bovine pancreatic sPLA2's showing that the accumulation of reaction products in GPC vesicles promotes interfacial binding and subsequent catalytic activity[88a]. We find that human $sPLA_2$-GIIA does not bind to GPC-rich vesicles (10% DOetPS/DOetPC) even with 2mM phospholipid present, and we cannot confirm the previous result of K_d ~0.1 μM for hGIIA dissociating from dihexadecyl GPC vesicles in the presence and absence of calcium (measured by surface plasmon resonance)[104].

Tryptophan on the membrane binding surface of human $sPLA_2$-GV is important for the high catalytic activity of this $sPLA_2$ on GPC-rich membranes[91c], and addition of a tryptophan to the membrane binding surface of human $sPLA_2$-GIIA renders this enzyme about 2 orders of magnitude more active on GPC-rich membranes[50a]. We have shown recently that the presence of a tryptophan on the membrane binding surface of human

$sPLA_2$-GX and its absence on that of human $sPLA_2$-GIIA is more important than the presence or absence of cationic residues (lysine and arginine) on the membrane binding surface of these $sPLA_2$s in permitting high affinity binding events to GPC-rich membranes[91a]. Furthermore, addition of a tryptophan to human $sPLA_2$-GIIA reduces the lag phase observed during the hydrolysis of GPC vesicles and allows this enzyme to liberate AA better when added to mammalian cells[91a]. Based on overlaying the sequences of the mouse and human $sPLA_2$'s onto the known three-dimensional x-ray structure of human $sPLA_2$-GIIA, the following enzymes are predicted to contain one or more tryptophans on their membrane binding surface: human $sPLA_2$-GIB, human $sPLA_2$-GIID, human $sPLA_2$-GV, human $sPLA_2$-GX, mouse $sPLA_2$-GIB, mouse $sPLA_2$-GIIC, mouse $sPLA_2$-GIID, mouse $sPLA_2$-GV, mouse $sPLA_2$-GX (human $sPLA_2$-GXII has a distinct primary structure making it difficult to locate the putative membrane binding surface). With the exception of mouse $sPLA_2$-GIB, all of these $sPLA_2$s hydrolyze PC vesicles without a discernible lag. All of the $sPLA_2$'s that do not contain a membrane binding surface tryptophan, human $sPLA_2$-GIIA, human $sPLA_2$-GIIE, human $sPLA_2$-GIIF, mouse $sPLA_2$-GIIA, mouse $sPLA_2$-GIIE, and mouse $sPLA_2$-GIIF, hydrolyze GPC vesicles only after a lag phase. There is no correlation between the predicted number of lysine and arginine residues on the membrane binding surface of the mouse and human $sPLA_2$'s and the occurrence of the lag.

There is a dramatic correlation between the ability of the $sPLA_2$s to hydrolyze

GPC-rich vesicles and the ability of these enzymes to liberate AA when added exogenously to mammalian cells. Human $sPLA_2$-GIB, mouse $sPLA_2$-GIB, human $sPLA_2$-GIIA, mouse $sPLA_2$-GIIA, mouse $sPLA_2$-GIIC, human $sPLA_2$-GIID, mouse $sPLA_2$-GIID, human $sPLA_2$-GIIE, mouse $sPLA_2$-GIIE, human $sPLA_2$-GIIF, mouse $sPLA_2$-GIIF, and human $sPLA_2$-GXII all fail to liberate AA from cells when added up to 1μg/ml, and all display specific activities on POPC vesicles less than 0.7 μmol/(min * mg). Human $sPLA_2$-GV, mouse $sPLA_2$-GV, human $sPLA_2$-GX, and mouse $sPLA_2$-GX are by far the most potent among the human and mouse $sPLA_2$'s to liberate AA from cells, and these enzymes display the highest specific activity on POPC. Furthermore, human $sPLA_2$-GV, mouse $sPLA_2$-GV, human $sPLA_2$-GX, and mouse $sPLA_2$-GX bind well to GPC-rich membranes (Table 7.2), a prelude for high catalytic turnover on these vesicles. The more efficient release of AA by human $sPLA_2$-GX *versus* human $sPLA_2$-GV from HEK293 and RBL-2H3 cells (Fig. 6, *A* and *C of* [25]) is consistent with the ~six-fold higher specific activity of the former enzyme *versus* the latter on POPC vesicles (Table III of [25]). On the other hand, mouse $sPLA_2$-GIIC, human $sPLA_2$-GIID, human $sPLA_2$-GIIF, and mouse $sPLA_2$-GIIF also bind relatively well to GPC-rich vesicles, but the specific activity of these enzymes for the hydrolysis of POPC vesicles is at least 10-fold less than that for human $sPLA_2$-GV (at least 60-fold less than that for human $sPLA_2$-GX). As noted above, mutagenesis studies have shown that tryptophan on the membrane binding surface of human $sPLA_2$-GV and human $sPLA_2$-GX is a key residue for supporting high affinity binding to GPC-rich

membranes[91a,91c]. The activity of exogenous human sPLA$_2$-GX on mammalian cells approaches that of cobra venom sPLA$_2$, an enzyme known for many years to display high activity on GPC-rich vesicles and on mammalian cells. Altogether, the results combined with our recent studies of wild type and mutant human sPLA$_2$-GIIA and human sPLA$_2$-GX[91a] form a strong argument that the ability to bind to and hydrolyze GPC-rich vesicles is required for efficient action of exogenously added sPLA$_2$ on mammalian cells. This seems reasonable given that the extracellular face of the mammalian cell plasma membrane is highly rich in zwitterionic GPL's (GPC and sphingomyelin), whereas most of the GPS and other anionic GPL's are on the inner leaflet of the membrane.

With the exception of human sPLA$_2$-GX and mouse sPLA$_2$-GX, there is a poor correlation between the ability of the various sPLA$_2$'s to liberate AA when added exogenously to mammalian cells (Figure 6 of [25]) and the ability of these enzymes to liberate this PUFA when forcibly overexpressed in mammalian cells. For example, HEK293 cells transfected with human sPLA$_2$-GIIA liberate AA[105] even though these cells are completely resistant to even high concentrations of this sPLA$_2$ (Figure 6 of [25]). Exogenous human sPLA$_2$-GV is inferior to human sPLA$_2$-GX in liberating AA when added exogenously to RBL-2H3 cells (Figure 6 of [25]), yet efficient AA liberation is seen when these cells are transfected with human sPLA$_2$-GV and human sPLA$_2$-GX cDNA[106]. The amount of AA produced by HEK293 cells forcibly overexpressing human sPLA$_2$-GIIF[107] is more than would be expect from the data with exogenously added enzyme (Figure 6 of

[25]). These results suggest that those $sPLA_2$s that liberate AA when overexpressed in mammalian cells but fail to do so when added exogenously to these cells are probably acting on a cellular membrane other than the extracellular face of the plasma membrane. Further work is needed to understand the site of action of $sPLA_2$'s expressed in mammalian cells.

In summary, the interfacial kinetic and binding data for the full set of human and mouse groups I, II, V, X, and XII $sPLA_2$'s show that these enzymes have dramatically different abilities to bind to GPL vesicles and to hydrolyze GPL's in these vesicles. These distinct interfacial binding properties coupled to the fact that the tissue distribution of the mammalian $sPLA_2$'s are also distinct argue strongly that these enzymes are not isoforms and that they are expected to have functions other than the release of lipid mediators such as AA for the biosynthesis of the eicosanoids[108].

List of References

1. Sud, M.; Fahy, E.; Cotter, D.; Brown, A.; Dennis, E. A.; Glass, C. K.; Merrill, A. H., Jr.; Murphy, R. C.; Raetz, C. R. H.; Russell, D. W.; Subramaniam, S., LMSD: LIPID MAPS structure database. *Nucleic Acids Res.* **2007,** *35* (Database Iss), D527-D532.
2. Fahy, E.; Subramaniam, S.; Brown, H. A.; Glass, C. K.; Merrill, A. H., Jr.; Murphy, R. C.; Raetz, C. R.; Russell, D. W.; Seyama, Y.; Shaw, W.; Shimizu, T.; Spener, F.; van Meer, G.; VanNieuwenhze, M. S.; White, S. H.; Witztum, J. L.; Dennis, E. A., A comprehensive classification system for lipids. *J. Lipid Res.* **2005,** *46* (5), 839-61.
3. Christie, W. W., *High-performance Liquid Chromatography and Lipids*. Pergamon Press: Maxwell House. Elmsford, New York 10523, 1987.
4. Anslyn, E. V.; Dougherty, D. A., *Modern physical organic chemistry*. University Science: Sausalito, CA, 2006.
5. Nelson, D. L.; Lehninger, A. L.; Cox, M. M., *Lehninger principles of biochemistry*. W.H. Freeman: New York, **2008**.
6. Ishii, I.; Fukushima, N.; Ye, X.; Chun, J., Lysophospholipid receptors: Signaling and biology. *Annu. Rev. Biochem.* **2004,** *73*, 321-354.
7. van Meer, G.; Voelker, D. R.; Feigenson, G. W., Membrane lipids: where they are and how they behave. *Nat Rev Mol Cell Biol* **2008,** *9* (2), 112-24.
8. Vance, D. E.; Vance, J. E.; Editors, *Biochemistry of Lipids, Lipoproteins and Membranes (5 th Edn.)*. Elsevier B. V.: 2008; p 631 pp.
9. Ford, D. A.; Gross, R. W., The Discordant Rates of sn-1 Aliphatic Chain and Polar Head Group Incorporation into Plasmalogen Molecular Species Demonstrate the Fundamental Importance of Polar Head Group Remodeling in Plasmalogen Metabolism in Rabbit Myocardium. *Biochemistry* **1994,** *33* (5), 1216-22.
10. Shimizu, T., Lipid mediators in health and disease: enzymes and receptors as therapeutic targets for the regulation of immunity and inflammation. *Annu. Rev. Pharmacol. Toxicol.* **2009,** *49*, 123-150.
11. Feldberg, W.; Holden, H. F.; Kellaway, C. H., The formation of lysocithin and of a muscle-stimulating substance by snake venoms. *J. Physiol. (Cambridge, U. K.)* **1938,** *94*, 232-48.
12. von Euler, U. S., The specific vasodilating and plain muscle-stimulating substances from accessory genital glands in man and certain animals (prostaglandin and vesiglandin). *J. Physiol. (Cambridge, U. K.)* **1936,** *88*, 213-34.
13. (a) Bergstrom, S.; Ryhage, R.; Samuelsson, B.; Sjovall, J., Prostaglandins and related factors. XV. The structures of prostaglandin E1, F1α, and F1β. *J. Biol. Chem.* **1963,** *238* (11), 3555-64; (b) Murphy, R. C.; Hammarstroem, S.; Samuelsson, B., Leukotriene C: A slow-reacting substance from murine mastocytoma cells. *Proc. Natl. Acad. Sci. U. S. A.* **1979,** *76* (9), 4275-9.

14. (a) Bergstrom, S.; Danielsson, H.; Klenberg, D.; Samuelsson, B., Prostaglandins and related factors. XXXIV. The enzymic conversion of essential fatty acids into prostaglandins. *J. Biol. Chem.* **1964,** *239* (11), PC4006-PC4008; (b) Bergstrom, S.; Danielsson, H.; Samuelsson, B., Enzymic formation of prostaglandin E2 from arachidonic acid. XXXII. *Biochim. Biophys. Acta, Gen. Subj.* **1964,** *90* (1), 207-10.
15. Vane, J. R., Inhibition of prostaglandin synthesis as a mechanism of action for aspirin-like drugs. *Nature (London), New Biol.* **1971,** *231* (25), 232-5.
16. Wymann, M. P.; Schneiter, R., Lipid signalling in disease. *Nat. Rev. Mol. Cell Biol.* **2008,** *9* (2), 162-176.
17. Blackwell, G. J.; Duncombe, W. G.; Flower, R. J.; Parsons, M. F.; Vane, J. R., The distribution and metabolism of arachidonic acid in rabbit platelets during aggregation and its modification by drugs. *Br. J. Pharmacol.* **1977,** *59* (2), 353-66.
18. (a) Clark, J. D.; Milona, N.; Knopf, J. L., Purification of a 110-kilodalton cytosolic phospholipase A2 from the human monocytic cell line U937. *Proc. Natl. Acad. Sci. U. S. A.* **1990,** *87* (19), 7708-12; (b) Kramer, R. M.; Roberts, E. F.; Manetta, J.; Putnam, J. E., The calcium-sensitive cytosolic phospholipase A2 is a 100-kDa protein in human monoblast U937 cells. *J. Biol. Chem.* **1991,** *266* (8), 5268-72; (c) Leslie, C. C.; Voelker, D. R.; Channon, J. Y.; Wall, M. M.; Zelarney, P. T., Properties and purification of an arachidonoyl-hydrolyzing phospholipase A2 from a macrophage cell line, RAW 264.7. *Biochim. Biophys. Acta, Lipids Lipid Metab.* **1988,** *963* (3), 476-92.
19. Burke, J. E.; Dennis, E. A., Phospholipase A2 structure/function, mechanism, and signaling. *J. Lipid Res.* **2009,** *50* (Supplement), S237-S242.
20. (a) Bradley, J. D.; Dmitrienko, A. A.; Kivitz, A. J.; Gluck, O. S.; Weaver, A. L.; Wiesenhutter, C.; Myers, S. L.; Sides, G. D., A randomized, double-blinded, placebo-controlled clinical trial of LY333013, a selective inhibitor of group II secretory phospholipase A2, in the treatment of rheumatoid arthritis. *The Journal of Rheumatology* **2005,** *32* (3), 417-423; (b) Suckling, K. E., Phospholipase A2 inhibitors in the treatment of atherosclerosis: a new approach moves forward in the clinic. *Expert opinion on investigational drugs* **2009,** *18* (10), 1425-30.
21. (a) Ghosh, M.; Tucker, D. E.; Burchett, S. A.; Leslie, C. C., Properties of the group IV phospholipase A2 family. *Prog. Lipid Res.* **2006,** *45* (6), 487-510; (b) Kennedy, B. P.; Payette, P.; Mudgett, J.; Vadas, P.; Pruzanski, W.; Kwan, M.; Tang, C.; Rancourt, D. E.; Cromlish, W. A., A Natural Disruption of the Secretory Group II Phospholipase A2 Gene in Inbred Mouse Strains. *Journal of Biological Chemistry* **1995,** *270* (38), 22378-22385.
22. Kita, Y.; Takahashi, T.; Uozumi, N.; Nallan, L.; Gelb, M. H.; Shimizu, T., Pathway-oriented profiling of lipid mediators in macrophages. *Biochem. Biophys. Res. Commun.* **2005,** *330* (3), 898-906.
23. Feng, L.; Prestwich, G. D., *Functional lipidomics*. Taylor & Francis: Boca Raton, 2006.

24. Lambeau, G.; Gelb, M. H., Biochemistry and physiology of mammalian secreted phospholipases A2. *Annu. Rev. Biochem.* **2008,** *77*, 495-520.
25. Singer, A. G.; Ghomashchi, F.; Le, C. C.; Bollinger, J.; Bezzine, S.; Rouault, M.; Sadilek, M.; Nguyen, E.; Lazdunski, M.; Lambeau, G.; Gelb, M. H., Interfacial Kinetic and Binding Properties of the Complete Set of Human and Mouse Groups I, II, V, X, and XII Secreted Phospholipases A2. *J. Biol. Chem.* **2002,** *277* (50), 48535-48549.
26. Homan, R.; Jain, M. K. In *Biology, pathology, and interfacial enzymology of pancreatic phospholipase A2*, Kluwer Academic/Plenum Publishers: 2001; pp 81-104.
27. Murakami, M.; Kudo, I., Lipid signaling. Phospholipase A2. *J. Biochem.* **2002,** *131* (3), 285-292.
28. Jemel, I.; Ii, H.; Oslund, R. C.; Payre, C.; Dabert-Gay, A.-S.; Douguet, D.; Chargui, K.; Scarzello, S.; Gelb, M. H.; Lambeau, G., Group X Secreted Phospholipase A2 Proenzyme Is Matured by a Furin-like Proprotein Convertase and Releases Arachidonic Acid inside of Human HEK293 Cells. *J. Biol. Chem.* **2011,** *286* (42), 36509-36521, S36509/1-S36509/10.
29. Scott, D. L.; Sigler, P. B., Structure and catalytic mechanism of secretory phospholipases A2. *Adv. Protein Chem.* **1994,** *45* (LIPOPROTEINS,APOLIPOPROTEINS, AND LIPASES), 53-88.
30. Rouault, M.; Bollinger, J. G.; Lazdunski, M.; Gelb, M. H.; Lambeau, G., Novel Mammalian Group XII Secreted Phospholipase A2 Lacking Enzymatic Activity. *Biochemistry* **2003,** *42* (39), 11494-11503.
31. Vadas, P.; Browning, J.; Edelson, J.; Pruzanski, W., Extracellular phospholipase A2 expression and inflammation: The relationship with associated disease states. *J. Lipid Mediators* **1993,** *8* (1), 1-30.
32. Mounier, C. M.; Ghomashchi, F.; Lindsay, M. R.; James, S.; Singer, A. G.; Parton, R. G.; Gelb, M. H., Arachidonic Acid Release from Mammalian Cells Transfected with Human Groups IIA and X Secreted Phospholipase A2 Occurs Predominantly during the Secretory Process and with the Involvement of Cytosolic Phospholipase A2-α. *J. Biol. Chem.* **2004,** *279* (24), 25024-25038.
33. (a) Muñoz, N. M.; Meliton, A. Y.; Meliton, L. N.; Dudek, S. M.; Leff, A. R., Secretory group V phospholipase A2 regulates acute lung injury and neutrophilic inflammation caused by LPS in mice. *American Journal of Physiology - Lung Cellular and Molecular Physiology* **2009,** *296* (6), L879-L887; (b) Giannattasio, G.; Fujioka, D.; Xing, W.; Katz, H. R.; Boyce, J. A.; Balestrieri, B., Group V Secretory Phospholipase A2 Reveals Its Role in House Dust Mite-Induced Allergic Pulmonary Inflammation by Regulation of Dendritic Cell Function. *The Journal of Immunology* **2010,** *185* (7), 4430-4438.
34. Henderson, W. R., Jr.; Chi, E. Y.; Bollinger, J. G.; Tien, Y.-t.; Ye, X.; Castelli, L.; Rubtsov, Y. P.; Singer, A. G.; Chiang, G. K. S.; Nevalainen, T.; Rudensky, A. Y.; Gelb, M. H., Importance of group X-secreted phospholipase A2 in allergen-induced airway inflammation and remodeling in a mouse asthma model. *J. Exp. Med.* **2007,** *204* (4), 865-877.

35. Beers, S. A.; Buckland, A. G.; Koduri, R. S.; Cho, W.; Gelb, M. H.; Wilton, D. C., The antibacterial properties of secreted phospholipases A2. A major physiological role for the group IIA enzyme that depends on the very high pI of the enzyme to allow penetration of the bacterial cell wall. *J. Biol. Chem.* **2002,** *277* (3), 1788-1793.
36. Koduri, R. S.; Gronroos, J. O.; Laine, V. J. O.; Le, C. C.; Lambeau, G.; Nevalainen, T. J.; Gelb, M. H., Bactericidal properties of human and murine groups I, II, V, X, and XII secreted phospholipases A2. *J. Biol. Chem.* **2002,** *277* (8), 5849-5857.
37. Cupillard, L.; Mulherkar, R.; Gomez, N.; Kadam, S.; Valentin, E.; Lazdunski, M.; Lambeau, G., Both group IB and group IIA secreted phospholipases A2 are natural ligands of the mouse 180-kDa M-type receptor. *J. Biol. Chem.* **1999,** *274* (11), 7043-7051.
38. Ancian, P.; Lambeau, G.; Lazdunski, M., Multifunctional activity of the extracellular domain of the M-Type (180 kDa) membrane receptor for secretory phospholipases A2. *Biochemistry* **1995,** *34* (40), 13146-51.
39. (a) Murakami, M.; Taketomi, Y.; Miki, Y.; Sato, H.; Hirabayashi, T.; Yamamoto, K., Recent progress in phospholipase A2 research: From cells to animals to humans. *Progress in Lipid Research* **2011,** *50* (2), 152-192; (b) Ghosh, M.; Loper, R.; Ghomashchi, F.; Tucker, D. E.; Bonventre, J. V.; Gelb, M. H.; Leslie, C. C., Function, Activity, and Membrane Targeting of Cytosolic Phospholipase A2ζ in Mouse Lung Fibroblasts. *J. Biol. Chem.* **2007,** *282* (16), 11676-11686.
40. Dessen, A.; Tang, J.; Schmidt, H.; Stahl, M.; Clark, J. D.; Seehra, J.; Somers, W. S., Crystal Structure of Human Cytosolic Phospholipase A2 Reveals a Novel Topology and Catalytic Mechanism. *Cell* **1999,** *97* (3), 349-360.
41. Tucker, D. E.; Stewart, A.; Nallan, L.; Bendale, P.; Ghomashchi, F.; Gelb, M. H.; Leslie, C. C., Group IVC cytosolic phospholipase A2γ is farnesylated and palmitoylated in mammalian cells. *J. Lipid Res.* **2005,** *46* (10), 2122-2133.
42. Xu, G.-Y.; McDonagh, T.; Yu, H.-A.; Nalefski, E. A.; Clark, J. D.; Cumming, D. A., Solution structure and membrane interactions of the C2 domain of cytosolic phospholipase A2. *Journal of Molecular Biology* **1998,** *280* (3), 485-500.
43. (a) Leslie, C. C., Properties and regulation of cytosolic phospholipase A2. *J. Biol. Chem.* **1997,** *272* (27), 16709-16712; (b) Dolan-O'Keefe, M.; Chow, V.; Monnier, J.; Visner, G. A.; Nick, H. S., Transcriptional regulation and structural organization of the human cytosolic phospholipase A2 gene. *American Journal of Physiology - Lung Cellular and Molecular Physiology* **2000,** *278* (4), L649-L657; (c) Clark, J. D.; Schievella, A. R.; Nalefski, E. A.; Lin, L.-L., Cytosolic phospholipase A2. *Journal of Lipid Mediators and Cell Signalling* **1995,** *12* (2–3), 83-117.
44. Funk, C. D., Prostaglandins and leukotrienes: advances in eicosanoid biology. *Science (Washington, DC, U. S.)* **2001,** *294* (5548), 1871-1875.
45. Tucker, D. E.; Ghosh, M.; Ghomashchi, F.; Loper, R.; Suram, S.; John, B. S.; Girotti, M.; Bollinger, J. G.; Gelb, M. H.; Leslie, C. C., Role of phosphorylation and basic residues in the catalytic domain of cytosolic phospholipase A2alpha in

regulating interfacial kinetics and binding and cellular function. *J Biol Chem* **2009,** *284* (14), 9596-611.

46. Tucker, D. E.; Ghosh, M.; Ghomashchi, F.; Loper, R.; Suram, S.; St, J. B.; Girotti, M.; Bollinger, J. G.; Gelb, M. H.; Leslie, C. C., Role of Phosphorylation and Basic Residues in the Catalytic Domain of Cytosolic Phospholipase A2α in Regulating Interfacial Kinetics and Binding and Cellular Function. *J. Biol. Chem.* **2009,** *284* (14), 9596-9611.
47. Surrel, F.; Jemel, I.; Boilard, E.; Bollinger, J. G.; Payre, C.; Mounier, C. M.; Talvinen, K. A.; Laine, V. J. O.; Nevalainen, T. J.; Gelb, M. H.; Lambeau, G., Group X phospholipase A2 stimulates the proliferation of colon cancer cells by producing various lipid mediators. *Mol. Pharmacol.* **2009,** *76* (4), 778-790.
48. Parrill, A. L., Lysophospholipid interactions with protein targets. *Biochim. Biophys. Acta, Mol. Cell Biol. Lipids* **2008,** *1781* (9), 540-546.
49. Pulfer, M.; Murphy, R. C., Electrospray mass spectrometry of phospholipids. *Mass Spectrom. Rev.* **2003,** *22* (5), 332-364.
50. (a) Baker, S. F.; Othman, R.; Wilton, D. C., Tryptophan-Containing Mutant of Human (Group IIa) Secreted Phospholipase A2 Has a Dramatically Increased Ability To Hydrolyze Phosphatidylcholine Vesicles and Cell Membranes. *Biochemistry* **1998,** *37* (38), 13203-13211; (b) Murph, M.; Tanaka, T.; Pang, J.; Felix, E.; Liu, S.; Trost, R.; Godwin, A. K.; Newman, R.; Mills, G., Liquid chromatography mass spectrometry for quantifying plasma lysophospholipids: potential biomarkers for cancer diagnosis. *Methods Enzymol.* **2007,** *433* (Lipidomics and Bioactive Lipids: Specialized Analytical Methods and Lipids in Disease), 1-25.
51. Baker, D. L.; Desiderio, D. M.; Miller, D. D.; Tolley, B.; Tigyi, G. J., Direct quantitative analysis of lysophosphatidic acid molecular species by stable isotope dilution electrospray ionization liquid chromatography-mass spectrometry. *Anal. Biochem.* **2001,** *292* (2), 287-295.
52. Kayganich, K. A.; Murphy, R. C., Fast atom bombardment tandem mass spectrometric identification of diacyl, alkylacyl, and alk-1-enylacyl molecular species of glycerophosphoethanolamine in human polymorphonuclear leukocytes. *Anal. Chem.* **1992,** *64* (23), 2965-71.
53. Bezzine, S.; Koduri, R. S.; Valentin, E.; Murakami, M.; Kudo, I.; Ghomashchi, F.; Sadilek, M.; Lambeau, G.; Gelb, M. H., Exogenously added human group X secreted phospholipase A2 but not the group IB, IIA, and V enzymes efficiently release arachidonic acid from adherent mammalian cells. *J. Biol. Chem.* **2000,** *275* (5), 3179-3191.
54. Eaton, B. R.; Dennis, E. A., Analysis of phospholipase C (Bacillus cereus) action toward mixed micelles of phospholipid and surfactant. *Arch. Biochem. Biophys.* **1976,** *176* (2), 604-9.
55. Pluckthun, A.; Dennis, E. A., Acyl and phosphoryl migration in lysophospholipids: importance in phospholipid synthesis and phospholipase specificity. *Biochemistry* **1982,** *21* (8), 1743-50.

56. Ejsing, C. S.; Sampaio, J. L.; Surendranath, V.; Duchoslav, E.; Ekroos, K.; Klemm, R. W.; Simons, K.; Shevchenko, A., Global analysis of the yeast lipidome by quantitative shotgun mass spectrometry. *Proc. Natl. Acad. Sci. U. S. A.* **2009,** *106* (7), 2136-2141.
57. Khaselev, N.; Murphy, R. C., Electrospray ionization mass spectrometry of lysoglycerophosphocholine lipid subclasses. *J. Am. Soc. Mass Spectrom.* **2000,** *11* (4), 283-291.
58. Aoki, J.; Taira, A.; Takanezawa, Y.; Kishi, Y.; Hama, K.; Kishimoto, T.; Mizuno, K.; Saku, K.; Taguchi, R.; Arai, H., Serum lysophosphatidic acid is produced through diverse phospholipase pathways. *J. Biol. Chem.* **2002,** *277* (50), 48737-48744.
59. Kishimoto, T.; Soda, Y.; Matsuyama, Y.; Mizuno, K., An enzymatic assay for lysophosphatidylcholine concentration in human serum and plasma. *Clin. Biochem.* **2002,** *35* (5), 411-416.
60. (a) Buczynski, M. W.; Stephens, D. L.; Bowers-Gentry, R. C.; Grkovich, A.; Deems, R. A.; Dennis, E. A., TLR-4 and Sustained Calcium Agonists Synergistically Produce Eicosanoids Independent of Protein Synthesis in RAW264.7 Cells. *J. Biol. Chem.* **2007,** *282* (31), 22834-22847; (b) Dickinson, J. S.; Murphy, R. C., Mass spectrometric analysis of leukotriene A4 and other chemically reactive metabolites of arachidonic acid. *J. Am. Soc. Mass Spectrom.* **2002,** *13* (10), 1227-1234.
61. (a) Lamos, S. M.; Shortreed, M. R.; Frey, B. L.; Belshaw, P. J.; Smith, L. M., Relative Quantification of Carboxylic Acid Metabolites by Liquid Chromatography-Mass Spectrometry Using Isotopic Variants of Cholamine. *Anal. Chem. (Washington, DC, U. S.)* **2007,** *79* (14), 5143-5149; (b) Pettinella, C.; Lee, S. H.; Cipollone, F.; Blair, I. A., Targeted quantitative analysis of fatty acids in atherosclerotic plaques by high sensitivity liquid chromatography/tandem mass spectrometry. *J. Chromatogr., B: Anal. Technol. Biomed. Life Sci.* **2007,** *850* (1-2), 168-176; (c) Yang, W.-C.; Adamec, J.; Regnier, F. E., Enhancement of the LC/MS Analysis of Fatty Acids through Derivatization and Stable Isotope Coding. *Anal. Chem. (Washington, DC, U. S.)* **2007,** *79* (14), 5150-5157.
62. Park, K. K.; Lee, J.; Han, D., Synthesis and proton-NMR of N-arylated nitrogen-containing aromatic heterocycles. *Bull. Korean Chem. Soc.* **1985,** *6* (3), 141-4.
63. McKew, J. C.; Lee, K. L.; Chen, L.; Vargas, R.; Clark, J. D.; Williams, C.; Clerin, V.; Marusic, S.; Pong, K. Indole derivatives as inhibitors of cytosolic phospholipase a2 and their preparation, pharmaceutical compositions, and use in the prevention and treatment of various diseases. WO2006128142A2, 2006.
64. Kita, Y.; Takahashi, T.; Uozumi, N.; Shimizu, T., A multiplex quantitation method for eicosanoids and platelet-activating factor using column-switching reversed-phase liquid chromatography-tandem mass spectrometry. *Anal. Biochem.* **2005,** *342* (1), 134-143.
65. Chung, T. W.; Turecek, F., Selecting fixed-charge groups for electron-based peptide dissociations. *Int. J. Mass Spectrom.* **2008,** *276* (2-3), 127-135.

66. McLafferty, F. W.; Turecek, F., *Interpretation of mass spectra*. University Science Books: Mill Valley, Calif., 1993.
67. Boilard, E.; Nigrovic, P. A.; Larabee, K.; Watts, G. F. M.; Coblyn, J. S.; Weinblatt, M. E.; Massarotti, E. M.; Remold-O'Donnell, E.; Farndale, R. W.; Ware, J.; Lee, D. M., Platelets Amplify Inflammation in Arthritis via Collagen-Dependent Microparticle Production. *Science (Washington, DC, U. S.)* **2010,** *327* (5965), 580-583.
68. (a) Rasmussen, L. B.; Kiens, B.; Pedersen, B. K.; Richter, E. A., Effect of diet and plasma fatty acid composition on immune status in elderly men. *Am J Clin Nutr* **1994,** *59* (3), 572-7; (b) Schaefer, E. J.; Lichtenstein, A. H.; Lamon-Fava, S.; McNamara, J. R.; Ordovas, J. M., Lipoproteins, nutrition, aging, and atherosclerosis. *The American Journal of Clinical Nutrition* **1995,** *61* (3), 726S-740S; (c) Simopoulos, A. P., Omega-3 fatty acids in health and disease and in growth and development. *The American Journal of Clinical Nutrition* **1991,** *54* (3), 438-463.
69. Serhan, C. N., Resolution phase of inflammation: novel endogenous anti-inflammatory and proresolving lipid mediators and pathways. *Annu. Rev. Immunol.* **2007,** *25*, 101-137.
70. Bicalho, B.; David, F.; Rumplel, K.; Kindt, E.; Sandra, P., Creating a fatty acid methyl ester database for lipid profiling in a single drop of human blood using high resolution capillary gas chromatography and mass spectrometry. *Journal of Chromatography A* **2008,** *1211* (1–2), 120-128.
71. Eder, K., Gas chromatographic analysis of fatty acid methyl esters. *Journal of Chromatography B: Biomedical Sciences and Applications* **1995,** *671* (1–2), 113-131.
72. Schmitz, B.; Egge, H.; Murawski, U., Capillary gas-chromatographic mass-spectrometric analysis of isomeric polyenoic fatty acids as their poly-O-trimethylsilyl derivatives. *Fresenius' Z. Anal. Chem.* **1976,** *279* (2), 166-7.
73. Lagerstedt, S. A.; Hinrichs, D. R.; Batt, S. M.; Magera, M. J.; Rinaldo, P.; McConnell, J. P., Quantitative determination of plasma C8-C26 total fatty acids for the biochemical diagnosis of nutritional and metabolic disorders. *Mol. Genet. Metab.* **2001,** *73* (1), 38-45.
74. Roberts, L. D.; McCombie, G.; Titman, C. M.; Griffin, J. L., A matter of fat: An introduction to lipidomic profiling methods. *Journal of Chromatography B* **2008,** *871* (2), 174-181.
75. (a) Carrier, A.; Parent, J., Liquid chromatography-mass spectrometry determination of free fatty acids in phospholipid-based formulations. *J. Liq. Chromatogr. Relat. Technol.* **2001,** *24* (1), 97-107; (b) Nagy, K.; Jakab, A.; Fekete, J.; Vekey, K., An HPLC-MS approach for analysis of very long chain fatty acids and other apolar compounds on octadecyl-silica phase using partly miscible solvents. *Anal. Chem.* **2004,** *76* (7), 1935-1941; (c) Perret, D.; Gentili, A.; Marchese, S.; Sergi, M.; Caporossi, L., Determination of free fatty acids in chocolate by liquid chromatography with tandem mass spectrometry. *Rapid Commun. Mass Spectrom.* **2004,** *18* (17), 1989-1994; (d) Sajiki, J.; Yonekubo, J.,

Determination of free polyunsaturated fatty acids and their oxidative metabolites by high-performance liquid chromatography (HPLC) and mass spectrometry (MS). *Anal. Chim. Acta* **2002,** *465* (1-2), 417-426; (e) Valianpour, F.; Selhorst, J. J. M.; van, L. L. E. M.; van, G. A. H.; Wanders, R. J. A.; Kemp, S., Analysis of very long-chain fatty acids using electrospray ionization mass spectrometry. *Mol. Genet. Metab.* **2003,** *79* (3), 189-196.

76. Zehethofer, N.; Pinto, D. M.; Volmer, D. A., Plasma free fatty acid profiling in a fish oil human intervention study using ultra-performance liquid chromatography/electrospray ionization tandem mass spectrometry. *Rapid Commun. Mass Spectrom.* **2008,** *22* (13), 2125-2133.

77. (a) Afonso, C.; Riu, A.; Xu, Y.; Fournier, F.; Tabet, J.-C., Structural characterization of fatty acids cationized with copper by electrospray ionization mass spectrometry under low-energy collision-induced dissociation. *J. Mass Spectrom.* **2005,** *40* (3), 342-349; (b) Hsu, F.-F.; Turk, J., Distinction among isomeric unsaturated fatty acids as lithiated adducts by electrospray ionization mass spectrometry using low energy collisionally activated dissociation on a triple stage quadrupole instrument. *J. Am. Soc. Mass Spectrom.* **1999,** *10* (7), 600-612.

78. (a) Andersson, B. A., Mass spectrometry of fatty acid pyrrolidides. *Prog. Chem. Fats Other Lipids* **1978,** *16* (New Concepts Lipid Res.), 279-308; (b) Andersson, B. A.; Heimermann, W. H.; Holman, R. T., Comparison of pyrrolidides with other amides for mass spectral determination of structure of unsaturated fatty acids. *Lipids* **1974,** *9* (7), 443-9; (c) Vetter, w.; Walther, w.; Vecchi, M., Pyrrolides as derivative groups for structural elucidation of aliphatic and alicyclic carboxylic acids using mass spectrometry. *Helv. Chim. Acta* **1971,** *54* (6), 1599-605.

79. (a) Destaillats, F.; Angers, P., One-step methodology for the synthesis of FA picolinyl esters from intact lipids. *J. Am. Oil Chem. Soc.* **2002,** *79* (3), 253-256; (b) Dubois, N.; Barthomeuf, C.; Berge, J.-P., Convenient preparation of picolinyl derivatives from fatty acid esters. *Eur. J. Lipid Sci. Technol.* **2006,** *108* (1), 28-32; (c) Hamilton, J. T. G.; Christie, W. W., Mechanisms for ion formation during the electron impact-mass spectrometry of picolinyl ester and 4,4-dimethyloxazoline derivatives of fatty acids. *Chem. Phys. Lipids* **2000,** *105* (1), 93-104; (d) Wolff, R. L.; Christie, W. W.; Pedrono, F.; Marpeau, A. M., Arachidonic, eicosapentaenoic, and biosynthetically related fatty acids in the seed lipids from a primitive gymnosperm, Agathis robusta. *Lipids* **1999,** *34* (10), 1083-1097.

80. (a) Christie, W. W.; Robertson, G. W.; McRoberts, W. C.; Hamilton, J. T. G., Mass spectrometry of the 4,4-dimethyloxazoline derivatives of isomeric octadecenoates (monoenes). *Eur. J. Lipid Sci. Technol.* **2000,** *102* (1), 23-29; (b) Fay, L.; Richli, U., Location of double bonds in polyunsaturated fatty acids by gas chromatography-mass spectrometry after 4,4-dimethyloxazoline derivatization. *J. Chromatogr.* **1991,** *541* (1-2), 89-98; (c) Zhuang, W.; McKague, B.; Reeve, D., Mass spectrometric elucidation of chlorine location in dichloro fatty acids following 4,4-dimethyloxazoline derivatization, and its application to chlorinated fatty acids in fish. *Int. J. Mass Spectrom.* **2004,** *232* (2), 127-137.

81. Tsukamoto, Y.; Santa, T.; Saimaru, H.; Imai, K.; Funatsu, T., Synthesis of benzofurazan derivatization reagents for carboxylic acids and its application to analysis of fatty acids in rat plasma by high-performance liquid chromatography-electrospray ionization mass spectrometry. *Biomed. Chromatogr.* **2005,** *19* (10), 802-808.
82. Barry, S. J.; Carr, R. M.; Lane, S. J.; Leavens, W. J.; Monte, S.; Waterhouse, I., Derivatization for liquid chromatography/electrospray mass spectrometry: Synthesis of pyridinium compounds and their amine and carboxylic acid derivatives. *Rapid Commun. Mass Spectrom.* **2003,** *17* (6), 603-620.
83. Bollinger, J. G.; Thompson, W.; Lai, Y.; Oslund, R. C.; Hallstrand, T. S.; Sadilek, M.; Turecek, F.; Gelb, M. H., Improved Sensitivity Mass Spectrometric Detection of Eicosanoids by Charge Reversal Derivatization. *Anal. Chem. (Washington, DC, U. S.)* **2010,** *82* (16), 6790-6796.
84. Quehenberger, O.; Armando, A.; Dumlao, D.; Stephens, D. L.; Dennis, E. A., Lipidomics analysis of essential fatty acids in macrophages. *Prostaglandins, Leukotrienes Essent. Fatty Acids* **2008,** *79* (3-5), 123-129.
85. Ghomashchi, F.; Naika, G. S.; Bollinger, J. G.; Aloulou, A.; Lehr, M.; Leslie, C. C.; Gelb, M. H., Interfacial Kinetic and Binding Properties of Mammalian Group IVB Phospholipase A2 (cPLA2β) and Comparison with the Other cPLA2 Isoforms. *J. Biol. Chem.* **2010,** *285* (46), 36100-36111.
86. (a) Ghosh, M.; Loper, R.; Gelb, M. H.; Leslie, C. C., Identification of the Expressed Form of Human Cytosolic Phospholipase A2β (cPLA2β): cPLA2β3 is a novel variant localized to mitochondria and early endosomes. *J. Biol. Chem.* **2006,** *281* (24), 16615-16624; (b) Hixon, M. S.; Ball, A.; Strifler, B. A.; Pickard, R. T.; Gelb, M. H., Calcium-Dependent and -Independent Interfacial Binding and Catalysis of Group IV Phospholipase A2. *Biochemistry* **1998,** *37* (23), 8516-8526.
87. (a) Six, D. A.; Dennis, E. A., The expanding superfamily of phospholipase A2 enzymes: classification and characterization. *Biochim. Biophys. Acta, Mol. Cell Biol. Lipids* **2000,** *1488* (1-2), 1-19; (b) Valentin, E.; Lambeau, G., Increasing molecular diversity of secreted phospholipases A2 and their receptors and binding proteins. *Biochim. Biophys. Acta, Mol. Cell Biol. Lipids* **2000,** *1488* (1-2), 59-70.
88. (a) Berg, O. G.; Gelb, M. H.; Tsai, M. D.; Jain, M. K., Interfacial enzymology: the secreted phospholipase A(2)-paradigm. *Chem Rev* **2001,** *101* (9), 2613-54; (b) Gelb, M. H.; Jain, M. K.; Hanel, A. M.; Berg, O. G., Interfacial enzymology of glycerolipid hydrolases: lessons from secreted phospholipases A2. *Annu. Rev. Biochem.* **1995,** *64*, 653-88.
89. (a) Ramirez, F.; Jain, M. K., Phospholipase A2 at the bilayer interface. *Proteins: Struct., Funct., Genet.* **1991,** *9* (4), 229-39; (b) Scott, D. L.; Otwinowski, Z.; Gelb, M. H.; Sigler, P. B., Crystal structure of bee-venom phospholipase A2 in a complex with a transition-state analogue. *Science* **1990,** *250* (4987), 1563-6.
90. Hendrickson, H. S.; Dennis, E. A., Kinetic analysis of the dual phospholipid model for phospholipase A2 action. *J. Biol. Chem.* **1984,** *259* (9), 5734-9.
91. (a) Bezzine, S.; Bollinger, J. G.; Singer, A. G.; Veatch, S. L.; Keller, S. L.; Gelb, M. H., On the Binding Preference of Human Groups IIA and X Phospholipases

A2 for Membranes with Anionic Phospholipids. *J. Biol. Chem.* **2002,** *277* (50), 48523-48534; (b) Gelb, M. H.; Cho, W.; Wilton, D. C., Interfacial binding of secreted phospholipases A2: more than electrostatics and a major role for tryptophan. *Curr. Opin. Struct. Biol.* **1999,** *9* (4), 428-432; (c) Han, S. K.; Kim, K. P.; Koduri, R.; Bittova, L.; Munoz, N. M.; Leff, A. R.; Wilton, D. C.; Gelb, M. H.; Cho, W., Roles of Trp31 in high membrane binding and proinflammatory activity of human group V phospholipase A2. *J. Biol. Chem.* **1999,** *274* (17), 11881-11888; (d) Lin, Y.; Nielsen, R.; Murray, D.; Hubbell, W. L.; Mailer, C.; Robinson, B. H.; Gelb, M. H., Docking phospholipase A2 on membranes using electrostatic potential-modulated spin relaxation magnetic resonance. *Science (Washington, D. C.)* **1998,** *279* (5358), 1925-1929; (e) Sumandea, M.; Das, S.; Sumandea, C.; Cho, W., Roles of Aromatic Residues in High Interfacial Activity of Naja naja atra Phospholipase A2. *Biochemistry* **1999,** *38* (49), 16290-16297.

92. Beers, S. A.; Buckland, A. G.; Giles, N.; Gelb, M. H.; Wilton, D. C., Effect of tryptophan insertions on the properties of the human group IIA phospholipase A2: Mutagenesis produces an enzyme with characteristics similar to those of the human group V phospholipase A2. *Biochemistry* **2003,** *42* (24), 7326-7338.
93. Wimley, W. C.; White, S. H., Experimentally determined hydrophobicity scale for proteins at membrane interfaces. *Nat. Struct. Biol.* **1996,** *3* (10), 842-848.
94. (a) Canaan, S.; Nielsen, R.; Ghomashchi, F.; Robinson, B. H.; Gelb, M. H., Unusual mode of binding of human group IIA secreted phospholipase A2 to anionic interfaces as studied by continuous wave and time domain electron paramagnetic resonance spectroscopy. *J. Biol. Chem.* **2002,** *277* (34), 30984-30990; (b) Han, S. K.; Yoon, E. T.; Scott, D. L.; Sigler, P. B.; Cho, W., Structural aspects of interfacial adsorption. A crystallographic and site-directed mutagenesis study of the phospholipase A2 from the venom of Agkistrodon piscivorus piscivorus. *J. Biol. Chem.* **1997,** *272* (6), 3573-3582.
95. Ghomashchi, F.; Lin, Y.; Hixon, M. S.; Yu, B. Z.; Annand, R.; Jain, M. K.; Gelb, M. H., Interfacial recognition by bee venom phospholipase A2: insights into nonelectrostatic molecular determinants by charge reversal mutagenesis. *Biochemistry* **1998,** *37* (19), 6697-710.
96. Bollinger, J. G.; Diraviyam, K.; Ghomashchi, F.; Murray, D.; Gelb, M. H., Interfacial Binding of Bee Venom Secreted Phospholipase A2 to Membranes Occurs Predominantly by a Nonelectrostatic Mechanism. *Biochemistry* **2004,** *43* (42), 13293-13304.
97. Dudler, T.; Chen, W.-Q.; Wang, S.; Schneider, T.; Dempcy, R. O.; Annand, R. R.; Crameri, R.; Gmachl, M.; Suter, M.; et, a., High-level expression in Escherichia coli and rapid purification of enzymically active honey bee venom phospholipase A2. *Biochim. Biophys. Acta, Lipids Lipid Metab.* **1992,** *1165* (2), 201-10.
98. Buser, C. A.; Sigal, C. T.; Resh, M. D.; McLaughlin, S., Membrane Binding of Myristylated Peptides Corresponding to the NH2 Terminus of Src. *Biochemistry* **1994,** *33* (44), 13093-101.

99. Berg, O. G.; Gelb, M. H.; Tsai, M.-D.; Jain, M. K., Interfacial Enzymology: The Secreted Phospholipase A2-Paradigm. *Chem. Rev. (Washington, D. C.)* **2001,** *101* (9), 2613-2653.
100. Ghomashchi, F.; Yu, B. Z.; Berg, O.; Jain, M. K.; Gelb, M. H., Interfacial catalysis by phospholipase A2: substrate specificity in vesicles. *Biochemistry* **1991,** *30* (29), 7318-29.
101. Elsbach, P.; Weiss, J.; Wright, G.; Forst, S.; Van, d. B. C. J.; Verheij, H. M., Regulation and role of phospholipases in host-bacteria interaction. *Prog. Clin. Biol. Res.* **1990,** *349* (Cytokines Lipocortins Inflammation Differ.), 1-9.
102. Jain, M. K.; Vaz, W. L., Dehydration of the lipid-protein microinterface on binding of phospholipase A2 to lipid bilayers. *Biochim Biophys Acta* **1987,** *905* (1), 1-8.
103. Jain, M. K.; Ranadive, G.; Yu, B. Z.; Verheij, H. M., Interfacial catalysis by phospholipase A2: monomeric enzyme is fully catalytically active at the bilayer interface. *Biochemistry* **1991,** *30* (29), 7330-40.
104. Stahelin, R. V.; Cho, W., Differential Roles of Ionic, Aliphatic, and Aromatic Residues in Membrane-Protein Interactions: A Surface Plasmon Resonance Study on Phospholipases A2. *Biochemistry* **2001,** *40* (15), 4672-4678.
105. Murakami, M.; Shimbara, S.; Kambe, T.; Kuwata, H.; Winstead, M. V.; Tischfield, J. A.; Kudo, I., The functions of five distinct mammalian phospholipase A_2s in regulating arachidonic acid release. Type IIA and type V secretory phospholipase A_2s are functionally redundant and act in concert with cytosolic phospholipase A2. *J. Biol. Chem.* **1998,** *273* (23), 14411-14423.
106. Enomoto, A.; Murakami, M.; Valentin, E.; Lambeau, G.; Gelb, M. H.; Kudo, I., Redundant and segregated functions of granule-associated heparin-binding group II subfamily of secretory phospholipases A2 in the regulation of degranulation and prostaglandin D2 synthesis in mast cells. *J. Immunol.* **2000,** *165* (7), 4007-4014.
107. Murakami, M.; Koduri, R. S.; Enomoto, A.; Shimbara, S.; Seki, M.; Yoshihara, K.; Singer, A.; Valentin, E.; Ghomashchi, F.; Lambeau, G.; Gelb, M. H.; Kudo, I., Distinct arachidonate-releasing functions of mammalian secreted phospholipase A2s in human embryonic kidney 293 and rat mastocytoma RBL-2H3 cells through heparan sulfate shuttling and external plasma membrane mechanisms. *J. Biol. Chem.* **2001,** *276* (13), 10083-10096.
108. Lambeau, G.; Lazdunski, M., Receptors for a growing family of secreted phospholipases A2. *Trends Pharmacol. Sci.* **1999,** *20* (4), 162-170.

Appendix A: Chronological Personal Publication List

A1 : Publications up to December 2012

1. Bezzine, S.; **Bollinger, J. G.**; Singer, A. G.; Veatch, S. L.; Keller, S. L.; Gelb, M. H., On the Binding Preference of Human Groups IIA and X Phospholipases A2 for Membranes with Anionic Phospholipids. *J. Biol. Chem.* **2002,** *277* (50), 48523-48534.
2. Singer, A. G.; Ghomashchi, F.; Le, C. C.; **Bollinger, J.**; Bezzine, S.; Rouault, M.; Sadilek, M.; Nguyen, E.; Lazdunski, M.; Lambeau, G.; Gelb, M. H., Interfacial Kinetic and Binding Properties of the Complete Set of Human and Mouse Groups I, II, V, X, and XII Secreted Phospholipases A2. *J. Biol. Chem.* **2002,** *277* (50), 48535-48549.
3. Rouault, M.; **Bollinger, J. G.**; Lazdunski, M.; Gelb, M. H.; Lambeau, G., Novel Mammalian Group XII Secreted Phospholipase A2 Lacking Enzymatic Activity. *Biochemistry* **2003,** *42* (39), 11494-11503.
4. **Bollinger, J. G.**; Diraviyam, K.; Ghomashchi, F.; Murray, D.; Gelb, M. H., Interfacial Binding of Bee Venom Secreted Phospholipase A2 to Membranes Occurs Predominantly by a Nonelectrostatic Mechanism. *Biochemistry* **2004,** *43* (42), 13293-13304.
5. Canaan, S.; Zadori, Z.; Ghomashchi, F.; **Bollinger, J.**; Sadilek, M.; Moreau, M. E.; Tijssen, P.; Gelb, M. H., Interfacial Enzymology of Parvovirus Phospholipases A2. *J. Biol. Chem.* **2004,** *279* (15), 14502-14508.
6. Smart, B. P.; Pan, Y. H.; Weeks, A. K.; **Bollinger, J. G.**; Bahnson, B. J.; Gelb, M. H., Inhibition of the complete set of mammalian secreted phospholipases A2 by indole analogues a structure-guided study. *Bioorg. Med. Chem.* **2004,** *12* (7), 1737-1749.
7. Granata, F.; Petraroli, A.; Boilard, E.; Bezzine, S.; **Bollinger, J.**; Del, V. L.; Gelb, M. H.; Lambeau, G.; Marone, G.; Triggiani, M., Activation of Cytokine Production by Secreted Phospholipase A2 in Human Lung Macrophages Expressing the M-Type Receptor. *J. Immunol.* **2005,** *174* (1), 464-474.
8. Gora, S.; Lambeau, G.; **Bollinger, J. G.**; Gelb, M.; Ninio, E.; Karabina, S.-A., The proinflammatory mediator Platelet Activating Factor is an effective substrate for human group X secreted phospholipase A2. *Biochim. Biophys. Acta, Mol. Cell Biol. Lipids* **2006,** *1761* (9), 1093-1099.
9. Morgan, D.; Cherny, V. V.; Finnegan, A.; **Bollinger, J.**; Gelb, M. H.; DeCoursey, T. E., Sustained activation of proton channels and NADPH oxidase in human eosinophils and murine granulocytes requires PKC but not cPLA2α activity. *J. Physiol. (Oxford, U. K.)* **2006,** *579* (2), 327-344.
10. Rouault, M.; Rash, L. D.; Escoubas, P.; Boilard, E.; **Bollinger, J.**; Lomonte, B.; Maurin, T.; Guillaume, C.; Canaan, S.; Deregnaucourt, C.; Schrevel, J.; Doglio, A.;

Gutierrez, J. M.; Lazdunski, M.; Gelb, M. H.; Lambeau, G., Neurotoxicity and Other Pharmacological Activities of the Snake Venom Phospholipase A2 OS2: The N-Terminal Region Is More Important Than Enzymatic Activity. *Biochemistry* **2006,** *45* (18), 5800-5816.

11. Ghomashchi, F.; **Bollinger, J. G.**; Gelb, M. H., Facile preparation of leukotrienes C4, D4 and E4 containing carbon-13 and nitrogen-15 for quantification of cysteinyl leukotrienes by mass spectrometry. *J. Labelled Compd. Radiopharm.* **2007,** *50* (8), 729-733.
12. Gillespie, J. R.; Yokoyama, K.; Lu, K.; Eastman, R. T.; **Bollinger, J. G.**; Van, V. W. C.; Gelb, M. H.; Buckner, F. S., C-terminal proteolysis of prenylated proteins in trypanosomatids and RNA interference of enzymes required for the post-translational processing pathway of farnesylated proteins. *Mol. Biochem. Parasitol.* **2007,** *153* (2), 115-124.
13. Henderson, W. R., Jr.; Chi, E. Y.; **Bollinger, J. G.**; Tien, Y.-t.; Ye, X.; Castelli, L.; Rubtsov, Y. P.; Singer, A. G.; Chiang, G. K. S.; Nevalainen, T.; Rudensky, A. Y.; Gelb, M. H., Importance of group X-secreted phospholipase A2 in allergen-induced airway inflammation and remodeling in a mouse asthma model. *J. Exp. Med.* **2007,** *204* (4), 865-877.
14. Rouault, M.; Le, C. C.; Boilard, E.; Surrel, F.; Singer, A.; Ghomashchi, F.; Bezzine, S.; Scarzello, S.; **Bollinger, J.**; Gelb, M. H.; Lambeau, G., Recombinant Production and Properties of Binding of the Full Set of Mouse Secreted Phospholipases A2 to the Mouse M-Type Receptor. *Biochemistry* **2007,** *46* (6), 1647-1662.
15. Wilensky, R. L.; Shi, Y.; Mohler, E. R., III; Hamamdzic, D.; Burgert, M. E.; Li, J.; Postle, A.; Fenning, R. S.; **Bollinger, J. G.**; Hoffman, B. E.; Pelchovitz, D. J.; Yang, J.; Mirabile, R. C.; Webb, C. L.; Zhang, L.-F.; Zhang, P.; Gelb, M. H.; Walker, M. C.; Zalewski, A.; Macphee, C. H., Inhibition of lipoprotein-associated phospholipase A2 reduces complex coronary atherosclerotic plaque development. *Nat. Med. (N. Y., NY, U. S.)* **2008,** *14* (10), 1059-1066.
16. Surrel, F.; Jemel, I.; Boilard, E.; **Bollinger, J. G.**; Payre, C.; Mounier, C. M.; Talvinen, K. A.; Laine, V. J. O.; Nevalainen, T. J.; Gelb, M. H.; Lambeau, G., Group X phospholipase A2 stimulates the proliferation of colon cancer cells by producing various lipid mediators. *Mol. Pharmacol.* **2009,** *76* (4), 778-790.
17. Tucker, D. E.; Ghosh, M.; Ghomashchi, F.; Loper, R.; Suram, S.; St, J. B.; Girotti, M.; **Bollinger, J. G.**; Gelb, M. H.; Leslie, C. C., Role of Phosphorylation and Basic Residues in the Catalytic Domain of Cytosolic Phospholipase A2α in Regulating Interfacial Kinetics and Binding and Cellular Function. *J. Biol. Chem.* **2009,** *284* (14), 9596-9611.
18. **Bollinger, J. G.**; Ii, H.; Sadilek, M.; Gelb, M. H., Improved method for the quantification of lysophospholipids including enol ether species by liquid chromatography-tandem mass spectrometry. *J. Lipid Res.* **2010,** *51* (2), 440-447.

19. **Bollinger, J. G.**; Thompson, W.; Lai, Y.; Oslund, R. C.; Hallstrand, T. S.; Sadilek, M.; Turecek, F.; Gelb, M. H., Improved Sensitivity Mass Spectrometric Detection of Eicosanoids by Charge Reversal Derivatization. *Anal. Chem. (Washington, DC, U. S.)* **2010,** *82* (16), 6790-6796.
20. Ghomashchi, F.; Naika, G. S.; **Bollinger, J. G.**; Aloulou, A.; Lehr, M.; Leslie, C. C.; Gelb, M. H., Interfacial Kinetic and Binding Properties of Mammalian Group IVB Phospholipase A2 (cPLA2β) and Comparison with the Other cPLA2 Isoforms. *J. Biol. Chem.* **2010,** *285* (46), 36100-36111.
21. Lai, Y.; Oslund, R. C.; **Bollinger, J. G.**; Henderson, W. R., Jr.; Santana, L. F.; Altemeier, W. A.; Gelb, M. H.; Hallstrand, T. S., Eosinophil Cysteinyl Leukotriene Synthesis Mediated by Exogenous Secreted Phospholipase A2 Group X. *J. Biol. Chem.* **2010,** *285* (53), 41491-41500.
22. Degousee, N.; Kelvin, D. J.; Geisslinger, G.; Hwang, D. M.; Stefanski, E.; Wang, X.-H.; Danesh, A.; Angioni, C.; Schmidt, H.; Lindsay, T. F.; Gelb, M. H.; **Bollinger, J.**; Payre, C.; Lambeau, G.; Arm, J. P.; Keating, A.; Rubin, B. B., Group V Phospholipase A2 in Bone Marrow-derived Myeloid Cells and Bronchial Epithelial Cells Promotes Bacterial Clearance after Escherichia coli Pneumonia. *J. Biol. Chem.* **2011,** *286* (41), 35650-35662, S35650/1-S35650/5.
23. Gelb, M. H.; Turecek, F.; **Bollinger, J.** Quaternary ammonium reagent and method for detection of carboxylic acids by mass spectrometry. US20110294153A1, 2011.
24. Henderson, W. R., Jr.; Oslund, R. C.; **Bollinger, J. G.**; Ye, X.; Tien, Y.-t.; Xue, J.; Gelb, M. H., Blockade of Human Group X Secreted Phospholipase A2 (GX-sPLA2)-induced Airway Inflammation and Hyperresponsiveness in a Mouse Asthma Model by a Selective GX-sPLA2 Inhibitor. *J. Biol. Chem.* **2011,** *286* (32), 28049-28055, S28049/1-S28049/9.
25. Thompson, W.; Oslund, R. C.; **Bollinger, J.**; Ewing, H.; Gelb, M. H., High-throughput assay of secreted phospholipases A2 inhibitors. *Methods Mol. Biol. (N. Y., NY, U. S.)* **2012,** *861* (Lipases and Phospholipases), 149-158.

Appendix B: List of Funded Proposals, Awards, and Presentations

B1: Funded Proposals

2010 Huckabay Teaching Fellowship
- Design and application of an experimental organic chemistry discussion section format

2010 University of Washington Student Technology Fee
- Acquisition of an Ultra High Pressure Liquid Chromatography (UPLC) System

2011 University of Washington Student Technology Fee
- Acquisition of an ambient pressure ionization source for use with departmental mass spectrometers

B2: Awards

2012 Department of Chemistry Outstanding Teaching Assistant Award

B3: Selected Presentations

2010 Pacific Northwest Mass Spectrometry Group (PacMass)
- Invited Speaker

2010 International Chemical Congress of Pacific Basin Science (Pacifichem)
- Poster presentation

2010 Institute of Translational Health Sciences (ITHS)
- Poster presentation, Industry relations event

2011 International Conference in Bioactive Lipids in Cancer, Inflammation, and Related Diseases
- Speaker

Vita

James G. Bollinger was born in Winifield, Illinois, and grew up in the north suburbs of Chicago. After high school, he attended University of Missouri-Columbia on an academic scholarship from Western Golf Association's Evans Scholars program. In the winter of 1999, James obtained a B.A. in Psychology and a B.S. in Biochemistry. Still deciding on a specific career path and endeavoring to experience more of the world, James travelled extensively after graduation and worked a series of odd jobs that included taxi cab driver, concessionaire for the Royal Haneford Circus, and research technician for Dr. Roy Morris in the Department of Biochemistry at the University of Missouri. Although extremely entertaining and fodder for a plethora of interesting stories, a lifestyle devoid of any specific intention or career arc ultimately left James unfulfilled. After moving to Seattle in pursuit of his eventual wife, James had the fortunate experience of being hired on as a research technician in the laboratory of Dr. Michael Gelb in the Department of Chemistry at the University of Washington. The interdisciplinary nature of Dr. Gelb's medicinal enzymology lab enabled James to interact with many talented scientists, learn a variety of chemical and biochemical techniques, and ultimately see the merit of a career in the academic sciences. After six years of working on a multitude of different projects, James decided to return to school to further explore the career options available in academia. Although initially not seriously considered at the outset, the opportunity to serve as a teaching assistant to many talented educators in the Department of Chemistry helped James develop a passion for science education. He earned a Ph.D. in Organic Chemistry at the University of Washington

under the tutelage of Professor Gelb in December, 2012, and is headed across the UW campus to the Department of Genome Sciences to begin his post-doctoral studies in the laboratory of Associate Professor Michael MacCoss. He ultimately desires to procure a position teaching organic chemistry at a small liberal arts or community college.